SYMBOLIC DYNAMICS OF BILLIARD FLOW IN ISOSCELES TRIANGLES

A Dissertation

Presented to the Faculty of the Graduate School

of Cornell University

in Partial Fulfillment of the Requirements for the Degree of

Doctor of Philosophy

by

Robyn L. Miller

January 2014

SYMBOLIC DYNAMICS OF BILLIARD FLOW

IN ISOSCELES TRIANGLES

Robyn L. Miller, Ph.D.

Cornell University 2014

We provide a complete characterization of billiard trajectory hitting sequences on $\left(\frac{\pi}{n}\right)$-isosceles triangles for $n \geq 2$. The case of the $\left(\frac{\pi}{4}\right)$-isosceles triangle is presented in detail. When n equals two or three, these triangles tile the plane. For n greater than or equal to four, this is no longer the case. On the two isosceles triangles that tile the plane, as well as the $\left(\frac{\pi}{4}\right)$-isosceles triangle, we provide combinatorial renormalization schemes that apply directly to hitting sequences given in a three letter aphabet of triangle side labels. Although cutting sequences have been characterized on related translation surfaces, this is the first analysis of billiard trajectory hitting sequences in triangles.

BIOGRAPHICAL SKETCH

Robyn received Bachelor's degrees in mathematics, statistics and economics from Mount Holyoke College in 2000. She participated in the NSF IGERT program in nonlinear dynamics during her first years at Cornell, and did research with a computational neuroscience group in the Neurobiology department during that time. Although she had not lost interest in biological applications, Robyn eventually decided that studying math would provide both greater intellectual satisfaction and a more solid disciplinary base from which to pursue any future interdisciplinary work. In 2004 she joined the Math department, earning her Masters in 2008. She continued her interdisciplinary adventures in 2012 with a research fellowship in biomedical image analysis, a position she still holds at this time.

Dedicated to the memories of David and Florence Miller, who passed away within months of each other, just before seeing this project brought to fruition.

ACKNOWLEDGMENTS

I would first like to thank my entire committee for its patience and support through what became a rather prolonged thesis process. My advisor John Smillie deserves special mention for patience, and more specifically for his guidance and many useful conversations about polygonal billiards and translation surfaces, topics that were new to me when I started working with him. The conversations I have had through the years with John Hubbard about various topics in dynamics have also enriched my doctoral experience tremendously. My interactions with Clifford Earle have been limited but always enjoyable, and I thank him for his consistent support and involvement.

The personal support of family and friends was incredibly important through the entire research and writing process. There are so many people to acknowledge here, and my list will inevitably be partial. First and foremost, my wonderful family: my consistently loving and encouraging parents Larry and Martha and my supportive dynamo of a brother Dan. Hercule Poirot, the now ancient toy poodle who accompanied me through graduate school and beyond was indispensible as a distraction and as a role model of relentless persistence. The friends who were so central to life and morale while I was in graduate school: Bruce Carter, Dan Pendleton, Donna Dietz and Michael Robinson, Erik Sherwood, Jeremy Kahn, Maria Terrell, Virginia Pasour and Vladimir Pistalo among many others. And more recent acquaintances in Albuquerque who have kept me going while I was away from the familiar environs of Cornell - especially Erik Erhardt, Robert Niemeyer and my terrific boss Vince Calhoun.

TABLE OF CONTENTS

LIST OF TABLES

LIST OF FIGURES

CHAPTER 1

INTRODUCTION

Let Q be a compact connected planar region bounded by a curve that is C^1 away from a finite set of points Σ. A billiard path is described by a point moving along a straight line at unit speed in the interior of Q, bouncing off the boundary according to the classical law of geometric optics that the angle of incidence equals the angle of reflection. We do not attempt to define a continuation for trajectories that hit points in Σ. Billiard trajectories in Q are in fact projections of trajectories of a flow defined on the unit tangent bundle of Q, where we identify certain incoming and outgoing vectors along the boundary of Q. The classical case of billiards in a domain with non-smooth boundary is that of square billiards. The rich results [46, 61, 71, 72] derived on the square encourage further investigation of billiard tables with polygonal boundary. We say a polygon is rational if all angles are rational multiples of π. In the rational case, the billiard flow on the three-dimensional phase space can be studied in terms of invariant surfaces.

Definition 1.0.0.1. *(Hitting Sequences) Let Q be a polygonal table with labeled sides. The* hitting sequence *of a billiard trajectory g_t is the sequence of labels corresponding to successive bounces of the trajectory off sides of Q.*

As the most elementary polygons, triangular billiards are of fundamental interest and have received a commensurate amount of attention [47, 33, 66, 84, 63, 64, 53, 30, 65]. Even in the setting of rational triangles however, many basic

questions remain open. This thesis addresses the problem of characterizing hitting sequences in rational triangles.

Triangles that tile the plane constitute a special class which is more easily analyzed than general triangles. The symbolic dynamics of triangles that tile the plane is related to *Sturmian sequences* [22, 61]. Results for the two *planar* isosceles triangles, the $\left(\frac{\pi}{2}\right)$-isosceles and equilateral triangle, are included here (Chapter 3 and Appendix A) both for completeness and as an introduction to techniques we will use in the thesis. More significantly, in this thesis we give the first complete analysis of a triangle that does not tile the plane, the $\left(\frac{\pi}{4}\right)$-isosceles triangle. There is an algorithm (see Section 4.2) that takes a word in the alphabet $\{\beta, \lambda, \rho\}$ of triangle sides (Figure 2.1 (a)) to a word in the alphabet $\{\beta_0, \beta_1, \beta_2, \beta_3, \rho^+, \rho^-\}$ corresponding to edges shown in Figure 2.1 (d). The results of our analysis are summarized below in Theorem 4.5.0.1.

Theorem 1.0.0.1 (Main Theorem)**.** *The set of infinitely deriveable (Definition 4.4.0.2) words in* $\{\beta_0, \beta_1, \beta_2, \beta_3, \rho^-, \rho^+\}$*(see Figure 2.1 (d)) which, at each derivation step, also satisfy a finite set of* coherence conditions *(Definition 4.5.0.1) coincides with the closure of the set of billiard trajectory hitting sequences on the* $\left(\frac{\pi}{4}\right)$*-isosceles triangle.*

Results of this form also hold in $\left(\frac{\pi}{n}\right)$-isosceles triangles when n is greater than four. In Chapter 5, we show how the methods we use to analyze the $\left(\frac{\pi}{4}\right)$-isosceles triangle extend to apply in $\left(\frac{\pi}{n}\right)$-isosceles triangles for n greater than four.

CHAPTER 2

PRELIMINARIES

One reason to focus on rational polygons is that in a rational polygon Q the billiard flow is readily recast [94, 24] as the linear flow on a translation surface S_Q (Section 2.1). Labeled sides of the reflected copies of Q are geodesic segments joining singular or marked points in S_Q.

Definition 2.0.0.2. *(Cutting Sequences) Let* S *be a translation surface,* Σ *a finite set of points in* S *including all singular points, and* $\mathcal{E}$ *a collection of labeled saddle connections joining points in* Σ*. The* cutting sequence $c(\gamma)$ *of a geodesic* γ_t *on* S *is the ordered bi-infinite sequence of labels arising from successive crossings of* γ_t *through labeled saddle connections in* $\mathcal{E}$*.*

One natural setting in which to investigate cutting sequences is S_Q where Q is a rational triangle. In this case Σ includes marked points of S corresponding to vertices of Q, and $\mathcal{E}$ includes of lifts of labeled sides of Q. If Q is a triangle that tiles the plane, then S_Q is the torus. The standard presentation of the torus as a square gives rise to *Sturmian sequences* [61, 71, 72] and our analysis of hitting sequences for triangles that tile the plane is closely connected with Sturmian sequences. When Q is the $\left(\frac{\pi}{4}\right)$-isosceles triangle, S_Q is a translation surface of genus two corresponding to the regular octagon with opposite sides identified. Arnoux and Hubert [1] raised the question of characterizing cutting sequences on this surface with respect to the sides of the octagon. Their question was answered by Smillie and Ulcigrai [74]. Partial results in this vein have been also

been obtained [19] for the so-called *double-regular* $(2m+1)$-gons.

Although the surface geometry of S_Q is the same when Q is either a regular $2n$-gon or a $\left(\frac{\pi}{n}\right)$-isosceles triangle, in the latter case, the marked point of S corresponding to the apex of Q is an endpoint of additional edges (Figure 2.1 (a)-(d)) that play a key role in the combinatorial encoding of geodesics on S_Q. Billiards in $\left(\frac{\pi}{n}\right)$-isosceles triangles and in regular $2n$-gons thus present distinct combinatorial problems.

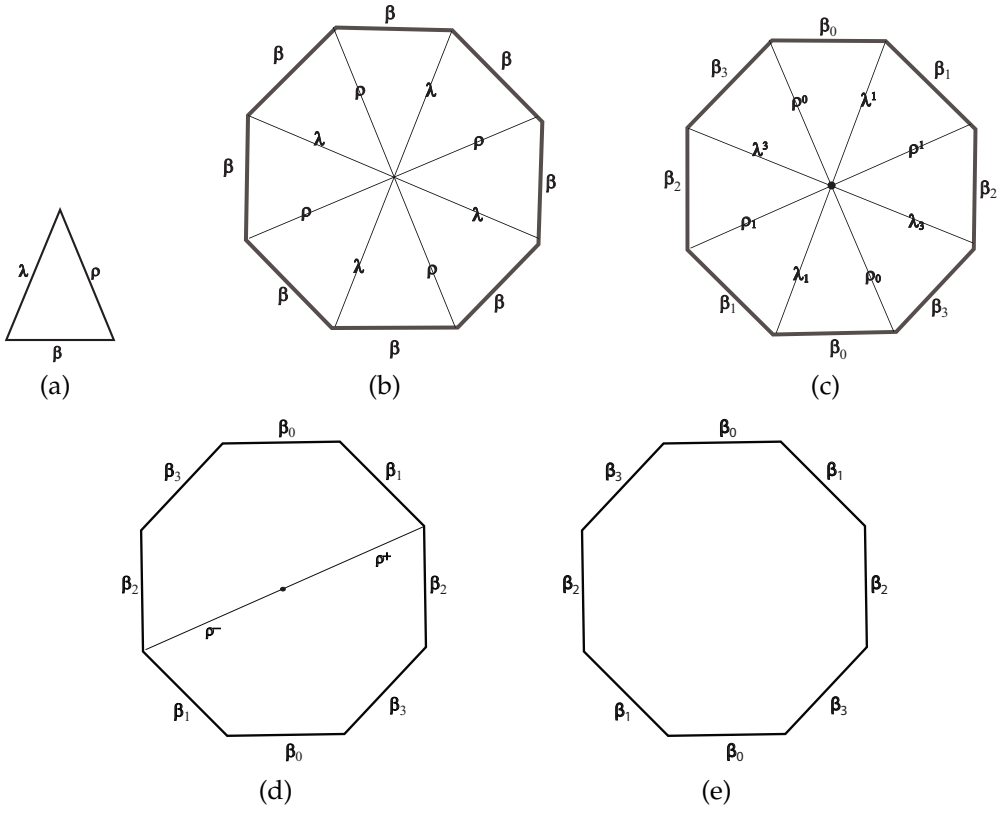

Figure 2.1: Edge labels for coding: billiard trajectories in the $\left(\frac{\pi}{4}\right)$-isosceles triangle ((a),(b)); directional flow in the $\left(\frac{\pi}{4}\right)$-isosceles triangle surface (c); directional flow in the centrally-punctured octagon surface (d), and directional flow on the regular octagon surface (e).

Although billiards in the regular $2n$-gon and in the $\left(\frac{\pi}{n}\right)$-isosceles triangle present distinct combinatorial problems, the symbolic dynamics of linear trajectories on the *centrally-punctured* $2n$-gon (Figure 2.1 (d)) and billiard trajectories in the $\left(\frac{\pi}{n}\right)$-isosceles triangle are closely related. There is a well-defined mapping between centrally-punctured $2n$-gon cutting sequences and $\left(\frac{\pi}{n}\right)$-isosceles hitting sequences that we describe in Section 4.2.

It has long been known [62] that some low-dimensional dynamical systems induce systems of the same class on restrictions of the original domain. This *renormalization* operation can be iterated, producing a dynamics on the given class of dynamical systems. If the original dynamical system has a combinatorial characterization, renormalization of the flow yields a renormalization of the combinatorics as well. This correspondence is well understood for interval exchange transformations [62, 87]. The directional flow on a rational polygon surface induces an interval exchange transformation on transversals, which has led to interest in renormalization of the polygonal billiard flow itself [88, 93]. Renormalization of dynamical systems is generally a challenging problem. It turns out that when Q is a $\left(\frac{\pi}{n}\right)$-isosceles triangle or a regular $2n$-gon, symmetries and properties of the affine automorphism group of S_Q make the renormalization problem for billiards on Q somewhat more tractable. In Chapter 4 we define a renormalization scheme for billiards on the $\left(\frac{\pi}{4}\right)$-isosceles triangle using symmetries of the triangle and an affine automorphism of the regular octagon surface. Analogous symmetries and affine automorphisms for $\left(\frac{\pi}{n}\right)$-isosceles triangles and regular $2n$-gons for $n \geq 5$ allow us to extend the renormalization scheme from Chapter 4 to billiards in $\left(\frac{\pi}{n}\right)$-isosceles triangles, $n \geq 5$, which we will do in Chapter 5.

2.1 Translation surfaces and rational polygons

A finite number of reflections through the sides of any rational polygon Q produces another polygon $\widetilde{Q}$ whose exterior edges come in same-length parallel pairs that can be identified by translation [24, 94]. In other words, under appropriate side identifications, $\widetilde{Q}$ closes up into a compact surface S_Q that is clearly Euclidean away from images of vertices of $\widetilde{Q}$. Furthermore, it is not hard to see that even neighborhoods of points on S_Q that were vertices in $\widetilde{Q}$ can fail to be Euclidean only in a limited sense: They are each 'hinge points' of a finite number of edge-pairs subtending angles $\{\theta_1, \theta_2, ..., \theta_k\}$ from copies of Q in $\widetilde{Q}$, and are thus *conical singularities* with cone angle $2\pi\Sigma_{i=1}^{k}\theta_i$.

Definition 2.1.0.1. *(Translation Surface: Basic Formulation) A surface* S *with charts* (ϕ_k, U_k) *is a translation surface if the overlap maps* $\phi_i \circ \phi_j^{-1}$ *are translations on* $\mathbb{R}^2$.

Clearly the surface S_Q for Q a rational polygon satisfies this definition, and is thus a translation surface. Generalizing the construction somewhat by specifying an *arbitrary* collection of polygons with the property that their sides taken as a group can be decomposed into same-length parallel pairs actually exhausts the set of compact translation surfaces.

Definition 2.1.0.2. *(Translation Surface: Polygonal Formulation) A collection of polygons* $\mathcal{P} = \{P^{(1)}, P^{(2)}, ..., P^{(d)}\}$ *whose sides decompose into same-length parallel pairs*

define a translation surface $\mathsf{S}_{\mathcal{P}}$*. Moreover, for any compact translation surface* S*, there exists a collection* $\mathcal{P} = \{P^{(1)}, P^{(2)}, ..., P^{(d)}\}$ *of polygons whose sides pair up by translation to produce* S*.*

Complex analysis offers yet another definition of translation surfaces. From this perspective, a translation surface is specified by the pairing of a Riemann surface with an abelian differential. The complex analytic definition is, in fact, equivalent to Definition 2.1.0.2 [95]. Here, we will only be using Definition 2.1.0.2.

The notation (S, Σ) will refer to a translation surface S with a specified collection of distinguished points Σ, that always includes singular points of S and may include additional marked points of the surface. In our case, Σ will include the marked point of the $2n$-gon surface S_{2n} that corresponds to the centerpoint of the regular $2n$-gon. When Σ is clear from the context, we will use S as shorthand for (S, Σ).

2.2 Veech surfaces and renormalization

Let S be a translation surface, Σ its set of singular and marked points and $\mathrm{A}(\mathsf{S}, \Sigma)$ the group of affine diffeomorphisms $\Phi : \mathsf{S} \mapsto \mathsf{S}$ such that $\Phi(\Sigma) = \Sigma$. The set of derivatives of elements of $\mathrm{A}(\mathsf{S}, \Sigma)$ plays an important role in understanding the dynamical properties of the geodesic flow on (S, Σ), and in constructing renormalization schemes on (S, Σ) that facilitate systematic study of the

behavior of individual linear trajectories on (S, Σ). $\mathrm{A}(\mathrm{S}, \Sigma)$ is the union of the set of orientation-preserving $\mathrm{A}^{+}(\mathrm{S}, \Sigma)$ and orientation-reversing $\mathrm{A}^{-}(\mathrm{S}, \Sigma)$ affine automorphisms of (S, Σ). The *Veech group* $\mathrm{V}(\mathrm{S}, \Sigma)$ of (S, Σ) is the subgroup of $GL(2, \mathbb{R})$ consisting of derivatives of elements of $\mathrm{A}(\mathrm{S}, \Sigma)$. One common convention restricts the Veech group to derivatives of orientation-preserving affine automorphisms of (S, Σ). Under this convention $\mathrm{V}(\mathrm{S}, \Sigma)$ is a subgroup of $SL(2, \mathbb{R})$. Since orientation-reversing automorphisms will play a role in our renormalization scheme, we will adopt a different convention. In this thesis, $\mathrm{V}(\mathrm{S}, \Sigma)$ will denote the group of derivatives of orientation-preserving *and* orientation-reversing affine automorphisms. Using this definition, $\mathrm{V}(\mathrm{S}, \Sigma)$ is a subgroup of $SL_{\pm}(2, \mathbb{R}) = \{M \in GL(2, \mathbb{R}) : \det(M) = \pm 1\}$.

If S is specified as a finite collection of polygons $\mathcal{P} = \{\mathrm{P}_1, .., \mathrm{P}_k\}$ with side-identifications (Definition 2.1.0.2), then $SL_{\pm}(2, \mathbb{R})$ acts on S by individually transforming each $\mathrm{P}_j \in \mathcal{P}$: for $M \in \mathrm{SL}_{\pm}(2, \mathbb{R})$, $M \cdot \mathrm{S}$ is the surface specified by $M \cdot \mathcal{P} = \{M \cdot \mathrm{P}_1, ..., M \cdot \mathrm{P}_k\}$, where $M \cdot \mathrm{P}_k$ is simply applying the linear transformation M to P_k in $\mathbb{R}^2$. The property of parallelism is preserved by $M \in SL_{\pm}(2, \mathbb{R})$ so if $\mathcal{P}$ defines a translation surface, then $M \cdot \mathcal{P}$ does.

The translation surface (S, Σ) is said to be a *Veech surface* or a *lattice surface* if its Veech group $\mathrm{V}(\mathrm{S}, \Sigma)$ is a lattice in $SL_{\pm}(2, \mathbb{R})$. Specifically (S, Σ) is a Veech or lattice surface if $\mathrm{V}(\mathrm{S}, \Sigma)$ is a discrete subgroup of $SL_{\pm}(2, \mathbb{R})$ that has finite covolume in $SL_{\pm}(2, \mathbb{R})$ but is not co-compact. This property implies that the Veech group of a lattice surface must [44] have at least one parabolic element. Recall that a linear transformation is parabolic if it has two identical eigenvalues and

is not equal to the identity. Parabolic elements of $\mathrm{V}(\mathrm{S})$ are derivatives of automorphisms that act as powers of *Dehn twists* of S along all cylinders in a fixed direction (see Figure 4.1 for example). The linear part of such an automorphism is a shear (for example, $\begin{pmatrix} 1 & 1 \\ 0 & 1 \end{pmatrix}$) in $SL_{\pm}(2,\mathbb{R})$. An affine automorphism whose derivative is the identity is a *translation equivalences*. Veech [85] established that surfaces defined from the regular n-gons are all Veech surfaces. It follows from work of Kenyon and Smillie, followed by Puchta [47, 64], that the $\left(\frac{2\pi}{m}\right)$-isosceles triangles that tile centrally-punctured regular m-gons define Veech surfaces only when m is even. A triangle is often said to be Veech if the triangle surface (S,Σ) where Σ consists *only* of singular points of S is Veech. The $\left(\frac{\pi}{n}\right)$-isosceles triangles that are the focus of this thesis actually satisfy a stronger version of the Veech property that that we will call the *strong Veech property for triangles*.

Definition 2.2.0.1 (Strong Veech Property for Triangles)**.** *A triangle whose reflections induce a translation surface* S *will be called be* strongly Veech *or said to be Veech in the stronger sense if the translation surface* (S,Σ) *is Veech even when* Σ *includes, in addition to the singular points of* S*, all points on* S *that correspond to vertices of the triangle.*

Proposition 2.2.0.1. *The Veech group of the regular* $2n$*-gon surface and the Veech group of the* $\left(\frac{\pi}{n}\right)$*-isosceles triangle surface (with a marked point corresponding to the triangle's apex) coincide.*

Proposition 2.2.0.1 was proven by Vorobets [89] (Propositions 4.2 and 4.3).

When n is even, the Veech group of both the regular n-gon surface and centrally punctured regular n-gon surface are generated by the rotation $\mathrm{r}_{\frac{2\pi}{n}}$ by $\frac{2\pi}{n}$, the shear $\mathrm{H}_n^+ = \begin{pmatrix} 1 & 2\cot\frac{\pi}{2n} \\ 0 & 1 \end{pmatrix}$ and the orientation-reversing reflection r_v through the vertical direction. When n is odd, the shear H_n^+ is the derivative of an affine automorphism of the regular n-gon surface, but *not* of the centrally-punctured regular n-gon surface: the marked central puncture on the surface is not mapped back to itself by the affine transformation with derivative H_n^+ (see Chapter 6).

In the cases treated here, the kernel of the Veech homomorphism $\mathrm{D} : \mathrm{A}((\mathsf{S}, \Sigma)) \mapsto GL(2, \mathbb{R})$ is trivial [76]. Thus, the automorphism with a given derivative is unique and we adopt the following convention.

Notational Convention. *To reduce notational overhead, we will sometimes use the same notation for a given affine automorphism and its derivative. For example, the notation* H_n^+ *above has been explicitly defined as a linear transformation. Consistent with this definition, when considered as an element of the Veech group of the* $2n$*-gon surface,* H_n^+ *will be exactly as originally defined. However, when the text explicitly refers to* H_n^+ *as an "affine automorphism," then* H_n^+ *denotes the actual affine automorphism whose derivative is* H_n^+.

Every direction on a Veech surface is either parabolic or is shortened by a parabolic element of the Veech group [89]. This feature of Veech surfaces makes them particularly amenable to renormalization. In the work reported here the

parabolic element H_n^- plays a central role.

2.3 Combinatorial renormalization in genus one

2.3.1 Cutting Sequences on the Square Torus

The canonical example of a Veech surface is the square torus. Its Veech group is $SL(2,\mathbb{Z})$, which is a lattice in $SL(2,\mathbb{R})$. Billiard trajectories in a square table can be viewed as geodesics on the torus. Parallel sides of the square billiard table appear as distinct saddle connections on the square torus $\mathbb{T}_\square$ joining the marked point of $\mathbb{T}_\square$ corresponding to the corners of the square to itself. Billiard trajectories that reflect off sides of the square back into its interior correspond to geodesics in $\mathbb{T}_\square$ that "cut" through the corresponding saddle connection on $\mathbb{T}_\square$.

The combinatorial rule that characterizes cutting sequences on the square torus is simple. The closure of the set of cutting sequences on $\mathbb{T}_\square$ consists exactly of the words $\mathrm{w} \in \{A, B\}^{\mathbb{Z}}$ such that:

1. w contains at most one of the subwords $[A\,A]$ or $[B\,B]$
2. For all $n \in \mathbb{N}$, property (1) is retained by each iterate $\mathrm{w}^{(n)}$ of w under the operation that replaces every $[A^k]$ or $[B^k]$, $k \geq 2$ in $\mathrm{w}^{(n-1)}$ ($k \geq 2$) with $[A^{k-1}]$ or $[B^{k-1}]$ in $\mathrm{w}^{(n)}$.

Proving the classical characterization following the presentation of Smillie and Ulcigrai ([76]) is instructive, and presents in a simplified setting many of the tools we use later.

Let $\Sigma_0 = [0, \frac{\pi}{4}]$ and $\mathcal{T}_0 = \{\text{trajectories } \tau \text{ in direction } \theta : \theta \in \Sigma_0\}$. The group D_4 of isometries of the square, where D_4 is the dihedral group with four elements, acts on cutting sequences by permuting letters: reflection in the horizontal and vertical axes preserve the labelings while reflection in the diagonals interchanges A and B. Without loss of generality we can consider only trajectories in $\mathcal{T}_0$ since any trajectory not in $\mathcal{T}_0$ can be sent to one in $\mathcal{T}_0$ by an element of D_4, and application of the permutation $\pi_1 = (A, B)$ to cutting sequences $\boldsymbol{c}(\tau)$ of $\tau \notin \mathcal{T}_0$ produces the cutting sequence of a trajectory $\mathcal{T}_0$.

Definition 2.3.1.1 (Normalization)**.** *Let $\nu \in \mathrm{D}_4$ denote reflection through the angle-$\left(\frac{\pi}{4}\right)$ diagonal in $\mathbb{T}_{\square}$. Whichever of τ or $\nu(\tau)$ is in $\mathcal{T}_0$ is called the* normalization $\mathtt{n}(\tau)$ *of τ.*

It is immediately evident that a cutting sequence $\boldsymbol{c}(\tau)$, $\tau \in \mathcal{T}_0$ cannot have repeating A's. This information is captured in the *transition diagram* $\mathfrak{D}_0$, a directed graph whose vertices are the labeled sides of the square torus. A directed edge joins two vertices v, v' in $\mathfrak{D}_0$ if a trajectory in $\mathcal{T}_0$ can exit side v and hit side v' of the square without crossing another side of the square.

Definition 2.3.1.2. *We will say that a word $\mathrm{w} \in \{A, B\}^{\mathbb{Z}}$ is* admissible *if either w or $\pi_1(\mathrm{w})$ is realizable as an infinite path in $\mathfrak{D}_0$. If $\pi_1(\mathrm{w})$ is realizable in $\mathfrak{D}_0$ then*

$\mathrm{n}(\mathrm{w}) = \pi_1(\mathrm{w})$ *is called the normalization of* w. *When* w *is realizable in* $\mathfrak{D}_0$, *then* $\mathrm{n}(\mathrm{w}) = \mathrm{w}$.

Definition 2.3.1.3. *The* derived sequence $\mathrm{w}' = \mathrm{D}(\mathrm{w})$ *of an admissible word* w *is obtained from* $\mathrm{n}(\mathrm{w})$ *by deleting one* B *from each block of one or more consecutive* B*'s.*

An admissible word w is *infinitely derivable* if $\mathrm{w}^{(n)} = \mathrm{D}^{(n)}(\mathrm{w})$ is admissible for all $n \in \mathbb{N}$.

Proposition 2.3.1.1. *Cutting sequences of billiard trajectories in the square are infinitely derivable.*

Proof (following [76]). This can be proven by showing that for any linear trajectory τ in the square, there is a linear trajectory τ' in the square such that $c(\tau') = (c(\tau))'$. The cutting sequence $\mathrm{w} = c(\tau)$ of a linear trajectory in the square is necessarily admissible and, as indicated before, it can be assumed without loss of generality that $\tau \in \mathcal{T}_0$. We will construct τ' by applying an affine cut-paste-shear diffeomorphism to the union of the square and the original trajectory τ. To track these steps combinatorially, we augment the square with a diagonal edge labeled c, joining its lower left corner to its upper right corner. Note that τ crosses c precisely when it is making a BB transition. So the *augmented cutting sequence* $\widetilde{c}(\tau)$ of τ gains a c between each pair of B's in $c(\tau)$ (Fig. 2.2).

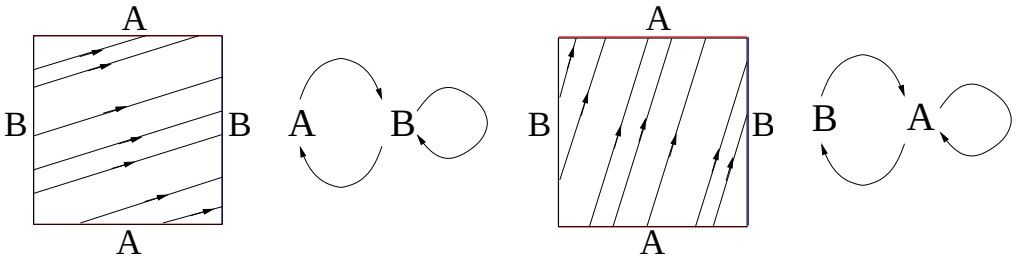

(a) $0 \leq \theta \leq \pi/2$ (b) $\mathscr{D}_0$ (c) $\pi/2 \leq \theta \leq \pi$ (d) $\mathscr{D}_1$

Figure 2.2: Possible transitions in the square. (Figure adapted from [74])

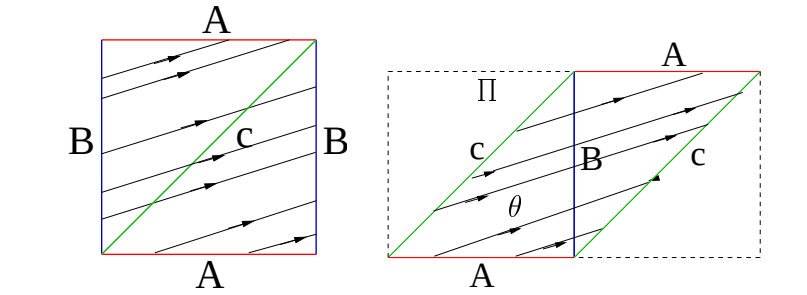

(a) Auxilliary diagonal (b) Parallelogram Π

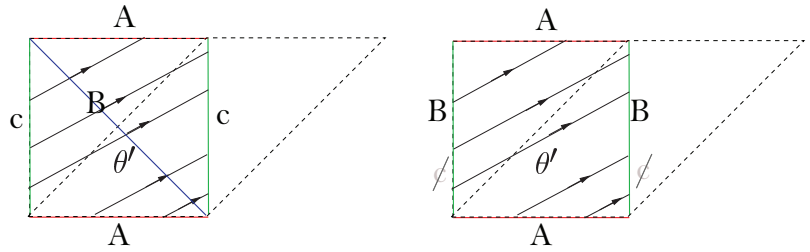

(c) Renormalized flow (d) Relabeling

Figure 2.3: Geometric renormalization of Σ_0 linear trajectories in the square. (Figure adapted from [74])

In the parallelogram Π (Figure 2.3 (b)) produced by cutting the augmented square along c, then gluing edge B to itself, the augmented cutting sequence $\widetilde{c}(\tau)$ is preserved. Application the shear $\mathrm{H} = \begin{pmatrix} -1 & 1 \\ 0 & 1 \end{pmatrix}$ that makes lines in direction $\frac{\pi}{4}$ vertical, sends τ to τ', another linear trajectory in the square torus (Figure 2.3 (c)). Unless τ itself is horizontal, the new trajectory τ' will not be in the same direction as τ; it has augmented cutting sequence $\widetilde{c}(\tau')$ in $\mathrm{H} \cdot \Pi$.

Removing the interior edge of $\mathrm{H} \cdot \Pi$ (Figure 2.3 (d)) and returning to original exterior side labeling has the effect first of dropping all B's in $\widetilde{\boldsymbol{c}}(\tau')$ and then of replacing each c in $\widetilde{\boldsymbol{c}}(\tau')$ with a B. Every c in $\widetilde{\boldsymbol{c}}(\tau')$ was sandwiched between two B's in some block of $j \geq 2$ B's from the original sequence $\boldsymbol{c}(\tau)$, so replacing this block with the $j-1$ sandwiched c's (then recoding those c's as B's again) leaves exactly $j-1$ B's. Singleton B's simply disappear ($ABA \mapsto AA$) and every A in $\boldsymbol{c}(\tau)$ is retained in $\boldsymbol{c}(\tau')$. In other words, $\boldsymbol{c}(\tau') = (\boldsymbol{c}(\tau))'$ according to Definition 2.3.1.3.

□

The converse to Proposition 2.3.1.1 is almost true ([71]):

Proposition 2.3.1.2 (Series)**.** *The set of infinitely deriveable sequences coincides with the closure of the set of cutting sequences on* $\mathbb{T}_{\square}$.

An example of an infinitely deriveable word that is not the cutting sequence of a trajectory in the square is $\mathrm{w} = \ldots B\,B\,A\,B\,B\ldots$, two half-infinite strings of B's joined by a single A. The two half-infinite blocks of B's in w code for semi-infinite horizontal geodesic rays. The subword $[BAB]$ joining the two half-infinite B-blocks in w can only be realized by a non-horizontal geodesic segment. Although w is not a cutting sequence, it is the limit of the sequence of periodic words $\mathrm{w}_n = \overline{A\,\mathrm{B}^n}$.

CHAPTER 3

EXTENDED TREATMENT OF GENUS ONE

3.1 An Alternative Characterization of Cutting Sequences on the Square Torus

This chapter introduces a renormalization strategy that will be used in remainder of the thesis. In the present section we detail a geometric renormalization scheme for square billiards that follows the same steps as our renormalization scheme for billiards in the $(\frac{\pi}{4})$-isosceles triangle. Section 3.2 uses this renormalization to induce a combinatorial renormalization for $(\frac{\pi}{2})$-isosceles hitting sequences coded in letters $\{A, B, L^{\pm}, R^{\pm}\}$ labeling sides of the $(\frac{\pi}{2})$-isosceles triangle. In Section 3.3 we employ this geometric renormalization to obtain a derivation rule for words in the alphabet $\{A, B, L^{\pm}\}$ in direct analogy to the way we will later derive cutting sequences on the centrally-punctured regular $2n$-gon, that correspond to hitting sequences in the $(\frac{\pi}{n})$-isoscles triangle $n \geq 4$. We will use the following terminology from Series [71].

Definition 3.1.0.1. *(Almost Constant Sequences) A word* $\mathrm{w} \in \{A, B\}^{\mathbb{Z}}$ *is* almost constant *if the following two conditions hold for either* w *or* $\pi_1(\mathrm{w}) = (A, B) \cdot \mathrm{w}$*:*

1. *At least one of* w *or* $\pi_1(\mathrm{w}) = (A, B) \cdot \mathrm{w}$ *is realizable as a bi-infinite path through the transition diagram* $\mathscr{D}_0$ *(Figure 2.2 (b)).*

2. *For at least one of* w *or* $\pi_1(\mathrm{w}) = (A, B) \cdot \mathrm{w}$*, there exists* $n \geq 1$ *such that between*

any two A's there are either n or $n+1$ B's.

Note that any infinitely deriveable Σ_0-admissible word is necessarily almost constant. If w is Σ_0-admissible, w satisfies condition (1) above. If in addition w is infinitely deriveable, then there is no $k \in \mathbb{N}$ for which $\mathrm{D}^{(k)}(\mathrm{w})$ contains both $[BB]$ and $[AA]$. This implies that blocks of B's in w cannot differ in length by more than one.

Definition 3.1.0.2. *(Sandwiched letters) The letter w_i in* w $= \ldots w_{i-2}w_{i-1}w_iw_{i+1}w_{i+2}\ldots$ *is said to be* sandwiched *in* w *if $w_{i-1} = w_{i+1}$.*

Proposition 3.1.0.1. *If* w $\in \{A, B\}^Z$ *is the cutting sequence of a linear trajectory on the torus, then:*

1. w *is* almost constant.
2. *For all $n \in \mathbb{N}$, property (1) is retained by each iterate* $\mathrm{w}^{(n)}$ *of* w *under the operation that retains in* $\mathrm{w}^{(n)}$ *only the letters that are sandwiched in* $\mathrm{w}^{(n-1)}$.

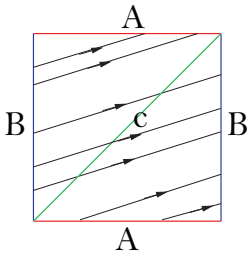

(a) Auxilliary diagonal

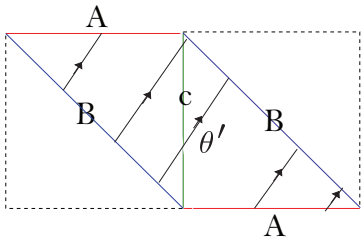

(b) Shear square and trajectory into parallelogram

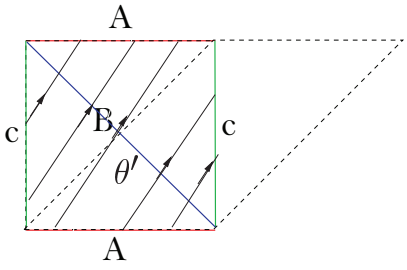

(c) Cut parallelogram along diagonal and paste into square shape

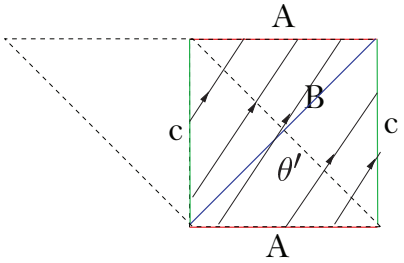

(d) Reflect square about central vertical axis

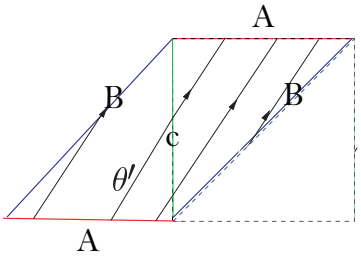

(e) Cut square along diagonal and paste into parallelogram.

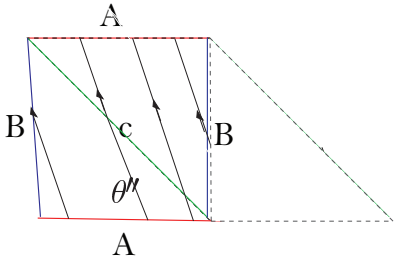

(f) Shear paralleogram and trajectory back into square shape.

Figure 3.1: Alternative renormalization of Σ_0 linear trajectories in the square. (Figure adapted from [74])

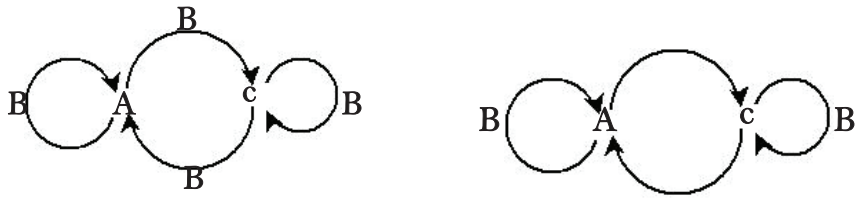

(a) Original transitions, $\mathscr{D}_0$

(b) Transitions after renormalization, $\mathscr{D}_1$

Figure 3.2: Possible transitions of original Σ_0 trajectories (a) and renormalized Σ_0 trajectories in "almost dual " form: horizontal and auxiliary edge are vertices, remaining exterior polygon edge(s) label directed graph edges.

For this section, we will re-use vocabulary from the previous section but slightly alter the definitions:

Definition 3.1.0.3. *Let π_1 be the permutation that interchanges A and B. A word* $\mathrm{w} \in \{A, B\}^{\mathbb{Z}}$ *is called* admissible *if either* w *or* $\pi_1(\mathrm{w}) = (AB) \cdot \mathrm{w}$ *is almost constant (Definition 3.1.0.1). If* $\pi_1(\mathrm{w})$ *is realizable in* $\mathfrak{D}_0$ *then* $\mathrm{n}(\mathrm{w}) = \pi_1(\mathrm{w})$ *is called the normalization of* w*. When* w *is realizable in* $\mathfrak{D}_0$*, then* $\mathrm{w} = \mathrm{n}(\mathrm{w})$.

Proposition 3.1.0.2. *Cutting sequences are admissible. Equivalently, the normalization of a cutting sequence is almost constant.*

Proof. If $\mathrm{w} = c(\tau)$ is the cutting sequence of a linear trajectory τ then by the contruction of $\mathfrak{D}_0$ either w or $\pi_1(\mathrm{w})$ is realizable in $\mathfrak{D}_0$ and the first condition of Definition 3.1.0.1 is satisfied. We now check that $\mathrm{w} = c(\tau)$ satisfies the second condition of Definition 3.1.0.1. Assume that $\mathrm{w} = c(\tau)$ is the cutting sequence of a normalized linear trajectory τ on the torus. Let $m \in [0, 1]$ be the slope of τ, set $\mu = m^{-1}$ to be the the inverse slope of τ and let $n = \lfloor \mu \rfloor$ denote the integer

part of μ (Figure 3.3). Let $\overline{\tau}$ be the segment of τ in $\mathbb{R}^2$ with one endpoint v_0 in the x-axis interval $[0, 1]$ and the other endpoint on $y = 1$. Projecting $\overline{\tau}$ onto the x-axis gives the interval $I_\mu = [v_0, v_0 + \mu]$, where:

$$n \leq v_0 + n \leq \mathrm{v}_0 + \mu < v_0 + (n+1) \leq n + 2$$

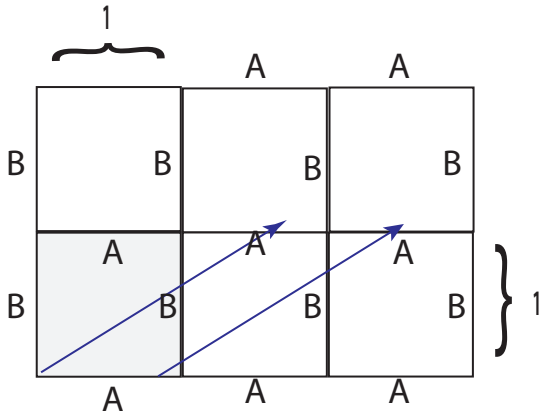

Figure 3.3: Line of slope $m \in [0, 1]$ can hit the vertical side of $\mathbb{T}_\square$ either $n = \lfloor m^{-1} \rfloor$ or $n + 1$ times between intersections with the horizontal side of $\mathbb{T}_\square$.

□

Definition 3.1.0.4. *The* derived sequence $\mathrm{w}' = \mathrm{D}(\mathrm{w})$ *of an admissible word* w *is obtained from* $\mathrm{n}(\mathrm{w})$ *by deleting the first and last* B *from each block of two or more consecutive* B*'s.*

Proposition 3.1.0.3. *Cutting sequences of billiard trajectories in the square are derivable, and the derived sequence of a cutting sequence is also a cutting sequence.*

Proof. Let $\mathrm{H}^+ = \begin{pmatrix} 1 & 2\cot(\frac{\pi}{4}) \\ 0 & 1 \end{pmatrix}$ be the horizontal shear in $\mathrm{V}^+(\mathbb{T}_\square)$, $r_v = \begin{pmatrix} -1 & 0 \\ 0 & 1 \end{pmatrix}$ be the vertical reflection in $\mathrm{V}^-(\mathrm{S}_{\mathbb{T}_\square})$ and $\mathrm{H}^- = \begin{pmatrix} -1 & 2\cot(\frac{\pi}{4}) \\ 0 & 1 \end{pmatrix} = \mathrm{H}^+ r_v$ in $\mathrm{V}^-(\mathbb{T}_\square)$. The linear transformation $\mathrm{h} = \begin{pmatrix} -1 & \cot(\frac{\pi}{4}) \\ 0 & 1 \end{pmatrix}$ that makes angle-$\left(\frac{\pi}{4}\right)$ vectors vertical (Figure 3.1 (b)) is *not* in $\mathrm{V} = \mathrm{V}^+(\mathbb{T}_\square) \cup \mathrm{V}^-(\mathbb{T}_\square)$. Let κ_1 be the cut-and-paste map shown in Figure 3.1 (c) and κ_2 the cut-and-paste map shown in Figure 3.1 (e). The effect of the affine automorphism $\Psi_{\mathbb{T}_\square} = \mathrm{h}^{-1} \circ \kappa_2 \circ r_v \circ \kappa_1 \circ \mathrm{h}$ on $\mathbb{T}_\square$ is illustrated in Figure 3.1 (b) through (e). $\Psi_{\mathbb{T}_\square}$ is an orientation-reversing affine automorphism of $\mathbb{T}_\square$ with derivative $\mathrm{H}^- \in \mathrm{V}(\mathbb{T}_\square)$. Moreoever, $\Psi_{\mathbb{T}_\square}$ is conjugate by the linear transformation h to the orientation-reversing isometry with derivative $r_v \in \mathrm{V}(\mathbb{T}_\square)$. Affine automorphisms of a translation surface that are conjugate to isometries by elements of $SL(2,\mathbb{R})$ that are *not* derivatives affine automorphisms are called *hidden symmetries* of the surface. They are discussed again in Section 4. The effect of $\Psi_{\mathbb{T}_\square}$ on $\mathbb{T}_\square$ is to horizontally shear by $2\cot(\frac{\pi}{4})$ though a reflection of $\mathbb{T}_\square$ about its central vertical axis. (Figure 3.4). As an affine automorphism of $\mathbb{T}_\square$, $\Psi_{\mathbb{T}_\square}$ sends linear trajectories in $\mathbb{T}_\square$ to linear trajectories.

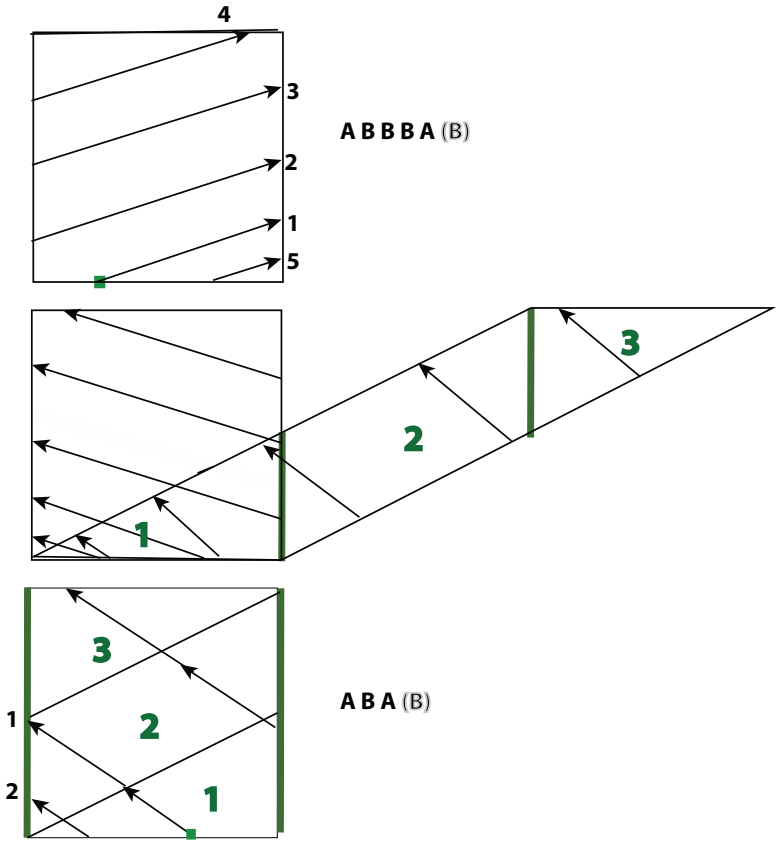

Figure 3.4: Top: A Σ_0 trajectory segment τ starting at the green dot and bouncing off sides in the order indicated by small black numbers. Cutting sequence w of τ in black letters to the right. Middle: Shearing the through the reflection of the top figure about its central vertical axis (left), then sheared by H^+ (right). Bottom: Cutting the sheared torus along vertical green lines and translating pieces back into the square. The trajectory segment in this figure is the renormalization τ' of τ. The cutting sequnce w′ of τ' is in black letters to the right. In w′ the only the sandwiched letters in w are retained.

Now assume that $\tau \in \mathcal{T}_0$ is a linear trajectory in $\mathbb{T}_\square$ and $\tau' = \Psi_{\mathbb{T}_\square}(\tau)$. By Proposition 3.1.0.2, $w = c(\tau)$ is admissible. Let p be the path that realizes w in $\mathscr{D}_0$. In the first two transformations illustrated in Figure 3.1 (b,c), the cutting sequence of the transformed trajectory is still $w = c(\tau)$. One can check that the cutting sequence $c(\tau_3)$ of the image τ_3 of τ following the third transformation (Figure 3.1, d) can be realized by following the path p through the transition diagram $\mathscr{D}_1$ (Figure 3.2, b). Call this new sequence $w' = c(\tau_3)$. No other changes

to the cutting sequence occur in subsequent steps of Figure 3.1, so $\mathrm{w}' = c(\tau')$ proving the proposition.

□

An admissible word w is *infinitely derivable* if $\mathrm{w}^{(n)} = \mathrm{D}^{(n)}(\mathrm{w})$ is admissible for all $n \in \mathbb{N}$.

Corollary 3.1.0.4. *Cutting sequences of billiard trajectories in the square are infinitely deriveable.*

Theorem 3.1.0.5. *The set of infinitely deriveable sequences is the closure of the set of torus cutting sequences.*

Proof. We have already shown (Proposition 2.3.1.2) that the set of *classically* (Definition 2.3.1.3) infinitely deriveable words in $\{A, B\}^Z$ is the closure of the set of torus cutting sequences. So here it suffices to show that there is a 1-to-1 correspondence between the set of *classically* infinitely deriveable sequences and *alternative-sense* infinitely deriveable sequences (Definition 3.1.0.4). Let D_c be the derivation from Definition 2.3.1.3 and D_a the derivation from Definition 3.1.0.4. Let $\mathrm{w} \in \{A, B\}^{\mathbb{Z}}$ be a word in which every A is isolated and B's appear in blocks of length n or $n+1$, i.e. w is what Series [71] calls an *almost constant* (Defintion 3.1.0.1) sequence. The classical derivation rule D_c gives the following transformation of sequences:

$$[A\underbrace{BB...B}_{k}] \mapsto [A\underbrace{BB...B}_{k-1}], \;\; k \geq 1$$

While the alternative rule D_a operates on sequences as indicated below:

$$[A\underbrace{BB...B}_{k}] \mapsto [A\underbrace{BB...B}_{k-2}], \;\; k \geq 2$$

So for fixed *almost constant* $\mathrm{w} \in \{A, B\}^{\mathbb{Z}}$, we can send $\mathrm{D}_a(\mathrm{w})$ to $\mathrm{D}_c(\mathrm{w})$ by applying D_a^c:

$$[ABA] \mapsto [AA] \text{ and}$$
$$[A\underbrace{BB...B}_{k}A] \mapsto [A\underbrace{BB...B}_{k+1}A], \;\; k = 0 \text{ and } k \geq 2$$

And we can obtain $\mathrm{D}_a(\mathrm{w})$ from $\mathrm{D}_c(\mathrm{w})$ by applying D_c^a:

$$[ABA] \mapsto [AA] \text{ and}$$
$$[A\underbrace{BB...B}_{k}A] \mapsto [A\underbrace{BB...B}_{k+1}A], \;\; k = 0 \text{ and } k \geq 2$$

Example 3.1.0.1. *Let* $\mathrm{w} = ...ABABABABBABBABBABBABABABABA....$

w =	... A B A B A B A B B A B B A B B A B B A B A B A B A B A ...
$D_c(\mathrm{w})$ =	... A A A A B A B A B A B A A A A A ...
$D_a(\mathrm{w})$ =	... A B A B A B A A A A A B A B A B A B A ...

Table 3.1:

□

For any almost constant word w there exist unique almost constant words v and u such that $\mathrm{D}_a^c(\mathrm{v}) = \mathrm{w}$ and $\mathrm{D}_c^a(\mathrm{u}) = \mathrm{w}$. The word v is the unique word that contains an $[ABA]$ wherever w has $[AA]$ and that contains, for $k = 0$ or any $k \geq 2$, the subword $[AB^kA]$ wherever w has the subword $[AB^{k+1}A]$. Similarly, u is the unique word that contains $[AA]$ where w has $[ABA]$ and that contains, for $k = 0$ or any $k \geq 2$, the subword $[AB^{k+1}A]$ where w has the subword $[AB^kA]$. One can check that if w is almost constant, then v and u are as well. This 1-to-1 correspondence suffices to prove the proposition.

3.2 Hitting Sequences in the $\left(\frac{\pi}{2}\right)$-Isosceles Triangle

Our initial approach the problem of characterizing $\left(\frac{\pi}{2}\right)$-isosceles triangle hitting sequences considers all edges in the $\left(\frac{\pi}{2}\right)$-isosceles triangle's reflected cover of the *centrally punctured* square $\mathbb{T}^{\odot}_{\square}$ (Figure 3.5). The geometric renormalization procedure for billiards in the square torus described in Section 3.1 is employed here without alteration: apply the affine automorphism $\Psi_{\mathbb{T}_{\square}}$ from Section 3.1 to $\mathbb{T}^{\odot}_{\square}$ tiled by four reflected copies of the $\left(\frac{\pi}{2}\right)$-isosceles triangle (Figure 3.5). The centerpoint is mapped back to itself under $\Psi_{\mathbb{T}_{\square}}$ so the operation $\Psi_{\mathbb{T}_{\square}}$ is an automorphism of $\mathbb{T}^{\odot}_{\square}$. In this setting however, the application of $\Psi_{\mathbb{T}_{\square}}$ has different combinatorial consequences.

In the unpunctured square torus, we say a sequence $\mathrm{w} \in \{A, B\}^{\mathbb{Z}}$ is admissible if either w or $\pi_1(\mathrm{w})$ can be realized as an infinite path through the one-step transition diagram $\mathfrak{D}_0$. Incorporating interior triangle sides breaks some

H

$$\begin{aligned}
\pi_1 =&(AB)(R^-R^+)\\
\pi_2 =&(AB)(R^-L^+R^+L^-)\\
\pi_3 =&(L^-R^-)(L^+R^+)\\
\pi_4 =&(R^-R^+)(L^-L^+)\\
\pi_5 =&(AB)(L^+L^-)\\
\pi_6 =&(AB)(R^-L^-R^+L^+)\\
\pi_7 =&(R^-L^+)(R^+L^-)
\end{aligned}$$

Table 3.2: The permutation π_k of $\{A, B, L^{\pm}, R^{\pm}\}$ maps edge and vertex labels of $\mathfrak{D}_k$ to those of $\mathfrak{D}_0$.

combinatorial symmetry. Specifically, the combinatorial transitions that can be realized by a given trajectory in forward and backward time are no longer identical. Transition diagrams $\mathfrak{D}_k$ for trajectories in angular sectors $\Sigma_k = [\frac{k\pi}{4}, \frac{(k+1)\pi}{4}]$, $k = 1, 2, ..., 7$ are obtained by relabeling $\mathfrak{D}_0$ and $\mathfrak{D}_0^*$ according to the permutations π_k:

It will be convenient to look at this coding alphabet as a disjoint union of exterior polygon sides $\mathscr{B} = \{A, B\}$ and interior triangle sides $\overline{\mathscr{B}} = \{L^-, R^-, L^+, R^+\}$ (Figure 3.5). For a word $\mathrm{w} \in \left(\mathscr{B} \cup \overline{\mathscr{B}}\right)^{\mathbb{Z}}$, we let $\mathrm{w}\Big|_{\mathscr{B}}$ and $\mathrm{w}\Big|_{\overline{\mathscr{B}}}$ denote the restrictions of w to $\mathscr{B}$ and $\overline{\mathscr{B}}$ respectively. The property most analogous to *admissibility* in the square torus we now call *weak admissibility*.

Definition 3.2.0.1. *We say a sequence* $\mathrm{w} \in \{A, B, L^{\pm}, R^{\pm}\}$ *is* weakly admissible *if* $\mathrm{w}\Big|_{\mathscr{B}}$ *is almost constant (Definition 3.1.0.1)* and *either* w *or* $\pi_i^{-1}(\mathrm{w})$ *is realizable as an infinite path through* $\mathfrak{D}_0$. *If* $\pi_i(\mathrm{w})$ *is realizable in* $\mathfrak{D}_0$ *then* $\mathrm{n}(\mathrm{w}) = \pi_i(\mathrm{w})$ *is a* normalization *of* w.

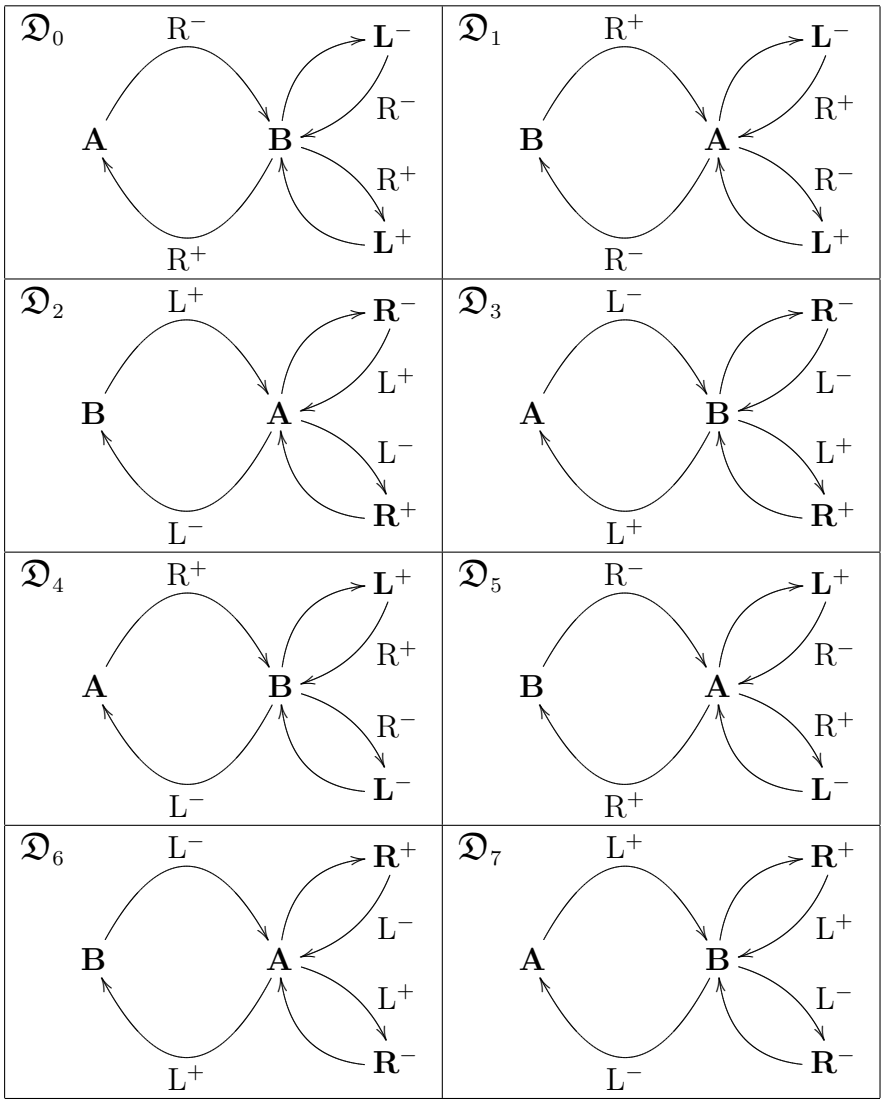

Table 3.3: All One-Step Transition Diagrams for the $\left(\frac{\pi}{2}\right)$-Isosceles Triangle-Tiled Square

One distinction between the classical square torus and the case we present here is the existence of a subword realizable in the one-step transition diagram $\mathfrak{D}_0$ that clearly cannot be realized as part of the cutting sequence of a linear trajectory $\tau \in \mathcal{T}_0$. Specifically, the subword $\mathfrak{u} = [L^+BL^-]$ cannot be realized by a trajectory with slope in $[0, \frac{\pi}{4}]$. The "almost dual" diagram $\mathfrak{D}_0^*$ (Table 3.4) whose vertices are labeled by horizontal and tipped edges of the $\left(\frac{\pi}{2}\right)$-isosceles tiled square admits fewer subwords than $\mathfrak{D}_0$. Every subword of length 3 arising

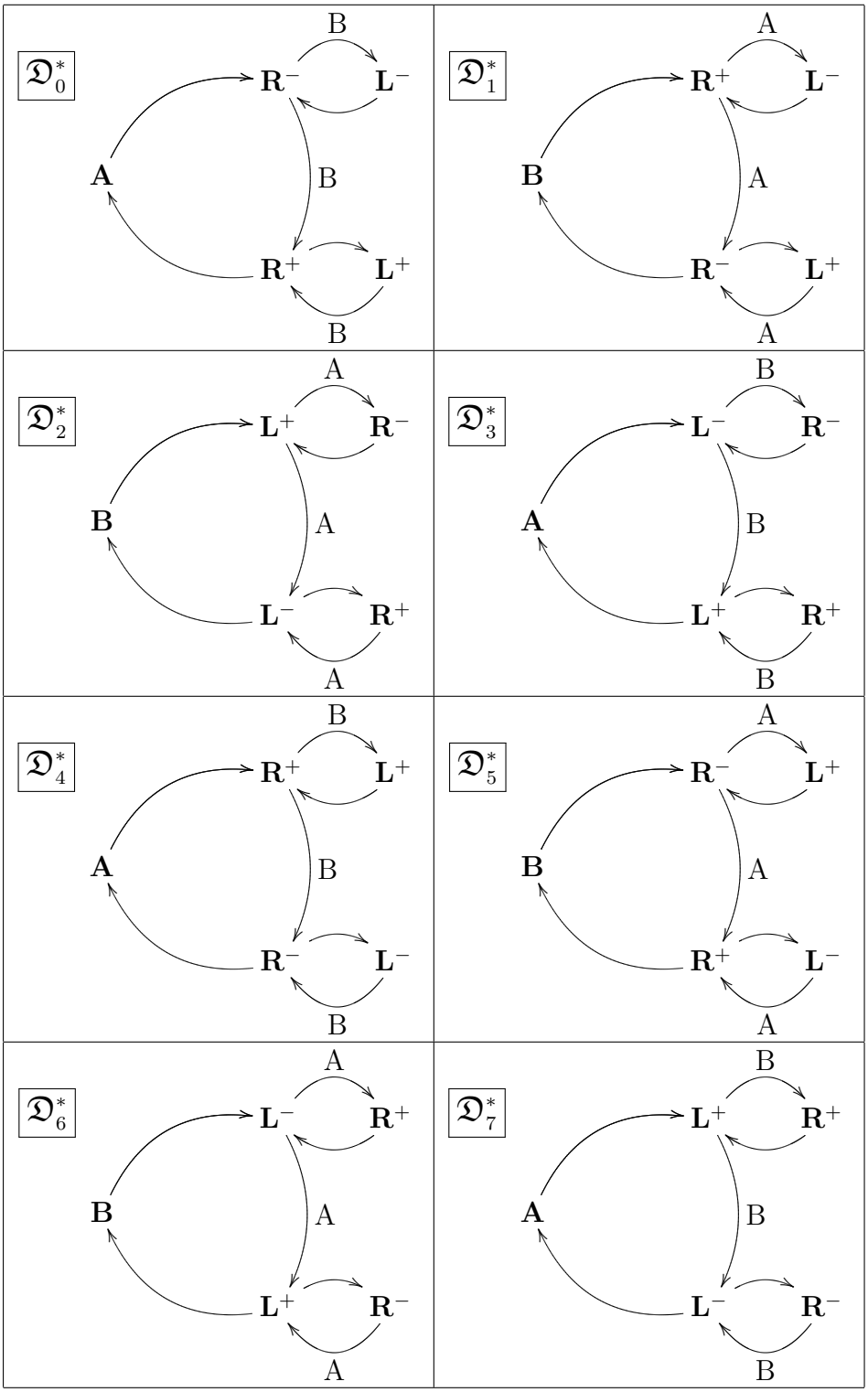

Table 3.4: All Nearly-Dual Transition Diagrams for the $\left(\frac{\pi}{2}\right)$-Isosceles Triangle-Tiled Square

from a path through $\mathfrak{D}_0^*$ can be realized by a linear trajectory segment with angle $\theta \in [0, \frac{\pi}{4}]$. Weakly admissible words not containing u are admissible.

Definition 3.2.0.2. *A weakly admissible word* w *with normalization* n(w) *is* admissible *if* n(w) *is realizable in* $\mathfrak{D}_0^*$.

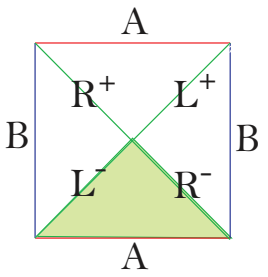

(a) Centrally Punctured Square from $(\frac{\pi}{2})$-Isosceles Triangle

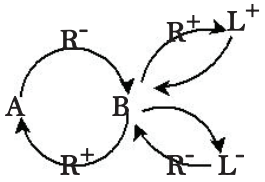

(b) One-Step Transition Diagram $\mathfrak{D}_0$ for $0 \leq \theta \leq \frac{\pi}{2}$

Figure 3.5

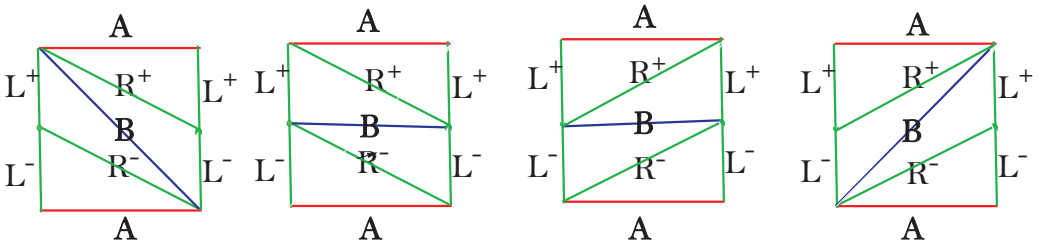

(a) Stage 0. Cut and paste along diagonal, then shear back to square shape.

(b) Stage 1. Flip main diagonal.

(c) Stage 2. Reflect about central vertical axis.

(d) Stage 3. Flip main diagonal again.

Figure 3.6

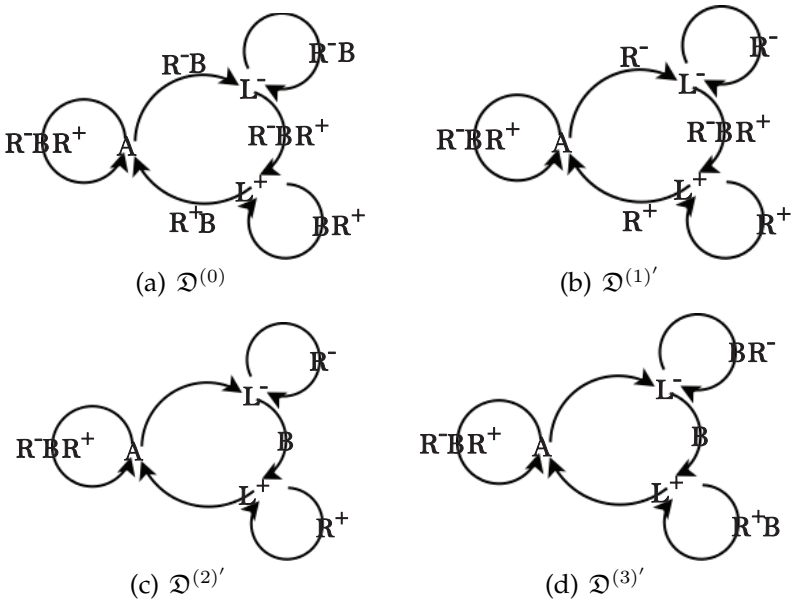

Figure 3.7: Possible transitions of renormalized Σ_0 trajectories, in "almost dual" form: horizontal and vertical edges of Figure 3.6 (a) are vertices, remaining edge(s) in Figure 3.6 (a) label directed graph edges

Proposition 3.2.0.1. *The "almost dual" transition diagram $\mathfrak{D}_0^*$ realizes exactly the same words as the transition diagram $\mathfrak{D}^{(0)}$ (Figure 3.7).*

Proof. The transformation shown in Figure 3.6 (a), in which we first cut and paste along the diagonal of Figure 3.5 (a) and then shear back to a square shape, sends each linear trajectory $\tau \in \Sigma_0$ to a linear trajectory τ' in $\Sigma_0' = [0, \frac{\pi}{2}]$. The intersections between trajectories and edges in Figure 3.5 (a) are preserved under this transformation, so $c(\tau) = c(\tau')$. Thus. it suffices to check that that $\mathfrak{D}^{(0)}$ realizes all two-step transitions possible for Σ_0' trajectories in Figure 3.6 (a).

□

The effect of this geometric renormalization on cutting sequences $w \in \left(\mathscr{B} \cup \overline{\mathscr{B}}\right)^{\mathbb{Z}}$ is to:

1. drop every B that is not sandwiched between either two A's or two B's in $\mathrm{w}\big|_{\mathscr{B}}$,

2. drop every R that is not sandwiched between two L's or two R's in $\mathrm{w}\big|_{\overline{\mathscr{B}}}$,

3. (*3-letter subword swap*) replace every occurance of $[LRB]$ with $[LBR]$, and every occurence of $[BRL]$ with $[RBL]$.

Definition 3.2.0.3. *The* derived sequence $\mathrm{w}' = \mathrm{D}(\mathrm{w})$ *of an admissible word* w *is obtained from* $\mathrm{n}(\mathrm{w})$ *by deleting the first and last* B *from each block of two or more consecutive* B*'s in* $\mathrm{w}\big|_{\mathscr{B}}$*, and every* R *that is not sandwiched between two* L*'s or two* R*'s in* $\mathrm{w}_{\overline{\mathscr{B}}}$*, then performing the subword swap (point 3. above).*

Example 3.2.0.1. *Suppose*

$$\mathrm{w} = ...AR^{-}BL^{-}R^{-}BL^{-}R^{-}BL^{-}R^{-}BR^{+}L^{+}BR^{+}L^{+}BR^{+}L^{+}BR^{+}A...$$

encodes part of a linear trajectory $\tau \in \mathcal{T}_0$ *in the* $\left(\frac{\pi}{2}\right)$*-isosceles-tiled centrally punctured square. Since* w *is admissible, it is realizable by a path* p $\mathfrak{D}^{(0)}$*. The effect of tracking* p *through transition diagrams* $\mathfrak{D}^{(0)}$*,* $\mathfrak{D}^{(1)'}$*,* $\mathfrak{D}^{(2)'}$*, and* $\mathfrak{D}^{(3)'}$ *(Figure 3.7) successively are shown in Table 3.5. The derived sequence* w′ *of* w *is given in the last row of Table 3.5. It is the word obtained by taking the path* p *through* $\mathfrak{D}^{(3)}$

Start	A	R^-	$\boldsymbol{B}$	L^-		R^-	$\boldsymbol{B}$	L^-		R^-	$\boldsymbol{B}$	L^-	R^-	$\underline{\boldsymbol{B}}$	R^+	L^+	$\boldsymbol{B}$	R^+		L^+	$\boldsymbol{B}$	R^+		L^+	$\boldsymbol{B}$	R^+	A
Step 1	A	R^-		L^-		R^-		L^-		R^-		L^-	R^-	$\underline{\boldsymbol{B}}$	R^+	L^+		R^+		L^+		R^+		L^+		R^+	A
Step 2	A			L^-		R^-		L^-		R^-		L^-		$\underline{\boldsymbol{B}}$		L^+		R^+		L^+		R^+		L^+			A
Final	A			L^-	$\boldsymbol{B}$	R^-		L^-	$\boldsymbol{B}$	R^-		L^-		$\underline{\boldsymbol{B}}$		L^+		R^+	$\boldsymbol{B}$	L^+		R^+	$\boldsymbol{B}$	L^+			A

Table 3.5

An admissible word w is *infinitely derivable* if $\mathrm{w}^{(n)} = \mathrm{D}^{(n)}(\mathrm{w})$ is admissible for all $n \in \mathbb{N}$.

Proposition 3.2.0.2. *Cutting sequences of linear trajectories in the $\left(\frac{\pi}{2}\right)$-isosceles tiled square are infinitely deriveable.*

The proof of Proposition 3.2.0.2 follows the same strategy as the proof of Proposition 2.3.1.1. If $\mathrm{w} = c(\tau)$ is the cutting sequence of a linear trajectory τ on the $\left(\frac{\pi}{2}\right)$-isosceles tiled square, then $\mathtt{n}(\mathrm{w})$ exists and is realizable in the "almost dual" Σ_0 transition diagram $\mathfrak{D}_0^*$ (Figure 3.4 (a)). By Proposition 3.2.0.1, $\mathfrak{D}^{(0)}$ realizes the same words as $\mathfrak{D}_0^*$. Thus $\mathtt{n}(\mathrm{w})$ can be realized by a path $\mathtt{p}$ through $\mathfrak{D}^{(0)'}$. The derived sequence w′ of w is obtained by tracing the path $\mathtt{p}$ through $\mathfrak{D}^{(3)'}$ (Figure 3.7 (d)). The word w′ is the cutting sequence of the trajectory $\tau_{(3)}$ that results from applying the affine automorphism illustrated in Figure 3.6 (a) through (d) to the isosceles-tiled square.

It is not hard to see that, restricted to just exterior square sides $\{A, B\}$, this process amounts to dropping the first and last B in any B-block of length greater

than 2. So, in its restriction to the smaller alphabet, this operation has exactly the combinatorial effect of performing this geometric renormalization procedure from Section 3.1 on trajectories in the square torus. Also note that the geometric renormaliation process has no effect on trajectory crossings of the two interior triangle edges in direction $\frac{\pi}{4}$; as a result, every L^+ and L^- in a cutting sequence w is retained in the derived sequence w′ (Figure 3.7). Specifically, geometric renormalization of trajectories preserves *all* crossings of edges that are either vertical or horizontal under $\kappa_1 \cdot$ h (see Figure 3.9).

It is also clear that the letters L^- and L^+ suffice to encode the passage of a trajectory $\tau \in \mathcal{T}_0$ under (resp. over) the centerpoint of the $\mathbb{T}^{\odot}_{\square}$. Our treatment of the $\left(\frac{\pi}{n}\right)$-isosceles triangles use two parallel interior segments joining the marked $2n$-gon centerpoint to exterior $2n$-gon vertices. We now apply this approach to the simpler $\left(\frac{\pi}{2}\right)$-isosceles case below.

3.3 Cutting Sequences in the $\left(\frac{\pi}{2}\right)$-Isosceles Triangle: Working in the Centrally-Punctured Square

The fundamenal difference between the coding of linear trajectories on square torus and on the $\left(\frac{\pi}{2}\right)$-isosceles triangle is the requirement, in the latter case, that we capture trajectory behavior relative to the marked centerpoint. Applying $\Psi_{\mathbb{T}_{\square}}$ (Figures 3.8, 3.9 and 3.10) gives the geometric renormalization familiar from Figure 3.1 in Section 3. Symmetries now give transition diagrams $\mathfrak{D}_k$, $\mathfrak{D}_k^*$ for trajectories with angles in sectors $\Sigma_k = [\frac{k\pi}{4}, \frac{(k+1)\pi}{4}]$ by label permutations π_k:

$$\pi_1 = (AB)$$

$$\pi_2 = (AB)(L^- L^+)$$

$$\pi_3 = id$$

$$\pi_4 = (L^- L^+)$$

$$\pi_5 = (AB)(L^- L^+)$$

$$\pi_6 = (AB)$$

$$\pi_7 = (L^- L^+)$$

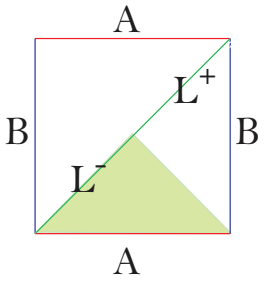

(a) Centrally Punctured Square from $(\frac{\pi}{2})$-Isosceles Triangle

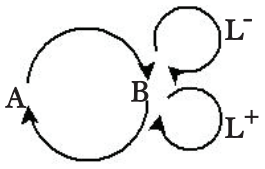

(b) One-Step Transition Diagram for $0 \leq \theta \leq \frac{\pi}{4}$

Figure 3.8

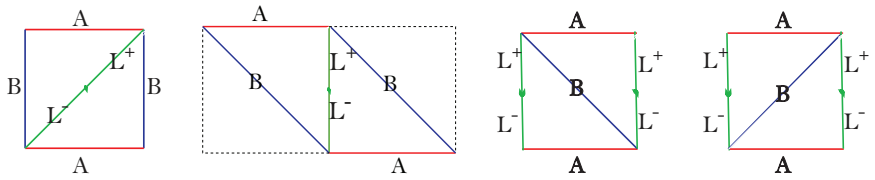

(a) Stage 0.00 Two copies of triangle leg along diagonal

(b) Stage 0.0 Sheared parallelogram ($0 \leq \theta' \leq \frac{\pi}{2}$)

(c) Stage 0. Cut along diagonal and paste back to square shape.

(d) Stage 1. Reflect about central vertical axis.

Figure 3.9

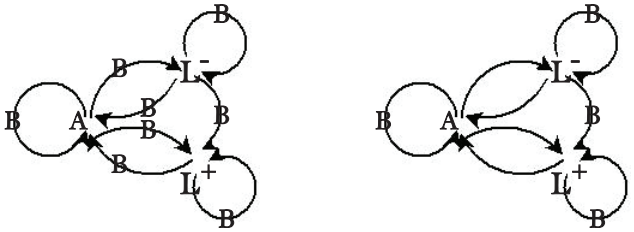

(a) $\mathfrak{D}^{(0)}$

(b) $\mathfrak{D}^{(1)'}$

Figure 3.10: Possible transitions of renormalized Σ_0 trajectories, in "almost dual" form: horizontal and interior triangle edges are vertices, remaining exterior polygon edge(s) label directed graph edges

Weakly admissible sequences defined here as they were in Section 3.1. They are words whose restrictions to $\mathscr{B}$ are almost constant and whose normalizations $\pi_i(\mathrm{w}) = \mathrm{n}(\mathrm{w})$ exist (i.e., are realizable in the one-step transition diagram $\mathfrak{D}_0$). Admissible sequences have normalizations realizable in the 'nearly dual' transition diagram $\mathfrak{D}_0^*$. Sub-alphabets $\mathscr{B} = \{A, B\}$, $\overline{\mathscr{B}} = \{L^{\pm}\}$ of exterior and interior edges are again useful here.

The intersections of a linear trajectories $\tau \in \mathcal{T}_0$ with interior triangle sides labeled by L^+ and L^- are invariant under $\Psi_{\mathbb{T}_\square}$ (examine Figure 3.9). Thus, the L^+'s and L^-'s that appear in the cutting sequence of τ are retained in the cutting sequence of the renormalized trajectory τ'. Differences between the cutting

sequence of τ and the cutting sequence of its renormalization $\tau' = \Psi_{\mathbb{T}_\square} \cdot \tau$ occur only over the subalphabet $\mathscr{B} = \{A, B\}$.

Definition 3.3.0.1. *The* derived sequence $\mathrm{w}' = \mathrm{D}(\mathrm{w})$ *of an admissible word* w *is obtained from* $\mathrm{n}(\mathrm{w})$ *by deleting the first and last* B *from each block of two or more consecutive* B*'s in* $\mathrm{w}\big|_{\mathscr{B}}$.

Example 3.3.0.1. *The derived sequence of:*

$$\mathrm{w} = ...ABL^-BL^-BL^-BL^+BL^+BL^+BA...$$

from Example 3.2.0.1 in this setting is given in Table 3.6.

Start	A		$\boldsymbol{B}$	L^-		$\boldsymbol{B}$	L^-		$\boldsymbol{B}$	L^-		$\underline{\boldsymbol{B}}$	L^+	$\boldsymbol{B}$		L^+	$\boldsymbol{B}$		L^+	$\boldsymbol{B}$		A
Final	A			L^-	$\boldsymbol{B}$		L^-	$\boldsymbol{B}$		L^-		$\underline{\boldsymbol{B}}$	L^+		$\boldsymbol{B}$	L^+		$\boldsymbol{B}$	L^+			A

Table 3.6

An admissible word w is *infinitely derivable* if $\mathrm{w}^{(n)} = \mathrm{D}^{(n)}(\mathrm{w})$ is admissible for all $n \in \mathbb{N}$. Furthermore:

Proposition 3.3.0.1. *Cutting sequences* $\mathrm{w} \in \{A, B, L^{\pm}\}^{\mathbb{Z}}$ *of linear trajectories in* $\mathbb{T}^{\odot}_{\square}$ *are infinitely deriveable.*

The proof of the Proposition follows the same strategy as the the proof of Proposition 2.3.1.1. If w is the cutting sequence of a linear trajectory on the centrally-punctured square, then $\mathrm{n}(\mathrm{w})$ exists and is realizable by a path p though

the "almost dual" Σ_0 transition diagram $\mathfrak{D}^{(0)}$ (Figure 3.10 (a)). The derived sequence w' of w is obtained by tracing the path p through $\mathfrak{D}^{(1)'}$ (Figure 3.10 (b)).

CHAPTER 4

GENUS TWO: THE $\left(\frac{\pi}{4}\right)$-ISOSCELES TRIANGLE

Our approach to the problem of characterizing billiard trajectory cutting sequences on the $\left(\frac{\pi}{4}\right)$-isosceles triangle utilizes techniques introduced in Section 3.3. These techniques use exploit the fact that the $\left(\frac{\pi}{4}\right)$-isosceles triangle unfolds into a centrally punctured regular octagon $\mathcal{O}^{\odot}$, which closes up under side-identifications into a surface $S_{\mathcal{O}}^{\odot}$ with the the same Veech group as $S_{\mathcal{O}}$. In $S_{\mathcal{O}}^{\odot}$ reflected isosceles triangle legs are among the boundary segments of cylinders in parabolic direction $\frac{\pi}{8}$ (Figure 4.1).

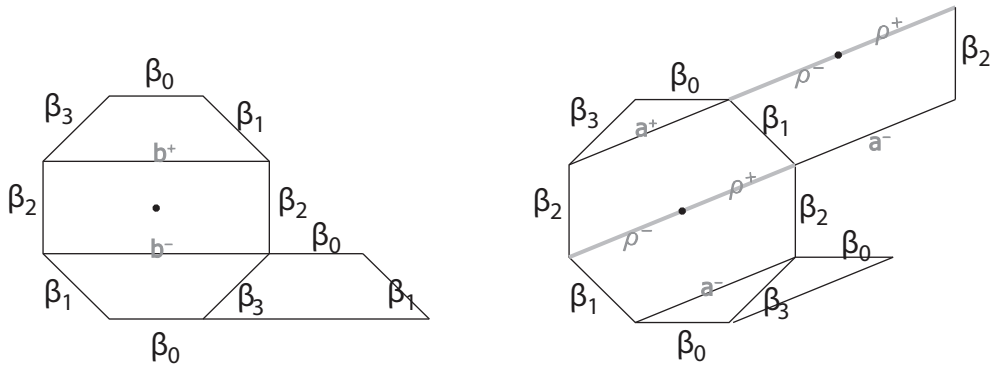

Figure 4.1: Horizontal and direction-$\left(\frac{\pi}{8}\right)$ cylinder decompositions of $\mathcal{O}^{\odot}$

Recall from Section 2.1 that the translation surface $S_{\mathcal{O}}^{\odot}$ is geometrically indistinguishable from $S_{\mathcal{O}}$, the (unpunctured) regular octagon surface. Coordinates in arbitrarily small neighborhoods of the central puncture in $\mathcal{O}^{\odot}$ are Euclidean; the puncture is a nonsigular marked point with cone angle 2π. Geometrically identical surfaces, such as $(S_{\mathcal{O}}, \Sigma)$ and $(S_{\mathcal{O}}^{\odot}, \Sigma^{\odot})$, with different sets of

marked points can have different affine automorphism groups. As indicated in Section2.1, however, regular $2n$-gon surfaces with and without a marked centerpoint do have the same Veech group (y Proposition 2.2.0.1). In the case of the surfaces $S_{\mathcal{O}}$ and $S_{\mathcal{O}}^{\odot}$, the Veech group $V(S^{\mathcal{O}})$ is generated by the rotation, $r_{\frac{\pi}{4}}$, the horizontal shear $H^+ = \begin{pmatrix} 1 & 2(1+\sqrt{2}) \\ 0 & 1 \end{pmatrix}$ and reflection r_v through the central vertical axis. The orientation-preserving subgroup, $V^+(S_{\mathcal{O}})$ of $V(S_{\mathcal{O}})$ is generated by just $r_{\frac{\pi}{4}}$ and H^+.

The linear transformation H^+ is the derivative of the automorphism illustrated in Figure 4.3. This automorphism induces a Dehn twist in the middle horizontal cylinder and two twists in the other cylinder (Figure 4.1)). It is, however, the orientation-reversing automorphism $\Psi = \Upsilon \circ H^+ \circ r_v$ with derivative $H^- = \begin{pmatrix} -1 & 2(1+\sqrt{2} \\ 0 & 1 \end{pmatrix} \in V(S_{\mathcal{O}}^{\odot})$ that plays a central role in our renormalization scheme. H^- is a *hidden symmetry* of $S_{\mathcal{O}}^{\odot}$. That is, H^- has finite order (in fact it is an involution) and there is a linear transformation not in the Veech group of $S_{\mathcal{O}}^{\odot}$ that conjugates H^- to an isometry of $S_{\mathcal{O}}^{\odot}$.

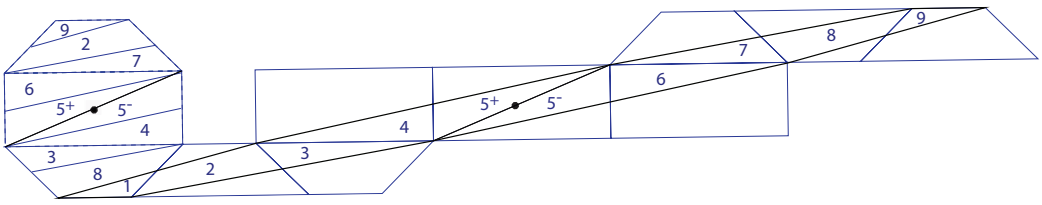

Figure 4.2: The figure shows $H^+ \cdot \mathcal{O}^{\odot}$ (right) and $(\Upsilon \circ H^+)$ (left) applied to $\mathcal{O}^{\odot}$. The shear H^+ is the derivative of the automorphism of $\mathcal{O}^{\odot}$ that postcomposes the cut-and-paste map Υ with H^+. (Figure adapted from [74])

Consider the shear $\mathrm{h} = \begin{pmatrix} -1 & 1+\sqrt{2} \\ 0 & 1 \end{pmatrix}$ that preserves the horizontal direction and takes lines tipped in direction $\frac{\pi}{8}$ to vertical lines (Figure 4.2). The linear transformation h is not the derivative of an affine automorphism of $\mathcal{O}^{\odot}$. The composition $\kappa^{-1} \circ r_v \circ \kappa$ of the cut-and-paste map κ that translates pieces of $\mathrm{h} \cdot \mathcal{O}^{\odot}$ to the L-shaped collection of rectangles in Figure 4.10 with $\kappa^{-1} \circ r_v$ is an isometry of $\mathrm{h} \cdot \mathcal{O}^{\odot}$. And

$$\mathrm{h}^{-1} \circ \kappa^{-1} \circ r_v \circ \kappa \circ \mathrm{h}$$

is an automorphism of $\mathcal{O}^{\odot}$ with derivative:

$$\mathrm{h}^{-1} \circ r_v \circ \mathrm{h} = \mathrm{H}^{-} \in \mathrm{V}(\mathrm{S}^{\odot}_{\mathcal{O}}).$$

Thus, $\mathrm{h} \circ \mathrm{H}^{-} \circ \mathrm{h}^{-1} = r_v$, implying that H^{-} is a hidden symmetry of $\mathrm{S}^{\odot}_{\mathcal{O}}$ conjugate to the orientation-reversing isometry r_v of by h, a linear transformation that is not the derivative of an affine automorphism of $\mathrm{S}^{\odot}_{\mathcal{O}}$.

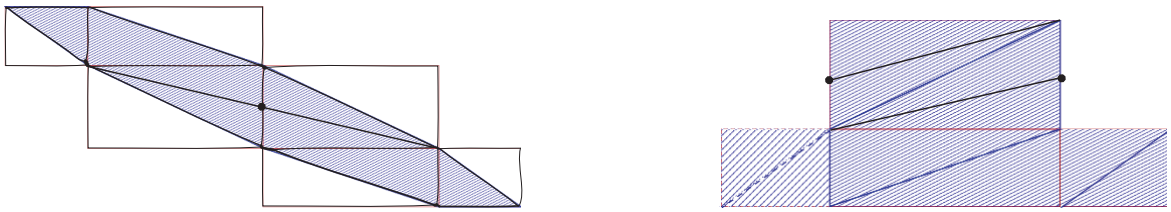

Figure 4.3: Left: the sheared octagon $\mathrm{h} \cdot \mathcal{O}^{\odot}$; Right: $(\kappa \circ \mathrm{h}) \cdot \mathcal{O}^{\odot}$ (Figure adapted from [74])

In the sheared octagon $\mathrm{h} \cdot \mathcal{O}^{\odot}$, the non-horizontal exterior sides of $\mathcal{O}$ become diagonals in circumscribed rectangles (Figure 4.3). Cutting and pasting into the L-shaped configuration $\mathcal{L}^{\odot}$ in Figure 4.3 yields a set of exterior rectangle sides that represent *interior* horizontal edges and edges tipped in direction $\frac{\pi}{8}$ in $\mathcal{O}^{\odot}$. These will be called *auxiliary edges*; they are labeled with $\{a^-, b^-, b^+, a^+\}$ (Figure 4.10). The auxiliary edges correspond to exterior edges of horizontal cyliders and cylinders in direction $\frac{\pi}{8}$ on $\mathcal{O}$. Use of the augmented alphabet $\widetilde{\mathscr{A}}^{\odot} = \mathscr{B} \cup \{\rho^-, \rho^+\} \cup \{a^-, b^-, b^+, a^+\}$ permits greater flexibility in tracking how trajectories pass through cylinders in $\mathcal{L}^{\odot}$ (Figure 4.10). The value of this flexibility is evident in Section 4.1.

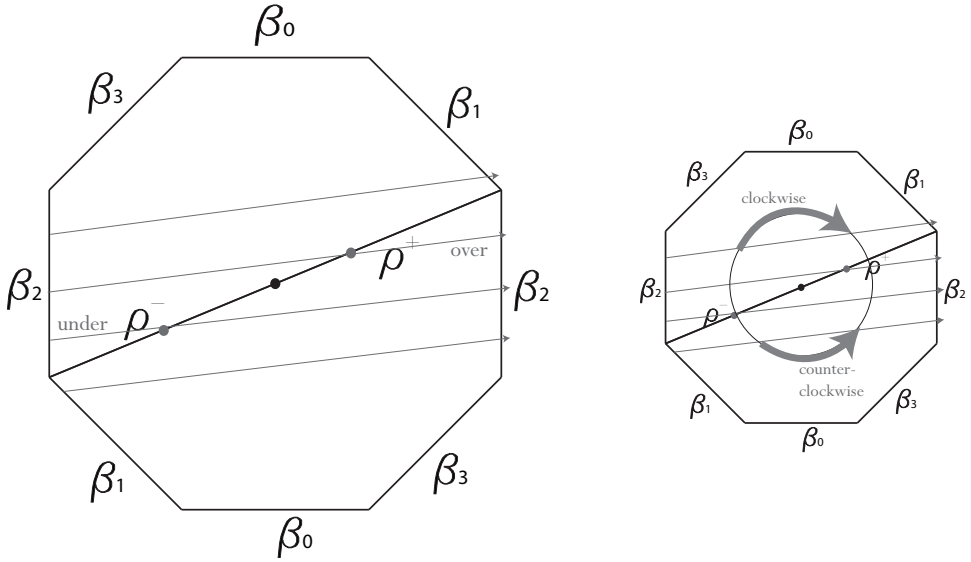

Figure 4.4: Example of a Σ_0-trajectory segment passing under/over the central puncture in $\mathcal{O}^{\odot}$ while making a β_2-to-β_2 transition.

4.1 Admissibility Criteria for $\mathcal{O}^{\odot}$ Cutting Sequences

Although the octagon and centrally-punctured octagon surfaces $\mathrm{S}_{\mathcal{O}}$ and $\mathrm{S}_{\mathcal{O}}^{\odot}$ share the same intrinsic geometry, interior edges included to account for trajectory behavior with respect to the marked centerpoint of $\mathcal{O}^{\odot}$ lead to more complex symbolic dynamics for geodesics on $\mathrm{S}_{\mathcal{O}}^{\odot}$.

Geodesic segments on $\mathrm{S}_{\mathcal{O}}^{\odot}$ that pass through the same labeled edge twice in succession are further identified by their orientation with respect to the centerpoint $p^{\odot}$. The projection of any such trajectory segment onto the minor arc it forms with a circle centered at $p^{\odot}$ moves either clockwise or counterclockwise, a distinction encoded by which of the interior triangle-leg edges, $\rho^{\pm}$ it crosses (Figure 4.4). Let $\overline{\tau}$ be a closed linear segment in direction $\theta \in \Sigma_0 = [0, \frac{\pi}{8}]$ that intersects the octagon boundary $\delta\mathcal{O}$ only at its endpoints. The diagram $\mathfrak{D}_0$ (Figure 4.8, right) summarizes the combinatorics of such segments with respect to the alphabet $\mathscr{A}^{\odot} = \{\beta_0, \beta_1, \beta_2, \beta_3, \rho^-, \rho^+\}$ (Figure 4.8, left). Vertices of $\mathfrak{D}_0$ represent octagon sides, directed edges are labeled by any interior edges that must be crossed by a Σ_0 trajectory in $\mathcal{O}^{\odot}$ passing between exterior octagon sides corresponding to the base and leading vertices of the directed edge.

Summary of Notational Conventions

The alphabet $\mathscr{B} = \{\beta_0, \beta_1, \beta_2, \beta_3\}$ labels distinct-angle segments of $\delta\mathcal{O}$. $\overline{\mathscr{B}} = \{\rho^-, \rho^+\}$ labels interior *spoke* segments of $\mathcal{O}^\odot$ that are reflected legs of the isosceles-$\left(\frac{\pi}{8}\right)$ triangle. $\mathscr{A}^\odot = \mathscr{B} \cup \overline{\mathscr{B}}$ is the coding alphabet for trajectories in $\mathcal{O}^\odot$. $\widetilde{\mathscr{A}}^\odot = \mathscr{B} \cup \{\rho^\pm\} \cup \{a^-, b^-, b^+, a^+\}$ includes all interior edges in $\mathcal{O}^\odot$ bounding horizontal and angle-$\left(\frac{\pi}{8}\right)$ cylinders. The restriction of a larger word to its elements in a particular sub-alphabet, for example of $\mathrm{w} \in \left(\mathscr{A}^\odot\right)^{\mathbb{Z}}$ to $\mathscr{B}$, is given as

$$\mathrm{w}\Big|_{\mathscr{B}}$$

$\mathcal{CS}_i^\odot$ is the set cutting sequences of linear trajectories in $\Sigma_i = [\frac{i\pi}{8}, \frac{(i+1)\pi}{8}]$.

Objects connected with the angular sectors Σ_{i+8} containing backward time trajectories from sectors $\Sigma_i = [\frac{i\pi}{8}, \frac{(i+1)\pi}{8}]$, $i \in \{0, 1, ..., 7\}$ will sometimes be denoted with subscript i^-. The objects associated with Σ_i, $i \in \{0, 1, ..., 7\}$ always have an *implied* subscript i^+. This becomes relevant when we speak of subscripts i^ϵ, $\epsilon \in \{+, -\}$. For example:

$$\Sigma_{i^-} \equiv \Sigma_{i+8}, \quad \mathcal{CS}_{i^-}^\odot \equiv \mathcal{CS}_{i+8}^\odot, \quad \mathfrak{D}_{i^-}^\odot \equiv \mathfrak{D}_{i+8}^\odot$$

and

$$\mathcal{T}_{i^\epsilon} = \mathcal{T}_{i+8}, \ (\epsilon = +), \quad \mathcal{T}_{i^\epsilon} = \mathcal{T}_i, \ (\epsilon = -)$$

Large bold Σ's, $\mathcal{T}$s, and $\mathcal{CS}^\odot$'s are unions over $i = 0, 1, 2, ..., 15$

$$\boldsymbol{\mathcal{T}} \equiv \bigcup_{i=0}^{15} \mathcal{T}_i, \quad \boldsymbol{\Sigma}_i \equiv \bigcup_{i=0}^{15} \Sigma_i$$

Both set closures and infinite periodic words are denoted by an *overline*. For example:

$$\text{the closure of } \boldsymbol{\mathcal{CS}}^\odot \text{ is } \overline{\boldsymbol{\mathcal{CS}}}^\odot$$

and

$$\text{the word } \overline{\beta_1\,\beta_3\beta_2} \text{ is shorthand for } ...\beta_1\,\beta_3\,\beta_2\,\beta_1\,\beta_3\beta_2\beta_1\,\beta_3\,\beta_2...$$

Figure 4.5

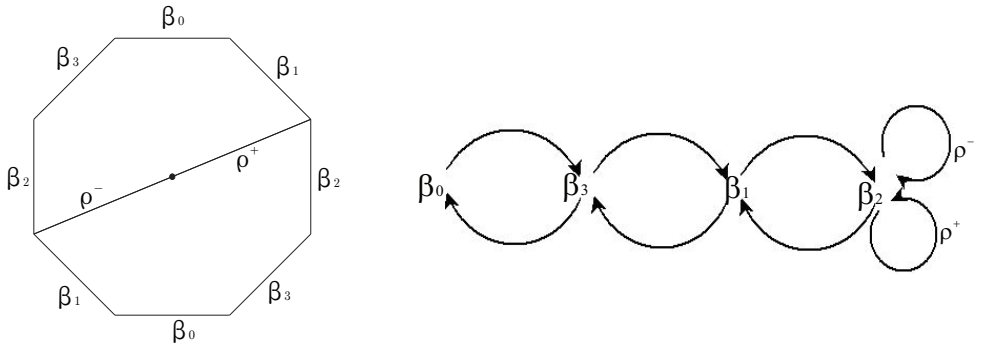

Figure 4.8: $\mathcal{O}^\odot$ and $\mathfrak{D}_0$, the transition diagram for Σ_0 linear trajectories in $\mathcal{O}^\odot$

$$\nu_0^+ = \begin{pmatrix} 1 & 0 \\ 0 & 1 \end{pmatrix} \quad \nu_1^+ = \begin{pmatrix} \frac{1}{\sqrt{2}} & \frac{1}{\sqrt{2}} \\ \frac{1}{\sqrt{2}} & -\frac{1}{\sqrt{2}} \end{pmatrix} \quad \nu_2^+ = \begin{pmatrix} \frac{1}{\sqrt{2}} & \frac{1}{\sqrt{2}} \\ -\frac{1}{\sqrt{2}} & \frac{1}{\sqrt{2}} \end{pmatrix} \quad \nu_3^+ = \begin{pmatrix} 0 & 1 \\ 1 & 0 \end{pmatrix}$$

$$\nu_4^+ = \begin{pmatrix} 0 & 1 \\ -1 & 0 \end{pmatrix} \quad \nu_5^+ = \begin{pmatrix} -\frac{1}{\sqrt{2}} & \frac{1}{\sqrt{2}} \\ \frac{1}{\sqrt{2}} & \frac{1}{\sqrt{2}} \end{pmatrix} \quad \nu_6^+ = \begin{pmatrix} -\frac{1}{\sqrt{2}} & \frac{1}{\sqrt{2}} \\ -\frac{1}{\sqrt{2}} & -\frac{1}{\sqrt{2}} \end{pmatrix} \quad \nu_7^+ = \begin{pmatrix} -1 & 0 \\ 0 & 1 \end{pmatrix}$$

Table 4.1: *Positive normalizing isometries* ν_i^+ of $\mathcal{O}^\odot$ that take Σ_i to Σ_0, $i = 0, 1, 2, ..., 7$. The remaining positive normalizing isometries are orientation reversing: $\nu_{i^-}^+ \equiv \nu_{i+8}^+ = \nu_i^+ \circ \mathrm{r}_\pi$, $i = 0, 1, ..., 7$. The *negative normalizing isometries* ν_i^- sending Σ_i to $\Sigma_{i^-} \equiv \Sigma_{i+8}$, $i = 0, 1, 2, ..., 15$ are given by $\nu_i^- = \mathrm{r}_\pi \circ \nu_i^+$.

The topology of transition diagrams $\mathfrak{D}_i$, $i = 1, 2, .., 7$ for trajectories in

$$\mathcal{T}_i \equiv \{\tau^\theta \text{ a linear trajectory on } \mathcal{O}^\odot : \theta \in \Sigma_i = \left[\frac{i\pi}{4}, \frac{(i+1)\pi}{4}\right]\}$$

and of transition diagrams $\mathfrak{D}_{i^-} \equiv \mathfrak{D}_{i+8}$, $i = 0, 1, 2, ..., 7$

$$\mathcal{T}_{i^-} \equiv \{\tau^\theta \text{ a linear trajectory on } \mathcal{O}^\odot : \theta \in \Sigma_{i^-} \equiv \Sigma_{i+8} = \left[\frac{(i+8)\pi}{4}, \frac{(i+9)\pi}{4}\right]\}$$

is exactly the same as that of $\mathfrak{D}_0$, and symmetries of the octagon ensure that

vertex labels of $\mathfrak{D}_0$ are *positive normalizing vertex permutations* $\pi_i^+ : \mathscr{B} \to \mathscr{B}$ of those in each of the $\mathfrak{D}_i$, $i = 0, 1, 2, ..., 15$ (Figure 4.9). Moreoever, $\pi_{i+8}^+ = \pi_i^+$ $\forall i \in \{0, 1, 2, ..., 7\}$. and the *negative normalizing vertex permutations* that take vertex labels of $\mathfrak{D}_i$ to those of $\mathfrak{D}_{0^-}$ are identical to the positive normalizing permutations. So $\pi_i^- = \pi_i^+$, $i = 0, 1, 2, ..., 15$.

Definition 4.1.0.1. *The* Σ_0 *trajectory* $\mathrm{n}(\tau) = \mathrm{n}^+(\tau) = \nu_i^+(\tau)$ *obtained from* $\tau \in \mathcal{T}_i$, $i \in \{0, 1, ..., 7\}$ *is called the* normalization *of* τ. *The normalization of* $\tau \in \mathcal{T}_{i^-}$, $i \in \{0, 1, ..., 7\}$ *is the* Σ_{0^-} *trajectory given by* $\mathrm{n}(\tau) = \mathrm{n}^-(\tau) = \nu_{i^-}(\tau)$.

Starting from the directed edge joining β_0 to β_3 in $\mathfrak{D}_0$ and proceeding clockwise around the diagram, enumerate the successive edges $\{\mathrm{e}_1, \mathrm{e}_2, .., \mathrm{e}_{10}\}$ of $\mathfrak{D}_0$. Denote by $\mathscr{R}^{\odot}$ the subset of $\{\emptyset, \rho^-, \rho^+\}^{10}$ consisting of an alternating length $2k$, $k = 1, 2, 3, 4, 5$ strings of $\rho^{\pm}$'s padded by $\frac{10-2k}{2}$ leading and trailing $\emptyset$'s, i.e. words such as $[\emptyset\ \emptyset\ \emptyset\ \rho^-\ \rho^+\ \rho^-\ \rho^+\ \emptyset\ \emptyset\ \emptyset]$. These words are parameterized by the length and initial sign of their alternating string of $\rho^{\pm}$'s, so $\mathscr{R}^{\odot} \equiv \{2^{\pm}, 4^{\pm}, 6^{\pm}, 8^{\pm}\}$. Edges of $\mathfrak{D}_0$ are labeled by $2^- \in \mathscr{R}^{\odot}$. Let $\pi_i^{\odot +}$ be the permutation on $\mathscr{R}^{\odot}$ that sends the element of $\mathscr{R}^{\odot}$ labeling edges of $\mathfrak{D}_i$ to 2^-. So relabeling $\mathfrak{D}_i$ according to $\boldsymbol{\pi}_i^+ \equiv \left(\pi_i^+, \pi_i^{\odot +}\right)$, $i = 0, 1, ..., 15$ yields $\mathfrak{D}_0$. Note that $\pi_{i+8}^{\odot +} = (2^-\ 2^+) \circ \pi_i^{\odot +}$ so $\widehat{\boldsymbol{\pi}}_i^+ \equiv \boldsymbol{\pi}_{i+8}^+ = (\pi_i^+, (2^-\ 2^+) \circ \pi_i^{\odot +})$. Edges of $\mathfrak{D}_{0^-}$ are labeled by $2^+ \in \mathscr{R}^{\odot}$ so $\pi_i^{\odot -} = (2^-\ 2^+) \circ \pi_i^{\odot +}$ and $\boldsymbol{\pi}_i^- = (\pi_i^+, (2^-\ 2^+) \circ \pi_i^{\odot +})$.

Definition 4.1.0.2. *A word* $\mathrm{w} \in \left(\mathscr{A}^{\odot}\right)^{\mathbb{Z}}$ *is* weakly admissible *if it can be realized as an infinite path in one of the diagrams* $\mathfrak{D}_i$, $i = 0, 1, 2, ..., 15$. *If weakly admissible* w *can be realized in* $\mathfrak{D}_j$, *then* w *is said to be* weakly Σ_j-admissible *or weakly admissible*

with respect to Σ_j.

Notational Convention. *In what follows, the notation* $\boldsymbol{\pi}_i$ *will be used in two related ways. When applied to the set of edge and vertex labels of* $\mathfrak{D}_i$, $\boldsymbol{\pi}_i$ *is the composition* $(\pi_i, \pi_i^{\odot})$ *of permutations discussed above. When applied to a* Σ_i*-admissible word* w, $\boldsymbol{\pi}_i$ *will denote the word* $\mathrm{n}(\mathrm{w}) = \boldsymbol{\pi}_i(\mathrm{w})$ *realized by following the* p *that realizes* w *in* $\mathfrak{D}_i$ *through* $\mathfrak{D}_0$.

Definition 4.1.0.3. *The word* $\mathrm{w} \in \left(\mathscr{A}^{\odot}\right)^{\mathbb{Z}}$ *is* normalizable *if for some* $i \in \{0, 1, ..., 15\}$, $\boldsymbol{\pi}_i(\mathrm{w})$ *is realizable as an infinite path in* $\mathfrak{D}_0$. *The word* w *is normalizable if and only if it is weakly* $\mathfrak{D}_i$*-admissible for some* $i \in \{0, 1, ..., 15\}$. *In this case,* normalizations *of* Σ_i*-admissible* w *and* Σ_{i^-}*-admissible* v *are given respectively by* $\mathrm{n}(\mathrm{w}) = \mathrm{n}^+(\mathrm{w}) = \boldsymbol{\pi}_i^+(\mathrm{w})$ *and* $\mathrm{n}(\mathrm{v}) = \mathrm{n}^-(\mathrm{v}) = \boldsymbol{\pi}_i^-(\mathrm{v})$.

Proposition 4.1.0.1. *Cutting sequences of linear trajectories in* $\mathcal{O}^{\odot}$ *are weakly admissible.*

Proof. Each linear trajectory τ^{θ}, $\theta \in \Sigma_i$, $i = 1, 2, ..., 15$ on $\mathcal{O}^{\odot}$ can be viewed as a concatenation of closed segments $\overline{\tau}_j$, $j \in \mathbb{N}$ in direction θ that intersect the octagon boundary $\partial\mathcal{O}$ only at their endpoints. By construction, there is a two-vertex path p_j in $\mathfrak{D}_i$ realizing the cutting sequence $c(\overline{\tau}_j)$ of each segment, so the cutting sequence $c(\tau^{\theta})$ of τ^{θ} is realizable in $\mathfrak{D}_i$ as an ordered concatenation $\mathrm{p}(\tau^{\theta}) = \mathrm{p}_1\mathrm{p}_2\cdots$

□

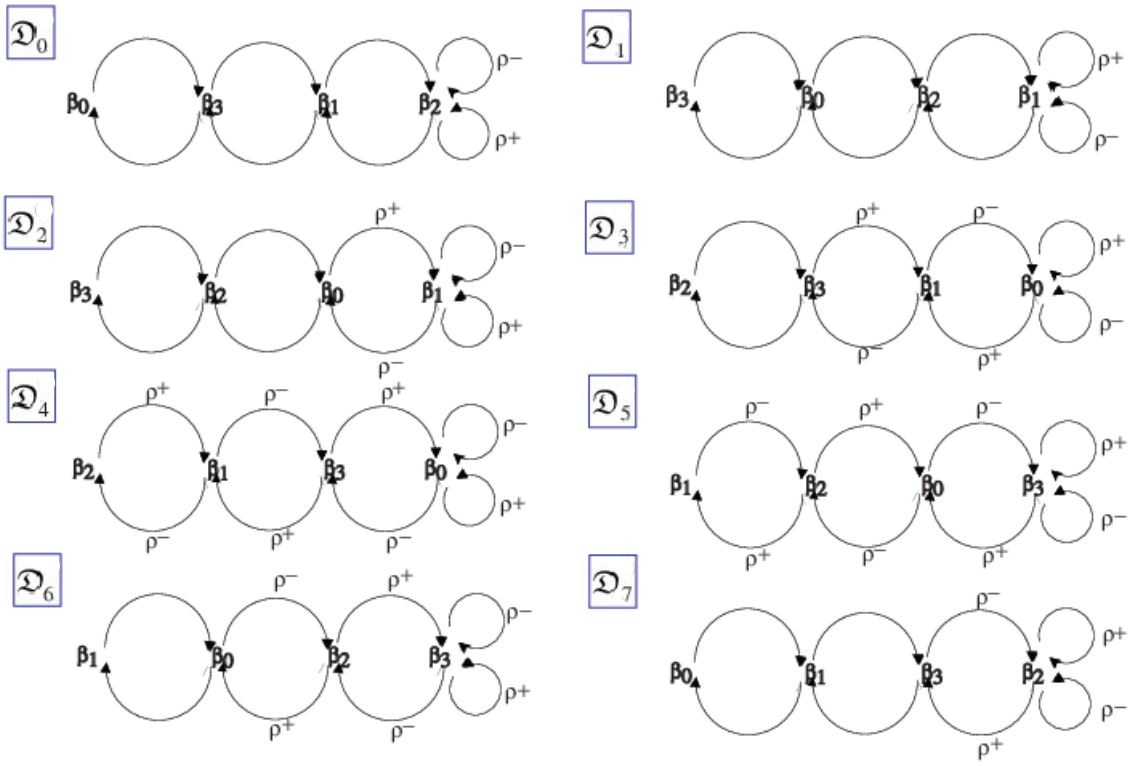

Figure 4.9: $\mathfrak{D}_i$, $i = 0, 1, 2, ..., 7$, transition diagrams for Σ_i, $i = 0, 1, 2, ..., 7$ linear trajectories in $\mathcal{O}^{\odot}$; $\mathfrak{D}_{i^-} \equiv \mathfrak{D}_{i+8}$, $i = 0, 1, 2, ..., 7$ is $\mathfrak{D}_i$ with signs of each $\rho^{\pm}$ switched. A word in $\left(\mathscr{A}^{\odot}\right)^{\mathbb{Z}}$ that is realizable as path through $\mathfrak{D}_i$ is *weakly* Σ_i-*admissible*.

It is clear from inspection that neighboring diagrams $\mathfrak{D}_k$, $\mathfrak{D}_{k+1 \,(\mathrm{mod}\ 8)}$ realize two common periodic period 1 or 2 restrictions of words from $\mathscr{A}^{\odot}$ to $\mathscr{B} = \{\beta_0, \beta_1, \beta_2, \beta_3\}$. It is also clear from inspection that any word w $\in \left(\mathscr{A}^{\odot}\right)^{\mathbb{Z}}$ that makes all transitions realizable in $\mathfrak{D}_k$ is realizable only in $\mathfrak{D}_k$.

$$\pi_0^+ = Id \qquad \pi_1^+ = (\beta_0\beta_3)(\beta_1\beta_2) \quad \pi_2^+ = (\beta_0\beta_1\beta_2\beta_3) \quad \pi_3^+ = (\beta_0\beta_2)$$
$$\pi_4^+ = (\beta_0\beta_2)(\beta_1\beta_3) \quad \pi_5^+ = (\beta_0\beta_1)(\beta_2\beta_3) \quad \pi_6^+ = (\beta_0\beta_3\beta_2\beta_1) \quad \pi_7^+ = (\beta_1\beta_3)$$

Table 4.2: Permutations π_i^+ that convert vertex labels of $\mathfrak{D}_i$ and of $\mathfrak{D}_{i^-} \equiv \mathfrak{D}_{i+8}$ to those of $\mathfrak{D}_0$, $i = 0, 1, 2, ..., 7$.

$$\pi_0^{\odot +} = Id \qquad \pi_1^{\odot +} = (2^+\, 2^-) \quad \pi_2^{\odot +} = (4^+\, 2^-) \quad \pi_3^{\odot +} = (6^+\, 2^-)$$
$$\pi_4^{\odot +} = (8^+\, 2^-) \quad \pi_5^{\odot +} = (8^-\, 2^-) \quad \pi_6^{\odot +} = (6^-\, 2^-) \quad \pi_7^{\odot +} = (4^-\, 2^-)$$

Table 4.3: Permutations $\pi_i^{\odot +}$ that convert edge labels of $\mathfrak{D}_i$ to those of $\mathfrak{D}_0$, $i = 0, 1, 2, ...$ The edge-label permutations for $\mathfrak{D}_{i^-} \equiv \mathfrak{D}_{i+8}$ are given by $\pi_{i^-}^{\odot} \equiv \pi_{i+8}^{\odot} = (2^-\, 2^+) \circ \pi_i^{\odot}$.

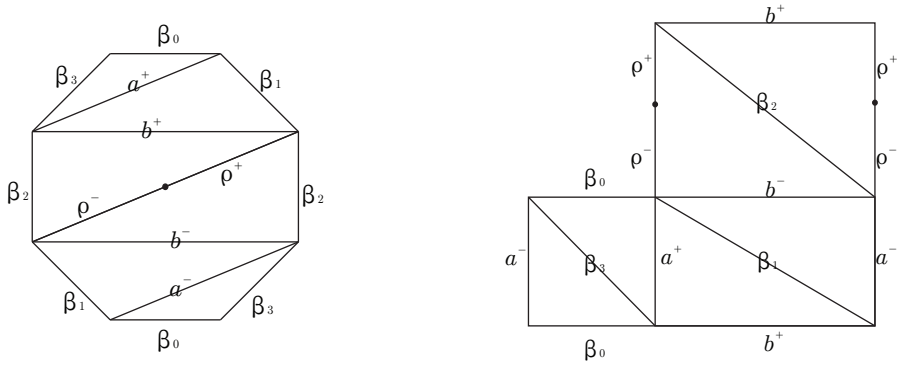

Figure 4.10: Augmented centrally punctured octagon $\widetilde{\mathcal{O}}^{\odot}$ (left) and L-shaped table $\mathcal{L}^{\odot} = (\kappa \circ \mathrm{h}) \cdot \widetilde{\mathcal{O}}^{\odot}$ (right).

Extending the procedure introduced for the torus in Section 2.3.1, we now label edges of the one-step transition diagram $\mathfrak{D}_0$ by the auxiliary segments crossed by trajectories $\tau \in \mathcal{T}_0$ passing from the octagon side labeled by the vertex at the base of the edge to the octagon side labeled by the vertex at its tail (Figure 4.11). This augmented transition diagram will be denoted $\widetilde{\mathfrak{D}}_0$.

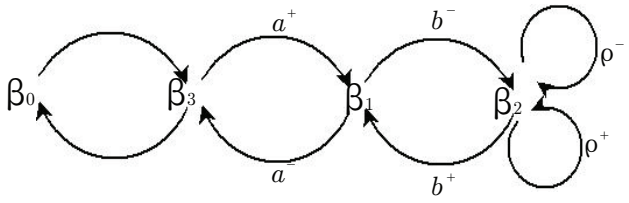

Figure 4.11: The figure shows $\widetilde{\mathfrak{D}}_0$, the transition diagram for Σ_0 trajectories in $\widetilde{\mathcal{O}}^{\odot}$.

The role of the augmented alphabet becomes clearer when we switch point of view, creating a new transition diagram $\widetilde{\mathfrak{D}}_0^*$ for Σ_0 trajectories that is "nearly dual" to $\widetilde{\mathfrak{D}}_0$. These nearly-dual transition diagrams labeled by letters in the augmented alphabet will prove useful in determining a derivation rule on words in $\mathscr{A}^{\odot}$ that corresponds to the geometric renormalization scheme we detail in Section 4.28. In $\widetilde{\mathfrak{D}}_0^*$, vertices are labeled by horizontal and vertical edges of $\mathcal{L}^{\odot}$ and directed edges labeled by the interior diagonals in $\mathcal{L}^{\odot}$ crossed by Σ_0 trajectories passing between the rectangle side labeled by the initial vertex to the rectangle side labeled by the terminal vertex (Figure 4.19).

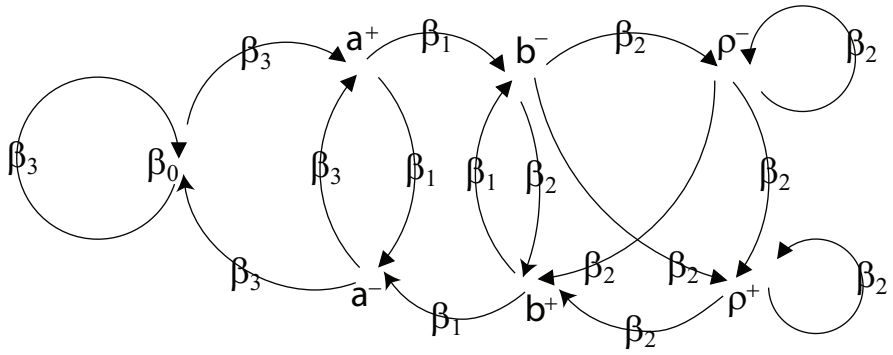

Figure 4.12: $\widetilde{\mathfrak{D}}_0^*$, the dual Σ_0 transition diagram: here the vertices are the edges of $\widetilde{\mathcal{O}}^{\odot}$ that are cylinder boundary components in horizontal and angle-$\left(\frac{\pi}{8}\right)$ cylinder decompositions of $\mathcal{O}^{\odot}$ while edges are labeled by exterior sides of $\mathcal{O}^{\odot}$ that are interior diagonals of the cylinders. The dual Σ_{0^-} diagram $\widetilde{\mathfrak{D}}_{0^-}^*$ is obtained from $\widetilde{\mathfrak{D}}_0^*$ by switching the signs of those vertex labels that have sigs as superscripts.

Observation 4.1.0.1. *The original transition diagram $\mathfrak{D}_0$ from which weak admissibility was defined (Figure 4.9) allows two finite words that are impossible for a trajectory $\tau \in \mathcal{T}_0$ to realize: words containing the subword $[\rho^+ \beta_2 \rho^-]$ (Figure 4.20). To be clear, these are not the only words realizable in $\mathfrak{D}_0$ that are not realizable as the cutting sequence of a linear trajectory on $\mathcal{O}^\odot$. These words are distinctive however in that simply looking at two-step transitions immediately reveals that they cannot be contained in cutting sequences.*

Definition 4.1.0.4. *The* augmentation *of a weakly Σ_i-admissible word* w, $i \in \{0, 1, ..., 7\}$ *is the word* $\widetilde{\mathrm{w}}$ *obtained by tracing the path* $\mathrm{p}(\mathrm{n}^+(\mathrm{w}))$ *of its normalization in* $\mathfrak{D}_0$ *through* $\widetilde{\mathfrak{D}}_0$. *The augmentation of a* Σ_{i^-}*-admissible* w *is the word obtained by tracing* $\mathrm{p}(\mathrm{n}^-(\mathrm{w}))$ *through* $\widetilde{\mathfrak{D}}_{0^-}$.

Definition 4.1.0.5. *A weakly $\Sigma_{j\epsilon}$-admissible, $\epsilon \in \{+, -\}$ word* w *is* admissible *if its augmented normalization* $\widetilde{\mathrm{n}}(\mathrm{w})$ *is realizable as a path in* $\widetilde{\mathfrak{D}}^*_{0\epsilon}$. *An admissible word is said to be* $\Sigma_{j\epsilon}$-admissible *or* admissible with respect to $\Sigma_{j\epsilon}$ *if it is weakly* $\Sigma_{j\epsilon}$*-admissible (Definition 4.1.0.2).*

Proposition 4.1.0.2. *Cutting sequences of linear trajectories on $\mathcal{O}^\odot$ are admissible.*

Proof. If $c(\tau)$ is the cutting sequence of a linear trajectory τ on $\mathcal{O}^\odot$, and $\mathrm{w} = \mathrm{n}(c(\tau))$ its normalization then, by Proposition 4.1.0.1 , w is weakly admissible. Moreover, by Observation 4.1.0.1, the 3-letter subword $[\rho^+ \beta_2 \rho^-]$ occurs nowhere in w, and hence cannot occur in the augmentation $\widetilde{\mathrm{w}}$ of w. Since any word $\widetilde{\mathrm{w}}$ realizable in $\widetilde{\mathfrak{D}}^\odot_0$ not containing the subword $[\rho^+ \beta_2 \rho^-]$ is also realizable in $\widetilde{\mathfrak{D}}^*_0$,

this proves the proposition.

□

4.2 Combinatorial correspondence between $\left(\frac{\pi}{4}\right)$-isosceles and centrally punctured regular octagon billiards

With the language of admissibility at our disposal we now establish the correspondence between cutting sequences of linear trajectories on the centrally punctured regular octagon and hitting sequences of billiard trajectories on the $\left(\frac{\pi}{4}\right)$-isosceles triangle.

Proposition 4.2.0.1. *Let* $\mathrm{w} = c(\tau)$ *be the cutting sequence of a linear trajectory on* $\mathcal{O}^{\odot}$. *There is a well-defined mapping* $a : (\mathscr{A})^{\mathbb{Z}} \mapsto \{\beta, \lambda, \rho\}^{\mathbb{Z}}$ *that yields a word* $\mathrm{w}^{\triangle} = a(\mathrm{w}) \in \{\beta, \lambda, \rho\}^{\mathbb{Z}}$ *that is the hitting sequence of a billiard trajectory* τ' *on the* $\left(\frac{\pi}{4}\right)$*-isosceles triangle.*

Proof. By Proposition 4.1.0.1, $\mathrm{w} = c(\tau)$ is weakly Σ_i-admissible for some $i \in \{0, 1, ..., 15\}$. The normalization $\mathrm{n}(\mathrm{w})$ of w exists and either $\mathrm{n}(\mathrm{w})$ or $(\rho^{+}\,\rho^{-}) \cdot \mathrm{n}(\mathrm{w})$ is realizable in $\mathfrak{D}_0$. First assume that $\mathrm{n}(\mathrm{w})$ is realizable in $\mathfrak{D}_0$,so $\mathrm{n}(\mathrm{w})$ is the cutting sequence of the normalization $\mathrm{n}(\tau)$ of τ. Let p be the path through $\mathfrak{D}_0$ that realizes $\mathrm{n}(\mathrm{w})$. The *triangle augmented* transition diagram $\widetilde{\mathfrak{D}}^{\triangle}$ (Figure 4.14, diagram II.) labels directed edges of $\mathfrak{D}_0$ by the interior triangle legs (Figure 4.13 (b)) crossed by Σ_0 trajectories passing from the octagon side labeled by the initial vertex to the octagon side labeled by the terminal vertex. The unindexed

triangle augmented transition diagram $\mathfrak{D}^{\triangle}$ (Figure 4.14, diagram III.) drops superscripts and subscripts from edge and vertex labels of $\widetilde{\mathfrak{D}}^{\triangle}$. Since w is the cutting sequence of the linear trajectory τ on $\mathcal{O}^{\odot}$, the word $\mathrm{w}^{\triangle} = a(\mathrm{w})$ obtained by tracing p through $\mathfrak{D}^{\triangle}$ is clearly the hitting sequence of the $\left(\frac{\pi}{4}\right)$-isosceles billiard trajectory τ' that unfolds into $\mathrm{n}(\tau)$ on $\mathcal{O}^{\odot}$. If $(\rho^{+}\,\rho^{-}) \cdot \mathrm{n}(\mathrm{w})$ is realizable in $\mathfrak{D}_0$, then the same argument holds for $(\rho^{+}\,\rho^{-}) \cdot \mathrm{n}(\mathrm{w})$ and $r_v \cdot \mathrm{n}(\tau)$

□

Since the correspondence is many-to-one, there is more than one natural way to define the mapping from $\left(\frac{\pi}{4}\right)$-isosceles hitting sequences to $\mathcal{O}^{\odot}$ cutting sequences. We present a mapping that fixes the target angular sector of its image. Other natural choices might fix the indexed β in $\mathcal{O}^{\odot}$ to which the first appearance of β in the hitting sequence lifts.

Proposition 4.2.0.2. *Let* w *be the hitting sequence of a billiard trajectory on the* $\left(\frac{\pi}{4}\right)$*-isosceles triangle. There is a well-defined mapping from* $\mathrm{a} : \{\beta, \lambda, \rho\}^{\mathbb{Z}} \mapsto \left(\mathscr{A}^{\odot}\right)^{\mathbb{Z}}$ *that yields a word* $\mathrm{w}^{\odot} = \mathrm{a}(\mathrm{w}) \in \left(\mathscr{A}^{\odot}\right)^{\mathbb{Z}}$ *that is the cutting sequence of a linear trajectory* τ' *on* $\mathcal{O}^{\odot}$.

Proof. Let w be the hitting sequence of a billiard trajectory τ in the $\left(\frac{\pi}{4}\right)$-isosceles triangle. Either w of $(\lambda\,\rho) \cdot \mathrm{w}$ is realizable the *dual triangle transition diagram* $\mathfrak{D}^{\triangle^*}$ (Figure 4.14, Diagram IV.) in which edge labels of $\mathfrak{D}^{\triangle}$ are vertex labels, and directed edges of $\mathfrak{D}^{\triangle^*}$ are labeled with vertex labels from $\mathfrak{D}^{\triangle}$. First assume that w is realizable in $\mathfrak{D}^{\triangle^*}$. Let p be a path through $\mathfrak{D}^{\triangle^*}$ that realizes w. The path p is unique if w contains a β*-free subword* (Definition 4.2.0.1) of length four, or if w

contains two β-free subwords of different lengths.

Definition 4.2.0.1 (β-free subwords). *A β-free subword of* $\mathrm{w} \in \{\beta, \lambda, \rho\}^{Z}$ *is a subword without β's that cannot be extended in either direction while retaining this property.*

Diagram V. in Figure 4.14 is adapted from the almost-dual augmented Σ_0 transition diagram (Figure 4.12) by stripping vertex labels, leaving only labels from the alphabet $\mathscr{A}^{\odot}$. When p is unique, then $\mathrm{w}^{\odot} = \mathrm{a}(\mathrm{w}) \in \left(\mathscr{A}^{\odot}\right)^{\mathbb{Z}}$ is the word obtained by tracing p through Diagram V. of Figure 4.14. If every β-free subword of w is the same length, say $k < 4$, then there are exactly two paths p_1 and p_2 that realize w in $\mathfrak{D}^{\triangle}$. The words $\mathrm{w}_1^{\odot}$ and $\mathrm{w}_2^{\odot}$ obtained by tracing p_1 and p_2 through Diagram V. of Figure 4.14 are the same up to indexing, they are both period-one periodic words $\overline{\beta_i \beta_j}$, $i \neq j \in \{0, 1, 2\}$. In this case, $\mathrm{w}^{\odot} = \mathrm{a}(\mathrm{w})$ will be whichever of $\mathrm{w}_1^{\odot}$ or $\mathrm{w}_2^{\odot}$ has $\beta_{\min(i,j)}$ in the zero position. Since w is the cutting sequence of a billiard trajectory τ on the $\left(\frac{\pi}{4}\right)$-isosceles triangle, $\mathrm{w}^{\odot} = \mathrm{a}(\mathrm{w})$ is the cutting sequence of the normalization $\mathrm{n}(\tau') \in \mathcal{T}_0$ of the linear trajectory τ' in $\mathcal{O}^{\odot}$ that τ that unfolds into.

We have so far assumed that w is realizable in $\mathfrak{D}^{\triangle}$. Since w is a hitting sequence either w or $(\lambda\rho) \cdot \mathrm{w}$ is realizable in $\mathfrak{D}^{\triangle}$. If $(\lambda\rho) \cdot \mathrm{w}$ is realizable in $\mathfrak{D}^{\triangle}$ then the same argument above holds for $(\lambda\rho) \cdot \mathrm{w}$ and $r_v \cdot \tau$ and $\mathrm{w}^{\odot}$ is the cutting sequence of the normalization $\mathrm{n}(\tau') \in \mathcal{T}_0$ of the unfolding in $\mathcal{O}^{\odot}$ of the reflected billiard trajectory $r_v \cdot \tau$.

□

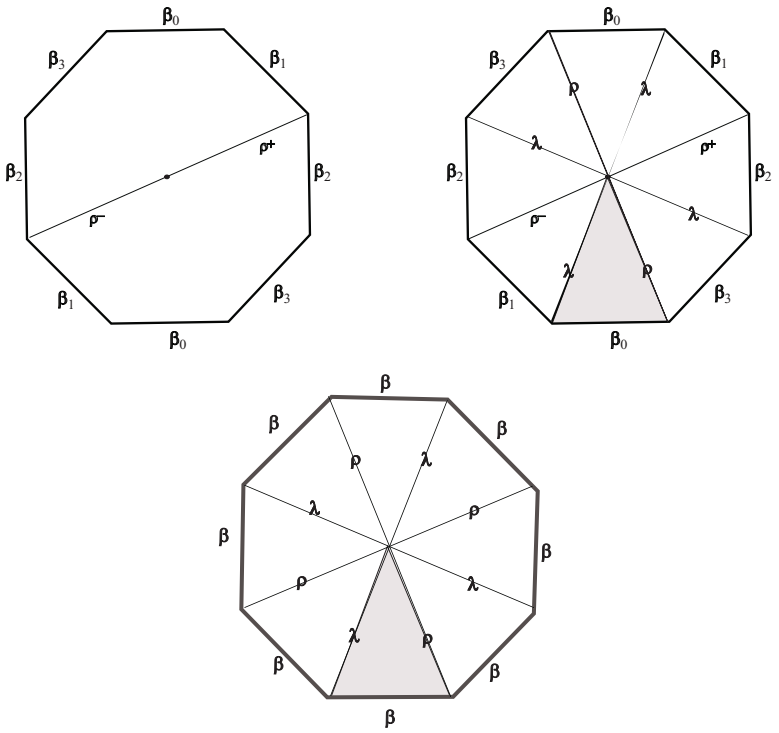
β0
β3
β1
β2
β2
ρ+
ρ−
β1
β3
β0
β0
β3
β1
ρ
λ
λ
ρ+
β2
β2
ρ−
λ
λ
ρ
β1
β3
β0
β
β
β
β
ρ
λ
λ
ρ
β
β
ρ
λ
λ
ρ
β
β
β

Figure 4.13

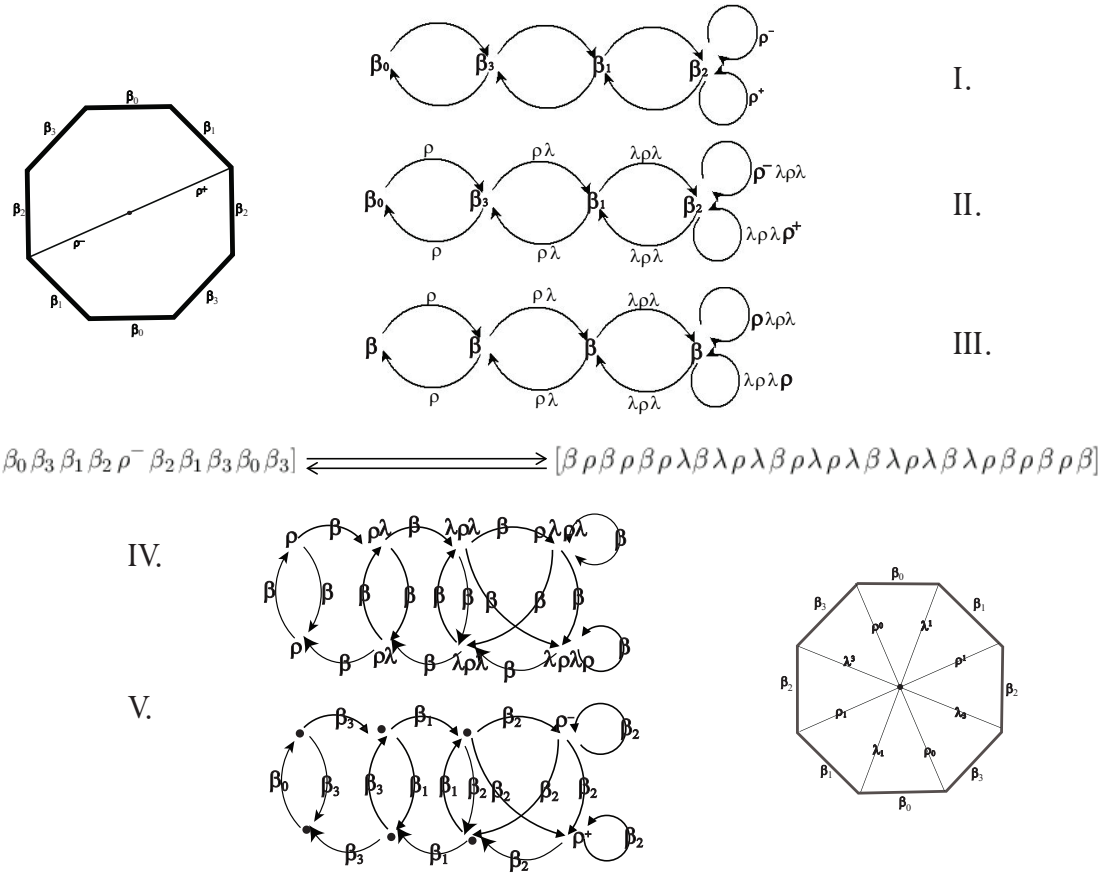

Figure 4.14: Cutting sequences of direction $\theta \in [0, \frac{\pi}{8}]$ trajectories on the centrally-punctured octagon can be realized by a path p through diagram I. Tracing p through diagram III. gives the corresponding hitting sequence on the $(\frac{\pi}{4})$-isosceles triangle. Hitting sequences, up to permutation by $(\lambda\, \rho)$, on the $(\frac{\pi}{4})$-isosceles triangle can be realized by a path p′ in diagram IV. Tracing p′ through diagram V. gives the corresponding cutting sequence for a direction $\theta \in [0, \frac{\pi}{8}]$ trajectory on the centrally punctured octagon.

4.3 Renormalization of Linear Trajectories in $\mathcal{O}^{\odot}$

Proposition 4.3.0.1. *If $\tau \in \boldsymbol{\mathcal{T}}$, then $\Psi(\mathrm{n}^{+}(\tau))$ and $\Psi(\mathrm{n}^{-}(\tau))$ are also linear trajectories on $\mathcal{O}^{\odot}$, and $\Psi(\mathrm{n}^{-}(\tau)) = \mathrm{r}_{\pi} \cdot \Psi(\mathrm{n}^{+}(\tau))$.*

Proof. Without loss of generality assume $\tau \in \mathcal{T}_0$ (so $\mathrm{n}^+(\tau) = \tau$). It is clear that $r_v(\tau)$ is a linear trajectory in $\mathcal{O}^{\odot}$ and thus $\mathrm{H}^-(\tau) = \left(\mathrm{H}^+ \circ r_v\right)(\tau)$ is a linear trajectory in $\left(\mathrm{H}^+ \circ r_v\right)(\mathcal{O}^{\odot}) = \mathrm{H}^-(\mathcal{O}^{\odot})$. The composition Ψ of the affine automorphism with derivative H^- and the cut-and-paste map Υ is an isometry, so $\tau' = \Psi(\mathrm{n}^+(\tau))$ is a linear trajectory in $\mathcal{O}^{\odot}$. Moreoever,

$$\begin{aligned}
\Psi(\mathrm{n}^-(\tau)) &= \left(\Upsilon \circ \mathrm{H}^- \circ r_v \circ \mathrm{r}_\pi\right)(\tau) \\
&= \left(\Upsilon \circ \mathrm{r}_\pi \circ \mathrm{H}^- \circ r_v\right)(\tau) \\
&= \left(\mathrm{r}_\pi \circ \Upsilon \circ \mathrm{H}^- \circ r_v\right)(\tau) \\
&= \mathrm{r}_\pi\left(\Psi(\mathrm{n}^+(\tau))\right) \\
&= \mathrm{r}_\pi(\tau')
\end{aligned}$$

is a rotation of $\tau' \in \boldsymbol{\mathcal{T}}$, thus also in $\boldsymbol{\mathcal{T}}$.

□

Observation 4.3.0.1. *(Figure 4.15) Note that the affine automorphism with derivative* H^+ *(which, abusing notation, we also refer to as* H^+*) takes* Σ_7 *to* $\bigcup_{i=1}^{7} \Sigma_i$ *so* $\mathrm{H}^- = \mathrm{H}^+ \circ r_v$ *takes* Σ_0 *to* $\bigcup_{i=1}^{7} \Sigma_i$ *and* $\Psi\left(\mathcal{T}_0\right) \cap \mathcal{T}_0 = \bigcup_{i=1}^{7} \Sigma_i$*. Similarly,* $\Psi\left(\mathcal{T}_{0^-}\right) = \bigcup_{i=1}^{7} \Sigma_{i^-}$*.*

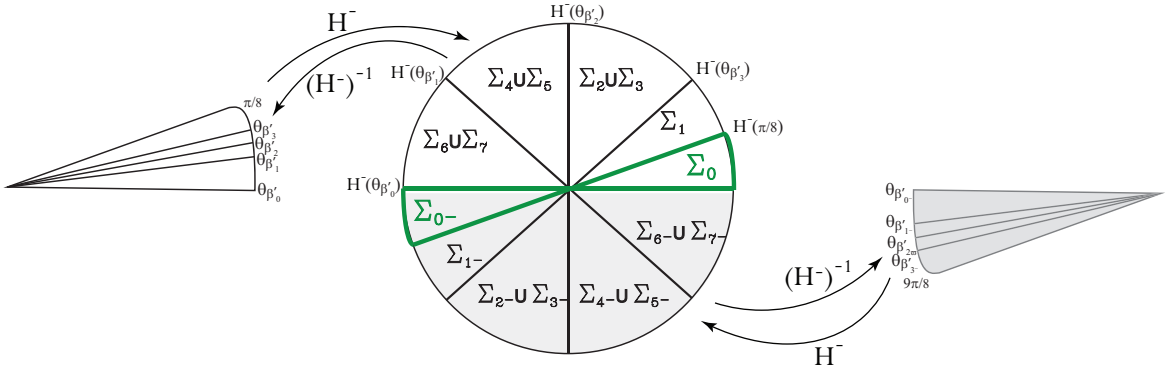

Figure 4.15: Images of $\left(\mathrm{H}^{-}\right)^{-1}\left(\bigcup_{i=1}^{7}\Sigma_{i^{\epsilon}}\right)$ in $\Sigma_{0\,\mathrm{sgn}\,(\epsilon)}$, with respect to angles of sheared exterior octagon sides $\mathrm{H}\cdot\delta\mathcal{O}$.

θ	θ'	β_1	β_2	β_3	
$0\leq\theta\leq\theta_{\beta'_1}$	$\theta'\in\overline{\Sigma}_6\cup\overline{\Sigma}_7$	β_3-sandwiched	β_2-sandwiched	β_1-sandwiched	$\mathfrak{G}_3$
$\theta_{\beta'_1}\leq\theta\leq\theta_{\beta'_2}$	$\theta'\in\overline{\Sigma}_4\cup\overline{\Sigma}_5$	β_2-sandwiched	β_2-sandwiched	β_1-sandwiched	$\mathfrak{G}_2$
$\theta_{\beta'_2}\leq\theta\leq\theta_{\beta'_3}$	$\theta'\in\overline{\Sigma}_2\cup\overline{\Sigma}_3$	β_2-sandwiched	β_1-sandwiched	B-sandwiched	$\mathfrak{G}_1$
$\theta_{\beta'_3}\leq\theta\leq\pi/8$	$\theta'\in\overline{\Sigma}_1$	β_2-sandwiched	β_1-sandwiched	β_0-sandwiched	$\mathfrak{G}_0$

Figure 4.16: Sandwiched letters in the normalized $\Sigma_{j^{\epsilon}}$-admissible derivatives of *coherent* $\Sigma_{i\,\mathrm{sgn}\,(\epsilon)}$-admissible words, in terms of the angular subsectors of $\Sigma_{0\,\mathrm{sgn}\,(\epsilon)}$ that the derivative falls into. (Figure adapted from [74])

Definition 4.3.0.1. *The operation of applying* Ψ *to* $\mathrm{n}^{+}(\tau)\in\mathcal{T}_0$ *or to* $\mathrm{n}^{-}(\tau)\in\mathcal{T}_{0^-}$ *for* $\tau\in\mathcal{T}_i$ *or* $\tau\in\mathcal{T}_{i^-}$, $i=0,1,2,..,7$ *respectively will be called* geometric derivation *or* renormalization *and denoted by* $\mathcal{D}(\tau)$.

As an immediate consequence of Proposition 4.3.0.1 we have the following corollary:

1

Corollary 4.3.0.2. *If* τ *is a linear trajectory on* $\mathcal{O}^{\odot}$, *then every successive geometric*

derivation $\tau^{(n)} = \mathcal{D}^{(n)}(\tau)$ of τ is also a linear trajectory on $\mathcal{O}^{\odot}$.

4.4 Renormalization of Symbolic Trajectories in $\mathcal{O}^{\odot}$

We now return to our main focus: the characterization of cutting sequences on $\mathrm{S}^{\odot}_{\mathcal{O}}$.

Definition 4.4.0.1. *The letter w_i in a word $\mathrm{w} = ...w_{i-1}\, w_i\, w_{i+1}... \in \mathscr{A}^{\mathbb{Z}}$ is said to be* sandwiched *if $w_{i-1} = w_{i+1}$.*

Let $\mathrm{D} : \left(\mathscr{A}^{\odot}\right)^{\mathbb{Z}} \to \left(\mathscr{A}^{\odot}\right)^{\mathbb{Z}}$ be the operator on *admissible* words $\mathrm{w} \in \left(\mathscr{A}^{\odot}\right)^{\mathbb{Z}}$ that retains every ρ^{-}, ρ^{+} in $\mathrm{n}(\mathrm{w})$ and the letters in $\mathrm{n}(\mathrm{w})$ that are sandwiched in $\mathrm{n}(\mathrm{w})\Big|_{\mathscr{B}}$. This operation will be called *combinatorial derivation*.

Definition 4.4.0.2. *An admissible word $\mathrm{w} \in \left(\mathscr{A}^{\odot}\right)^{\mathbb{Z}}$ is* deriveable *if $\mathrm{w}' = \mathrm{D}(\mathrm{w})$ is also admissible.*

Example 4.4.0.1. *Consider the word*

$$\mathrm{w} = ...\beta_0\ \beta_3\ \beta_1\ \beta_2\ \rho^{-}\ \beta_2\ \rho^{+}\ \beta_1\ \beta_3\beta_0\beta_3... \in \mathcal{A}_0$$

In this case, $\mathrm{n}(\mathrm{w}) = \mathrm{w}$, and

$$\mathrm{n}(\mathrm{w})\Big|_{\mathscr{B}} = ...\beta_0\ \beta_3\ \beta_1\ \beta_2\ \ \beta_2\ \ \beta_2\ \beta_1\ \beta_3\ \beta_0\ \beta_3...$$

The derived sequence retaining all $\rho^{\pm}$'s and sandwiched letters of $\mathrm{n}(\mathrm{w})\Big|_{\mathscr{B}}$ *is:*

$$\mathrm{D}(\mathrm{w}) = ...\rho^{-}\ \beta_2\ \rho^{+}\ \beta_0... \in \mathcal{A}_5, \mathcal{A}_6.$$

Let $\mathcal{CS}^{\odot} \subset \left(\mathscr{A}^{\odot}\right)^{\mathbb{Z}}$ be the set of cutting sequences of linear trajectories on $\mathcal{O}^{\odot}$.

Proposition 4.4.0.1. *If* $\mathrm{w} \in \mathcal{CS}^{\odot}$*, then* w *is deriveable and* $\mathrm{w}' = \mathrm{D}(\mathrm{w}) \in \mathcal{CS}^{\odot}$.

Proof of Proposition 4.4.0.1. Without loss of generality, we prove the proposition for $\tau \in \mathcal{T}_0$. Let $\mathrm{w} = c(\tau)$ be the cutting sequence of $\tau \in \mathcal{T}_0$. By Proposition 4.3.0.1, we know that

$$\begin{aligned}
\tau' &= \Psi(\tau) \\
&= \left(\Upsilon \circ \left(\mathrm{h}^{-1} \circ r_v \circ \mathrm{h}\right)\right) \cdot \tau \\
&= \left(\Upsilon \circ \left(\mathrm{h}^{-1} \circ \kappa^{-1} r_v \circ \kappa \circ \mathrm{h}\right)\right) \cdot \tau.
\end{aligned}$$

Let τ^{θ}, $\theta \in [0, \frac{\pi}{2}]$ be the image of τ in $\mathcal{L}^{\odot} = (\kappa \circ \mathrm{h}) \cdot \mathcal{O}^{\odot}$. Note that τ^{θ} has the same combinatorics as τ, i.e. $c(\tau^{\theta}) = c(\tau) = \mathrm{w}$. By Proposition 4.1.0.2, the augmentation $\widetilde{\mathrm{w}}$ of w is realizable in $\widetilde{\mathfrak{D}}_0^*$. Now reflect each rectangle in $\mathcal{L}^{\odot}$ about its central vertical axis. Call the result $\mathcal{L}^{\odot'} = r_v \cdot \mathcal{L}^{\odot}$ (see Figure 4.17). The diagonals in $\mathcal{L}^{\odot'}$ carry *primed* labels to indicate change in angle from the preimages in $\mathcal{L}^{\odot}$.

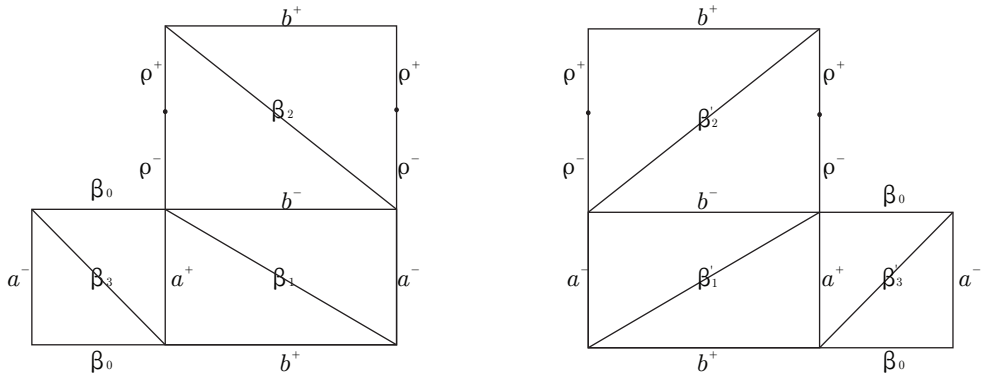

Figure 4.17: Left: $\mathcal{L}^{\odot} = (\kappa \circ \mathrm{h}) \cdot \widetilde{\mathcal{O}}^{\odot}$, the Σ_0-linear trajectory τ with cutting sequence w in $\widetilde{\mathcal{O}}^{\odot}$ is the angle $\theta \in [0, \frac{\pi}{8}]$ linear trajectory $\mathrm{h} \cdot \tau$ in $\mathcal{L}^{\odot}$ with the same cutting sequence. Right: $\mathcal{L}^{\odot\,\prime}$, the cutting sequence of $\mathrm{h} \cdot \tau$ in $\mathcal{L}^{\odot\,\prime}$ is $\mathrm{w}' = \mathcal{D}(\mathrm{w})$, the derived sequence of w.

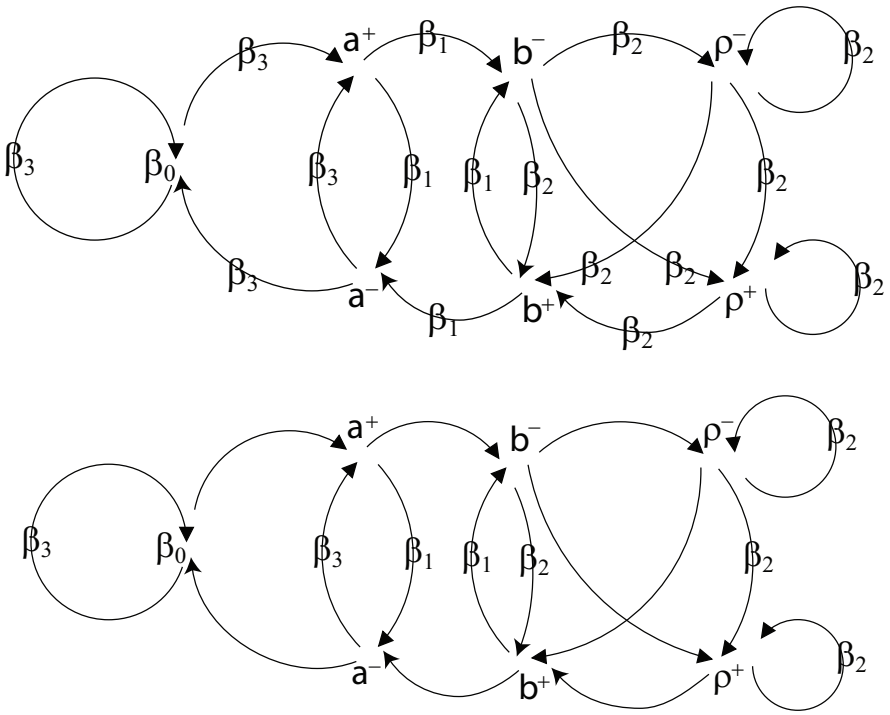

Figure 4.19: $\widetilde{\mathfrak{D}}_0^*$ (Top) the nearly-dual transition diagram for $\widetilde{\mathcal{O}}^{\odot}$; $\widetilde{\mathfrak{D}}_0^{*\prime}$ (Bottom) the nearly-dual transition diagram for $\widetilde{\mathcal{O}}^{\odot}$ following geometric renormalization. The nearly-dual transition diagrams $\widetilde{\mathfrak{D}}_{0-}^*$ and $\widetilde{\mathfrak{D}}_{0-}^{*\prime}$ before and after geometric renormalization are obtained by changing the polarity of the signed vertex labels in $\widetilde{\mathfrak{D}}_0^*$ and $\widetilde{\mathfrak{D}}_0^{*\prime}$.

Vertex labels of the transition diagram $\widetilde{\mathfrak{D}}_0^{*'}$ for linear trajectories τ^θ, $\theta \in [0, \frac{\pi}{2}]$ in $\mathcal{L}^{\odot'}$ are the same as those in $\widetilde{\mathfrak{D}}_0^{*}$, while directed edges are labeled according to the diagonals in $\mathcal{L}^{\odot'}$ a trajectory in $[0, \frac{\pi}{2}]$ must cross in getting from the rectangle side labeled by the initial vertex to the rectangle side labeled by the terminal vertex.

Let $\mathrm{p}(\widetilde{\mathrm{w}})$ be the path realizing $\widetilde{\mathrm{w}} = c(\widetilde{\tau}^\theta)$ in $\widetilde{\mathfrak{D}}_0^{*}$; the cutting sequence $\widetilde{\mathrm{w}}' = c'(\tau^\theta)$ of τ^θ in $\widetilde{\mathfrak{D}}_0^{*'}$ is the word obtained by tracing $\mathrm{p}(\widetilde{\mathrm{w}})$ through $\widetilde{\mathfrak{D}}_0^{*'}$. Examination of the diagrams $\widetilde{\mathfrak{D}}_0^{*}$ and $\widetilde{\mathfrak{D}}_0^{*'}$ reveals that:

1. Every occurrence of $\rho^{\pm}$ in $\widetilde{\mathrm{w}}$ is retained in $\widetilde{\mathrm{w}}'$.

2. Exactly the sandwiched letters in $\widetilde{\mathrm{w}}\Big|_{\mathscr{B}}$ are retained in $\widetilde{\mathrm{w}}'$

Applying $\left(\Upsilon \circ \mathrm{h}^{-1} \circ \kappa^{-1}\right)$ to τ^θ and $\mathcal{L}^{\odot'}$ produces the renormalized trajectory $\mathcal{D}(\tau)$ in $\widetilde{\mathcal{O}}^{\odot}$ with the same combinatorics as τ^θ in $\mathcal{L}^{\odot'}$. Dropping the auxiliary edges from $\widetilde{\mathcal{O}}^{\odot}$ and dropping *primes* from octagon side labels yields the cutting sequence of τ' in $\mathcal{O}^{\odot}$, and by observations 1 and 2 above, this sequence is precisely $c(\tau') = \mathrm{w}' = \mathrm{D}(\mathrm{w}) = c(\mathrm{w})'$. By symmetry, the corresponding statement holds for $c(\tau)$, $\tau \in \mathcal{T}_{0^-}$ with respect to $\widetilde{\mathfrak{D}}_{0^-}^{*}$ and $\widetilde{\mathfrak{D}}_{0^-}^{*'}$.

□

Corollary 4.4.0.2. *If* $\mathrm{w} \in \mathcal{CS}^{\odot}$, *then* w *is infinitely deriveable and* $\mathrm{w}^{(n)} = \mathrm{D}^{(n)}(\mathrm{w}) \in \mathcal{CS}^{\odot}$ $\forall\, n \in \mathbb{N}$.

Proof. This follows immediately from Proposition 4.3.0.1 and Definition 4.4.0.2 of the operator D on admissible words in $\left(\mathscr{A}^{\odot}\right)^{\mathbb{Z}}$.

□

4.5 Generation and Coherence on $\mathcal{O}^{\odot}$

The set of infinitely deriveable sequences is the closure of the set of cutting sequences on the square torus, but this is no longer the case in higher genus. Consider for example the following admissible periodic word:

Example 4.5.0.1.

$$\mathrm{w} = \overline{\beta_2\,\rho^-\,\beta_2\,\rho^+\,\beta_2\beta_1\,\beta_3\,\beta_1\,\beta_2\,\rho^+\,\beta_2\,\beta_1\,\beta_3\,\beta_1\,\beta_2\,\rho^-\,\beta_2\,\beta_1\,\beta_3\,\beta_1\,\beta_2\,\beta_1\,\beta_3\,\beta_0\,\beta_3\,\beta_1} \tag{4.1}$$

According to Definition 4.4.0.2, the derivative of w *is:*

$$\mathrm{w}' = \overline{\rho^-\,\beta_2\,\rho^+\,\beta_3\,\rho^+\,\beta_3\,\rho^-\,\beta_3\,\beta_2\,\beta_0}$$

Examining Figures 4.9 and 4.12 indicates thats w′ *is realizable in* $\mathfrak{D}_6$ *with normalization* $\mathrm{n}(\mathrm{w}') = \overline{\beta_1\,\beta_2\,\rho^-\,\beta_2\rho^+\,\beta_2\,\beta_1\,\beta_3}$ *whose augmentation* $\widetilde{\mathrm{n}}(\mathrm{w}')$ *is realizable in* $\widetilde{\mathfrak{D}}_0^*$*, making* w′ *admissible. After a second derivation, we get:*

$$\mathrm{w}'' = \overline{\rho^- \beta_2 \rho^+ \beta_0}$$

which is realizable in $\mathfrak{D}_5$ *and* $\mathfrak{D}_6$*, with normalizations* $\mathrm{n}_5(\mathrm{w}'') = \overline{\beta_3\,\beta_1} = \overline{\beta_1\,\beta_3} = \mathrm{n}_6(\mathrm{w}'')$ *whose augmentation* $\widetilde{\mathrm{w}''}$ *is realizable in* $\widetilde{\mathfrak{D}}_0^*$.

And all subsequent derivations, $n \geq 3$*, will be :*

$$\mathrm{w}^{(n)} = \overline{\beta_1\,\beta_3}$$

always realizable in $\mathfrak{D}_5$ *and* $\mathfrak{D}_6$ *with augmented normalization realizable in* $\widetilde{\mathfrak{D}}_0^*$*. Hence* w *is infinitely deriveable.*

However, any trajectory segment in Σ_0 *that realizes the first half of* w *could not also realize the second half. In particular, a segment in* Σ_0 *realizing* $[\beta_1\,\beta_2\,\rho^-\,\beta_2\,\rho^+\,\beta_2\,\beta_1]$ *has to have slope* $< \frac{1}{3}\tan(\frac{\pi}{8})$*, whereas a segment in* Σ_0 *realizing* $[\beta_1\,\beta_2\,\beta_1]$ *necessarily has slope greater than* $\frac{1}{2}\tan(\frac{\pi}{8})$ *(Figure 4.20).*

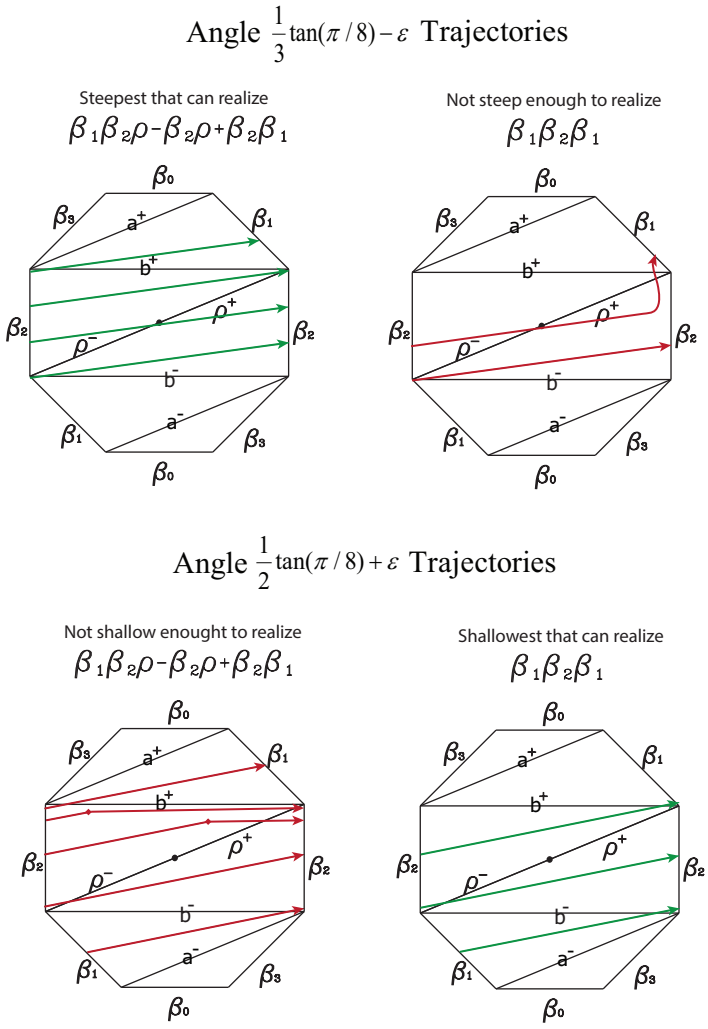

Figure 4.20

Theorem 4.5.0.1 (Set of Infinitely Coherent Sequences is the Closure of the Space of Cutting Sequences)**.** *The set of infinitely coherent sequences in* $\left(\mathscr{A}^{\odot}\right)^{\mathbb{Z}}$ *coincides with the closure* $\overline{\mathcal{CS}}^{\odot}$ *of the set of cutting sequences of linear trajectories on* $\mathcal{O}^{\odot}$.

Infinitely deriveable words, such as those in Example 4.5.0.1 encode concatenated sequences of linear segments whose angles in Σ_0 map to different angular sectors under geometric renormalization (Figure 4.15). Such concatenations are not geometric limits of any sequence of bi-infinite linear trajectories in $\mathcal{O}^{\odot}$, nor

are their cutting sequences limits of sequences of cutting sequences of linear trajectories. As a further constraint on deriveable sequences, we introduce the notion of *coherence*. Coherence or *coherence with respect to (i,j)* is a property involving the relationship between a deriveable word w, the sector Σ_i with respect to which it is admissible, the sandwiched letters in $\mathrm{n}(\mathrm{w})\Big|_{\mathscr{B}}$ and the sector Σ_j with respect to which w′ is admissible. An infinitely deriveable word $\mathrm{w} \in \left(\mathscr{A}^{\odot}\right)^{\mathbb{Z}}$ is *infinitely coherent* if $\forall\ n \in \mathbb{N}$, $\exists\ (i_n, j_n)$ with respect to which $\mathrm{w}^{(n)} = \mathrm{D}^{(n)}(\mathrm{w})$ is coherent.

Definition 4.5.0.1. *A deriveable word* $\mathrm{w} \in \left(\mathscr{A}^{\odot}\right)^{\mathbb{Z}}$ *realizable in* $\mathfrak{D}_i$, $i \in \{0, 1, 2, ..., 15\}$ *with* w′ *realizable in* $\mathfrak{D}_j$, $j \in \{1, 2, ..., 15\}$ *is* coherent with respect to (i,j) *when the sandwiched letters in the restriction* $\mathrm{n}(\mathrm{w})\Big|_{\mathscr{B}}$ *of* $\mathrm{n}(\mathrm{w})$ *to* $\mathscr{B} = \{\beta_0, \beta_1, \beta_2, \beta_3\}$ *fall only into the categories given for* $\mathcal{G}_k$, $k = \left[\frac{j \pmod 8}{2}\right]$ *(Table in Figure 4.23);* w *is* infinitely coherent *if it is infinitely deriveable, and for each* $n \in \{0, 1, 2, ...\}$ *there exist* i_n, j_n *such that* $\mathrm{D}^{(n)}(\mathrm{w})$ *is coherent with respect to* (i_n, j_n)

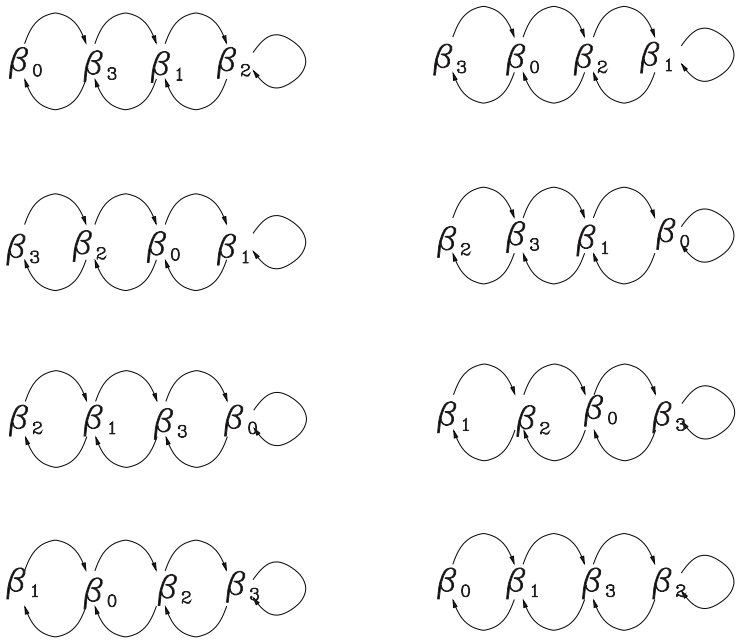

Figure 4.22: Transition diagrams for the unpunctured regular octagon. The property of coherence for sequences from $\mathrm{w} \in \left(\mathscr{A}^{\odot}\right)^{\mathbb{Z}}$ is defined on their restrictions $\mathrm{w}\Big|_{\mathscr{B}}$ to exterior octagon side labels.

sandwiched letter	β_0	β_1	β_2	β_3
in $\mathcal{G}_0$ sandwiched by	β_3	β_2	β_1	β_0
in $\mathcal{G}_1$ sandwiched by	β_3	β_2	β_1	β_1
in $\mathcal{G}_2$ sandwiched by	β_3	β_2	β_2	β_1
in $\mathcal{G}_3$ sandwiched by	β_3	β_3	β_2	β_1

Figure 4.23: A deriveable Σ_i-admissible word w with Σ_j-admissible derivative w′ is *coherent* with respect to (i, j) if the sandwiched letters in $\mathrm{n}(\mathrm{w}')\Big|_{\mathscr{B}}$ fall only into categories given for $\mathcal{G}_k$, $k = \lfloor \frac{j \pmod 8}{2} \rfloor$

The set of sequences coherent with respect to some finite or infinite sequence of sectors $\{s_k\} \in \mathrm{S}^*$ will be denoted by $\mathscr{C}(\{s_k\})$; the set of infinitely coherent sequences is $\mathscr{C}^\infty$.

Definition 4.5.0.2. *A* sequence of sectors *for a linear trajectory τ on $\mathcal{O}^\odot$, (resp. of its cutting sequence $\mathrm{w} = \boldsymbol{c}(\tau)$), is a sequence $\{s_j{}_\epsilon(\tau)\}_{j\in\mathbb{Z}}$ where $s_j \in \{0,1,2,...,7\}$, $\epsilon \in \{+,-\}$ is the index of the angular sector of the j^{th} geometric derivative $\tau^{(j)} = \mathcal{D}(\mathrm{n}(\tau^{(j-1)}))$ of τ. Equivalently, $s_j \in \{0,1,2,...,7\}$, $\epsilon \in \{+,-\}$ is the index of the sector with respect to which the j^{th} combinatorial derivative $\mathrm{w}^{(j)} = \mathrm{D}(\mathrm{n}(\mathrm{w})^{(j-1)})$ of $\mathrm{w} = \boldsymbol{c}(\tau)$ is admissible.*

For our purposes it suffices to consider the subset S^* of sector sequences for $\tau \in \mathcal{T}_0$, i.e. the sequences $\{\mathrm{s}_k(\tau)\}_{k\in\mathbb{Z}}$ where $s_0 = 0$, $s_k \neq 0$, $k \neq 0$.

4.5.1 Inverting Derivation and Interpolating Words

Let $\mathcal{O}^{\odot\prime} = \Psi\left(\mathcal{O}^\odot\right)$ be the renormalized version of $\mathcal{O}^\odot$ and $\mathcal{O}^{\odot\prime+} = \left(\Upsilon \circ \mathrm{H}^-\right)\cdot \mathcal{O}^\odot$ the image of $\mathrm{H}^- \cdot \mathcal{O}^\odot$ in $\mathcal{O}^{\odot\prime}$ (see Figure 4.26). Knowing the admissibility criteria and derivation rule for linear trajectories on $\mathcal{O}^\odot$ and sequences in $\left(\mathscr{A}^\odot\right)^{\mathbb{Z}}$ allows us to iteratively construct infinitely deriveable words from admissible words. Since geometric derivation takes place on normalized trajectories in $\tau \in \mathcal{T}_\epsilon$, $\epsilon \in \{0, 0^-\}$ and produces trajectories in $\mathcal{T}_{j^{\,\mathrm{sgn}\,(\epsilon)}}$, $j^{\,\mathrm{sgn}\,(\epsilon)} \neq 0$, the cutting sequence of the Σ_0 trajectory $\widetilde{\tau}_0$ from which τ was geometrically derived can be

recovered by examining the edge-crossings of τ through the image of $\mathcal{O}^{\odot\prime+}$ in $\mathcal{O}^{\odot\prime}$ (see Figures 4.26 and 4.27).

The generation diagram $\mathcal{G}_j$ is an augmentation of the transition diagram $\mathfrak{D}_j$; each pair of labeled vertices β,$\widetilde{\beta}$ joined by a directed edge in $\mathfrak{D}_j$ codes a Σ_j trajectory segment $\overline{\tau}$ in $\mathcal{O}^{\odot}$ whose intersection with $\partial\mathcal{O}$ consists of an initial point on β, and a terminal point on $\widetilde{\beta}$. In $\mathcal{G}_j$, the edge joining β and $\widetilde{\beta}$ is labeled by the labeled sides of $\mathcal{O}^{\odot\prime+}$ that $\overline{\tau}$ crosses between its final departure from β and its first encounter with $\widetilde{\beta}$.

Definition 4.5.1.1. *Let* w_0 *be admissible with respect to* Σ_i. *Let* $\mathrm{p}_0 = \mathrm{p}(\mathrm{w}_0)$ *be the path realizing* w_0 *in* $\mathfrak{D}_i$. *The fact that* w_0 *is admissible means there is also a path* $\widetilde{\mathrm{p}}_0 = \mathrm{p}(\widetilde{\mathrm{w}_0})$ *realizing the augmentation* $\widetilde{\mathrm{w}}_0$ *of (the normalization of)* w_0 *in* $\widetilde{\mathfrak{D}}_0^*$. *Let* $\mathfrak{g}_i^0 : \mathcal{A}_i \to \mathcal{A}_0$, $i = 1, 2, ..., 7$ *be operators defined to take* $\mathrm{w}_0 \in \mathcal{A}_i$ *to the* interpolated *word,* $\mathrm{w}_1 = \mathfrak{g}_i^0(\mathrm{w}_0) \in \mathcal{A}_0$, *by tracing path* p_0 *through the* Σ_i generation diagram $\mathcal{G}_i$ *(Figure 4.26).*

Remark 4.5.1.1. *Note that* w_0 *is assumed here to be* Σ_i*-admissible, not just weakly* Σ_i*-admissible. Thus, the order of* $\rho^{\pm}$*'s in* w_0 *is such that* w_0 *maps, under* $\boldsymbol{\pi}_i$, *to a word whose augmentation is realizable in* $\widetilde{\mathfrak{D}}_0^*$. *This means that the path* p_0 *through* $\mathfrak{D}_i$ *moves through edges labeled by* ρ^+ *and* ρ^- *in a way that will produce admissible words when followed through* $\mathcal{G}_i$.

Proposition 4.5.1.1. *If* $\mathrm{w} = c(\tau)$ *is a* Σ_j*-admissible cutting sequence and* $W = \mathfrak{g}_j^0(\mathrm{w})$, *then* $W' = \mathrm{w}$.

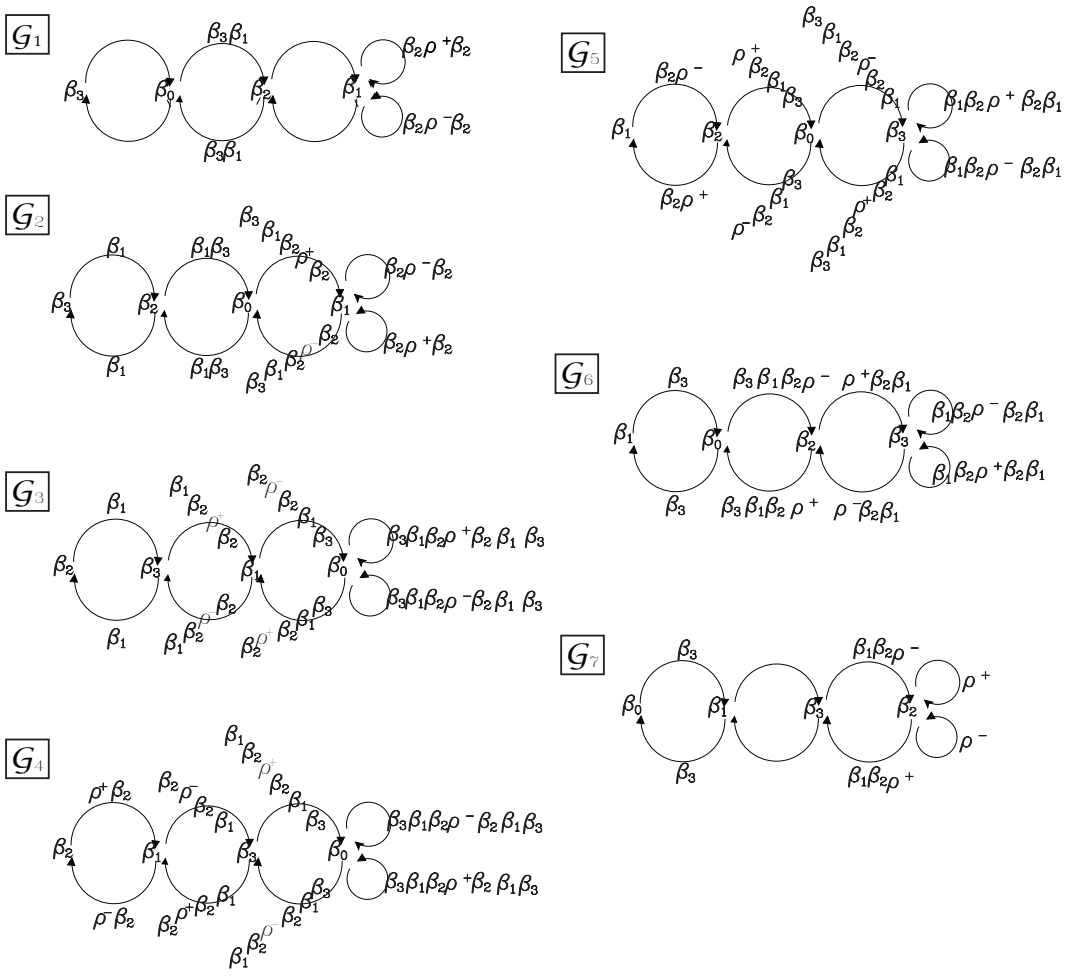

Figure 4.25: Generation diagrams, $\mathcal{G}_i$, $i \in \{1, 2, ..., 7\}$

Proof. Without loss of generality assume w $= \mathcal{c}(\tau)$ is the cutting sequence of a linear trajectory in direction $\theta \in \Sigma_{j^+}$ for some $j \in \{1, 2, ..., 7\}$. So by Proposition 4.1.0.2 w $= ...w_{i-1}\, w_i\, w_{i+1}... = \mathcal{c}(\tau)$ is Σ_j-admissible. Moreoever, the Σ_0-admissible word $W = \mathfrak{g}_j^0(\mathrm{w})$ corresponds, by construction, to the interpolated word that records between w_i and w_{i+1} the edge-crossings of τ in $\mathcal{O}^{\odot\prime+}$ that occur as τ moves from edge w_i to edge w_{i+1} in $\mathcal{O}^{\odot\prime}$, the geometric derivative of $\mathcal{O}^{\odot}$. This is necessarily a word in Σ_0 since the image of $\bigcup_{j=1}^{7} \mathcal{T}_j$ under Ψ is $\mathcal{T}_0$ by

Observation 4.3.0.1.

□

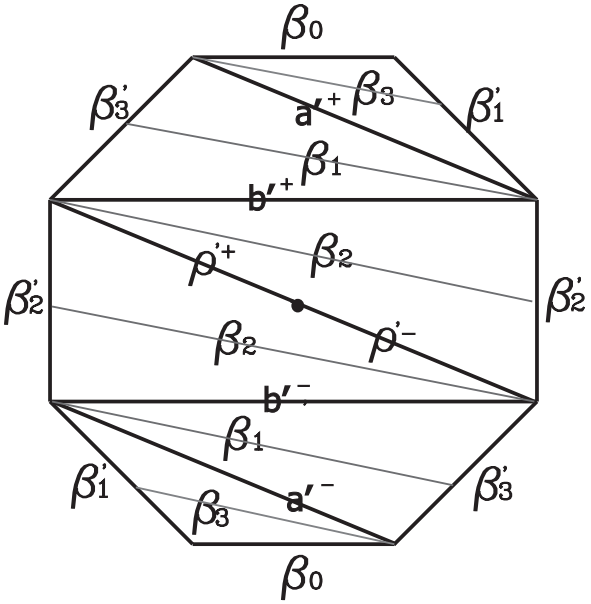

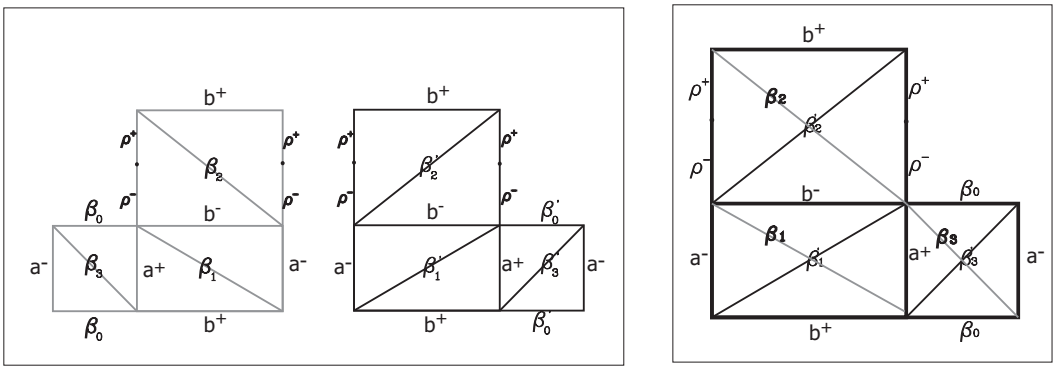

Figure 4.26: Top: $\mathcal{O}^{\odot\prime+}$ (gray) superimposed on $\mathcal{O}^{\odot\prime}$ (black); Bottom left: $\mathcal{L}^{\odot}$ and $\mathcal{L}^{\odot'}$; Bottom right: $\mathcal{L}^{\odot'}$ with diagonals from $\mathcal{L}^{\odot}$ superimposed.

Example 4.5.1.1. *The finite word*

$$\mathrm{w} = [\beta_3\,\rho^+\,\beta_1\,\rho^-\,\beta_0\,\rho + \beta_0\,\rho^-\,\beta_0\,\rho^+\,\beta_1]$$

is realizable by the finite path p *through* $\mathfrak{D}_3$. *Following* p *through* $\mathcal{G}_3$ *yields:*

$$\mathfrak{g}_3^0(\mathrm{w}) = [\beta_3\,\beta_1\,\beta_2\,\rho^+\,\beta_2\,\beta_1\,\beta_2\,\rho^-\,\beta_2\,\beta_1\,\beta_3\,\beta_0\,\beta_3\,\beta_1\,\beta_2\,\rho^+\,\beta_2\,\beta_1\,\beta_0\,\beta_3\,\beta_1\,\beta_2\,\rho^-\,\beta_2\,\beta_1\,\beta_0\,\beta_3\,\beta_1\,\beta_2\,\rho^+\,\beta_2\,\beta_1]$$

which is Σ_0-admissible. Moreover, if we adopt the convention that derivation on a finite word retains first and last letter, we readily verify that $\left(\mathfrak{g}_j^0(\mathrm{w})\right)' = \mathrm{w}$.

Definition 4.5.1.2. *Generating $W \in \mathcal{A}_i$, $i \neq 0^{\pm}$ such that $\mathrm{n}(W)' = \mathrm{w}$ for $\mathrm{w} \in \mathcal{A}_j$ is now straightforward: $\mathfrak{g}_j^i = \boldsymbol{\pi}_i^{-1} \circ \mathfrak{g}_j^0(\mathrm{w})$.*

Proposition 4.5.1.2. *If $\mathrm{w} \in \mathcal{A}_j$ and $W = \mathfrak{g}_j^i(\mathrm{w})$ then W is coherent with respect to (i, j) and $\mathrm{w} = \mathrm{n}(W)'$.*

Proof. Inspection of Figure 4.25 verifies that the possible sandwiched letters in the restriction to $\mathscr{B}$ of $W_1 = \mathfrak{g}_j^0(\mathrm{w}) = \boldsymbol{\pi}_i(\boldsymbol{\pi}_i^{-1}\mathfrak{g}_j^0(\mathrm{w})) = \boldsymbol{\pi}_i(\mathfrak{g}_j^i(\mathrm{w}) = \mathrm{n}(\mathfrak{g}_j^i(\mathrm{w}) = \mathrm{n}(W)$ are exactly those given in Figure 4.23 for $\mathcal{G}_k$, $k = \lfloor \frac{j \pmod 8}{2} \rfloor$. Deriving W_1 drops the sandwiched letters in $W_1\Big|_{\mathscr{B}}$ acquired during generation, so $W_1' = \mathrm{n}(W)' = \mathrm{w}$. □

As a corollary of Propositions 4.5.1.1 and 4.5.1.2 we have:

Corollary 4.5.1.3. *If $\mathrm{w} = c(\tau)$ is a cutting sequence on $\mathcal{O}^{\odot}$, then w is coherent. Specifically, if $\tau \in \mathcal{T}_i$ and $\tau' \in \mathcal{T}_j$, w is coherent with respect to (i, j)*

Even more is true however.

Corollary 4.5.1.4 (Cutting Sequences are Infinitely Coherent)**.** *If $\mathrm{w} = c(\tau)$ is the cutting sequence of a linear trajectory τ on $\mathcal{O}^{\odot}$, w is infinitely coherent.*

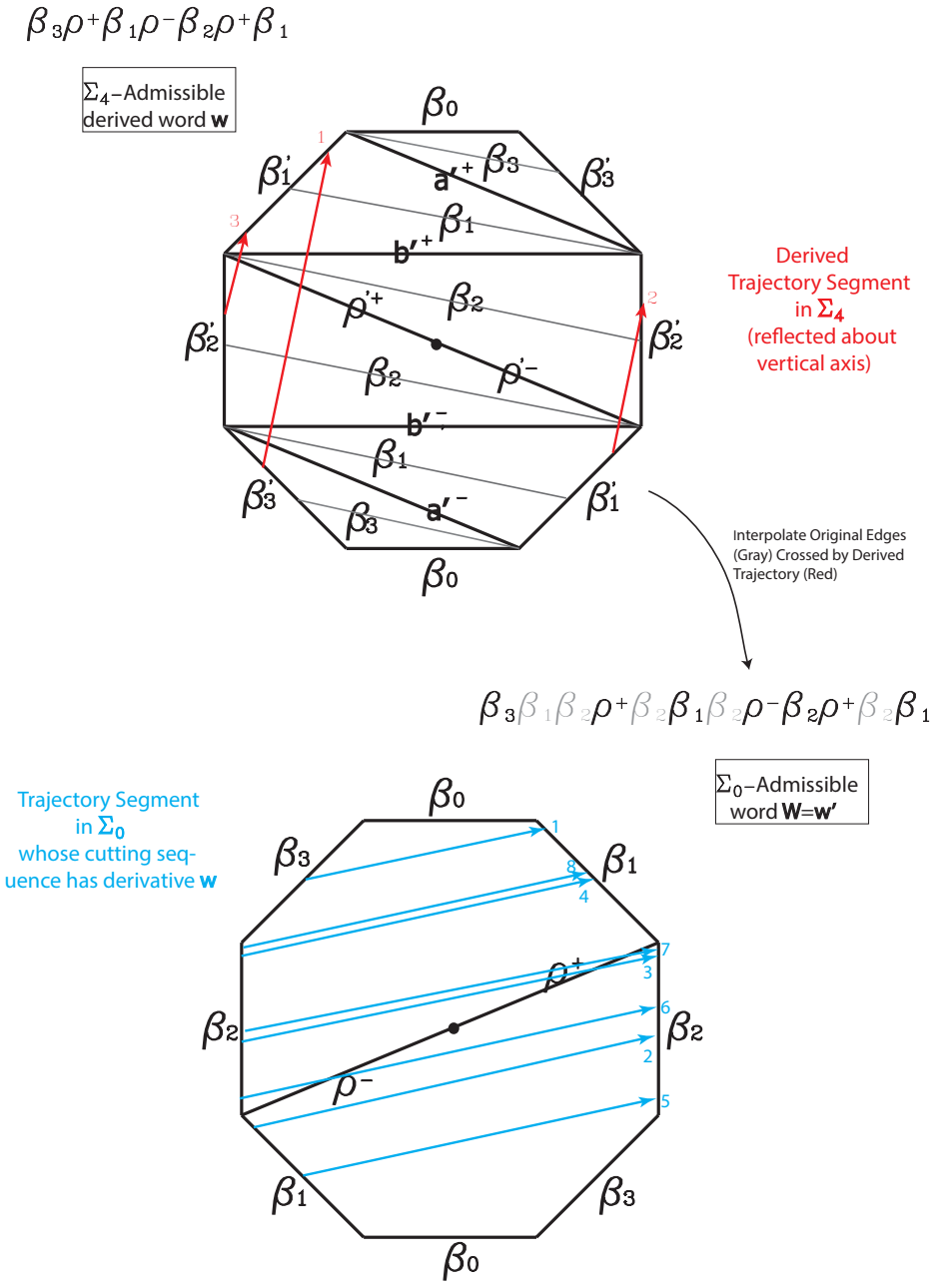
$\beta_3\rho^+\beta_1\rho^-\beta_2\rho^+\beta_1$
Σ_4–Admissible derived word **w**
β_0
β_1'
β_3
β_3'
a'^+
β_1
b'^+
ρ'^+
β_2
β_2'
β_2'
ρ'^-
β_2
b'^-
β_1
β_3'
β_3
a'^-
β_1'
β_0
Derived Trajectory Segment in Σ_4 (reflected about vertical axis)
Interpolate Original Edges (Gray) Crossed by Derived Trajectory (Red)
$\beta_3\beta_1\beta_2\rho^+\beta_2\beta_1\beta_2\rho^-\beta_2\rho^+\beta_2\beta_1$
Σ_0–Admissible word **W=w'**
Trajectory Segment in Σ_0 whose cutting sequence has derivative **w**
β_0
β_3
β_1
ρ^+
β_2
β_2
ρ^-
β_1
β_3
β_0
1
8
4
7
3
6
2
5

Figure 4.27

Proof. Corollary 4.4.0.2 ensures that w is infinitely deriveable. Let $\{s_k\}_{k\in\mathbb{N}}$ be the sequence of sectors (see Definition 4.5.0.2) for τ, so $\mathrm{w}^{(n)} = \mathrm{D}^{(n)}(\mathrm{w}) \in \mathcal{A}_{s_k}$ for all k. Now, by Corollary 4.5.1.3, we have that for every $j \in \mathbb{N}$, $\mathrm{w}^{(j)}$ is coherent with respect to (s_j, s_{j+1}).

□

It remains to show that infinitely coherent words are limits of cutting sequences of linear trajectories on $\mathcal{O}^{\odot}$. Toward this end we introduce some notation and results from [76]. After accounting for $\rho^{\pm}$'s in generation diagrams and for different admissibility conditions for words in $\left(\mathscr{A}^{\odot}\right)^{\mathbb{Z}}$, Smillie and Ulcigrai's results on generation and coherence for the unpunctured regular octagon translate directly to the centrally punctured case. These results are derived from an *additive continued fraction algorithm* for the octagon which is built on the *sequence of sectors* of a linear trajectory in $\mathcal{O}$. These sequences and their convergence properties are common to trajectories (modulo those that intersect the center-point of $\mathcal{O}$) in $\mathcal{O}$ and $\mathcal{O}^{\odot}$, and we will use the relevant results from [74] without adaptation.

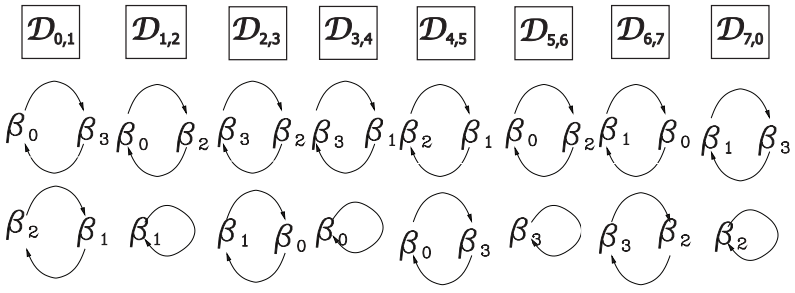

Figure 4.29: Period 2 and 1 transitions in unpunctured octagon shared by transition diagrams for adjacent angular sectors.

Let $\mathscr{P}_k$ denote the set of period 1 or 2 periodic words in $\mathfrak{D}_k$ (Figure 4.22), so for example $\mathscr{P}_6 = \{\overline{\beta_1\beta_0}, \overline{\beta_0\beta_2}, \overline{\beta_2\beta_3}, \overline{\beta_3}\}$. Further, for a sequence of sectors $\{s_k^\epsilon\}_{k\in\mathbb{N}} \in S^*$, define:

$$\mathscr{G}(s_0, s_1, ..., s_k) = \{\mathfrak{g}_{s_1}^{s_0}\mathfrak{g}_{s_2}^{s_1}...\mathfrak{g}_{s_k}^{s_{k-1}}\mathrm{u} : \mathrm{u} \in \mathcal{A}_{s_k}\}$$

and

$$\mathscr{P}(s_0, s_1, ..., s_k) = \{\mathfrak{g}_{s_1}^{s_0}\mathfrak{g}_{s_2}^{s_1}...\mathfrak{g}_{s_k}^{s_{k-1}}\mathrm{u} : \mathrm{u} \in \mathscr{P}_{s_k}\}$$

Lemma 4.5.1.5 (Smillie-Ulcigrai [76], Lemma 2.4.17)**.** *For any sequence of sectors $s = \{s_k^\epsilon\}_{k\in\mathbb{N}} \in S^*$ and for each k, all words in $\mathscr{P}(s_0, s_1, ..., s_k)$ are cutting sequences of periodic trajectories.*

Proposition 4.5.1.6 (Smillie-Ulcigrai [76], Prop. 2.4.20 (Infinite Coherence via Generation))**.** *A word* w *is infinitely coherent with respect to the sequence of sectors $s = \{s_k^\epsilon\}_{k\in\mathbb{N}} \in S^*$ if and only if:*

$$\mathrm{w} \in \bigcap_{k\in\mathbb{N}} \mathscr{G}(s_0, s_1, ..., s_k)$$

Thus, a word w *is infinitely coherent if and only if:*

$$\mathrm{w} \in \bigcap_{k\in\mathbb{N}} \bigcup_{\substack{s_0\in\{0,1,..,7\}\\ s_i\in\{1,2,..,7\},i>0}} \mathscr{G}(s_0, s_1, ..., s_k)$$

Proposition 4.5.1.7 (Smillie-Ulcigrai [76], Prop. 2.4.21)**.** *If* w *is an infinitely coherent word, every finite subword* w^* *of* w *is realized by a periodic trajectory* τ *in the sense that* $\mathrm{w}^* = c(\tau^*)$ *is the cutting sequence of some finite segment* τ^* *of* τ*. In particular, if* w *is infinitely coherent with respect to* $\{s_k\}_{k\in\mathbb{N}}$*, then each finite subword of* w *occurs as a subword of some periodic cutting sequence in*

$$\bigcup_{k\in\mathbb{N}} \mathscr{P}(s_0, s_1, ..., s_k)$$

Corollary 4.5.1.8 (Smillie-Ulcigrai [76], Cor. 2.4.22)**.** *If* w *is infinitely coherent with respect to* $\{s_k\}_{k\in\mathbb{N}}$ *then*

$$\mathrm{w} \in \overline{\bigcup_{k\in\mathbb{N}} \mathscr{P}(s_0, s_1, ..., s_k)}$$

Lemma 4.5.1.9 (Set of Infinitely Coherent Sequences Contains the Closure of the Space of Cutting Sequences)**.** *If* $\mathrm{w} \in \left(\mathscr{A}^{\circlearrowright}\right)^{\mathbb{Z}}$ *is infinitely coherent, then there exists a sequence* $\{\tau_j\}_{j\in\mathbb{N}}$ *of linear trajectories on* $\mathcal{O}^{\circlearrowright}$ *such that* $\mathrm{w} = \lim_{j\to\infty} c(\tau_j)$*.*

Proof. This is effectively a restatement of Corollary 4.5.1.8; it follows from

Lemma 4.5.1.5 and Proposition 4.5.1.7.

□

Proof of Theorem 4.5.0.1. Theorem 4.5.0.1 follows as a corollary from Corollary 4.5.1.4 Lemma 4.5.1.9 and Proposition 4.5.1.6. Specifically, from Corollary 4.5.1.4 we get the inclusion $\mathcal{CS}^{\odot} \subseteq \mathscr{C}^{\infty}$. The sets $\mathcal{A}_j$, $j \in \{0, 1, ..., 15\}$ are subshifts of finite type, thus they are closed. For each $j \in \{0, 1, ..., 15\}$, the length of any subword common to both w and $\mathrm{v} \in \mathcal{A}_j$ cannot decrease under $\mathfrak{g}_j^i$, $i \in \{0, 1, ..., 15\}$ so these operators and their compositions are continuous. Which makes $\mathscr{C}^{\infty} = \bigcap_{k \in \mathbb{N}} \bigcup_{\substack{s_0 \in \{0,1,..,7\} \\ s_i \in \{1,2,..,7\}, i>0}} \mathscr{G}(s_0, s_1, ..., s_k)$ (equality by Proposition 4.5.1.8) the countable intersection of finite unions of closed sets. So $\mathscr{C}^{\infty}$ is a closed set consisting of limit points of cutting sequences, i.e. $\mathscr{C}^{\infty} = \overline{\mathcal{CS}}^{\odot}$.

□

CHAPTER 5

ARBITRARY GENUS: THE $\left(\frac{\pi}{N}\right)$-ISOSCELES TRIANGLE

Hitting sequences on $\left(\frac{\pi}{n}\right)$-isosceles triangles for $n > 4$ can be characterized using machinery analogous to that employed for the $\left(\frac{\pi}{4}\right)$-isosceles triangle. All relevant geometric features of the $\left(\frac{\pi}{4}\right)$-isosceles triangle surface have analogues in higher genus $\left(\frac{\pi}{n}\right)$-isosceles triangle surfaces, $n > 4$. The $\left(\frac{\pi}{n}\right)$-isosceles triangle unfolds into a centrally punctured regular $2n$-gon $\mathrm{P}_{2n}^{\odot}$. The translation surface $\mathsf{S}_{\mathrm{P}_{2n}}^{\odot}$ is geometrically identical to the surface $\mathsf{S}_{\mathrm{P}_{2n}}$ that arises from identifying parallel sides of the unpunctured regular $2n$-gon. When $n = 2k \geq 4$, $\mathsf{S}_{\mathrm{P}_{2n}}$ has a singular point with cone angle $2\pi(n-1)$ and decomposes into k rationally commensurable horizontal cylinders, one with inverse modulus $\cot\frac{\pi}{2n}$, the others with inverse modulus $2\cot\frac{\pi}{2n}$. When $n = 2k+1 \geq 3$, $\mathsf{S}_{\mathrm{P}_{2n}}$ has two singular points, each with with cone angle $2\pi k$ and decomposes into k horizontal cylinders which all have inverse modulus $2\cot\frac{\pi}{2n}$. Consistent with our convention in previous chapters, we again take the Veech group of a surface to include derivatives of both orientation-preserving *and* orientation-reversing affine automorphisms. In this sense, the Veech group of $\mathsf{S}_{\mathrm{P}_{2n}}$ is generated by the rotation $\mathrm{r}_{\frac{\pi}{n}}$, the shear $\mathrm{H}_{2n}^{+} = \begin{pmatrix} 1 & 2\cot\frac{\pi}{2n} \\ 0 & 1 \end{pmatrix}$ and the reflection r_v about the central vertical axis. The linear transformation $\mathrm{h}_{2n} = \begin{pmatrix} -1 & \cot\frac{\pi}{2n} \\ 0 & 1 \end{pmatrix}$ is not in the Veech group of S_{2n}, but conjugates $\mathrm{H}^{-} = \begin{pmatrix} -1 & 2\cot\frac{\pi}{2n} \\ 0 & 1 \end{pmatrix} \in \mathrm{V}(\mathsf{S}_{\mathrm{P}_{2n}})$ to the orientation-reversing isometry r_v of $\mathsf{S}_{\mathrm{P}_{2n}}$, demonstrating that H^{-} is a hidden symmetry of $\mathsf{S}_{\mathrm{P}_{2n}}$.

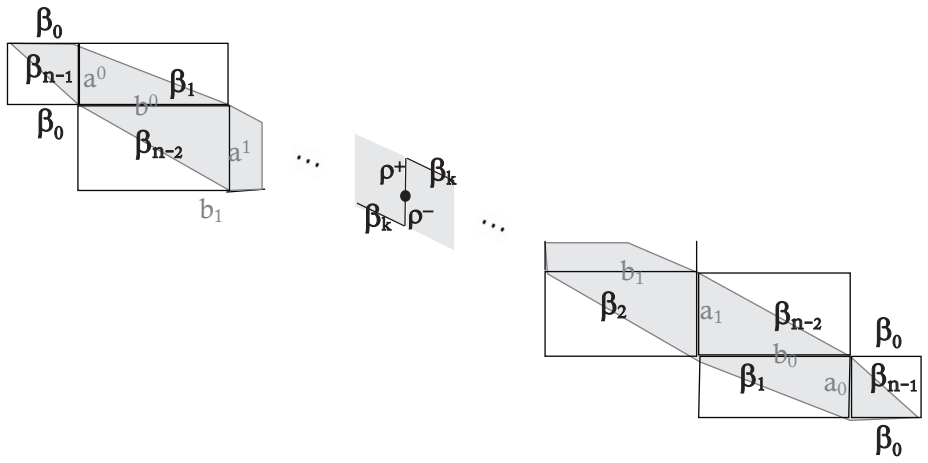

Figure 5.1: The augmented sheared $2n$-gon, $\mathrm{h}_{2n} \cdot \mathrm{P}^{\odot}_{2n}$ for $n = 2k \geq 4$. The indexed a's and b's are boundary edges of horizontal cylinders and cylinders in direction $\left(\frac{\pi}{2n}\right)$ in $\mathrm{P}^{\odot}_{2n}$ (see Figure 4.10 for octagon case). For $n = 2k+1 \geq 5$, the ρ^- is replaced by a λ^- indicating a reflected copy of the left leg of the base triangle.

The combinatorics of $\left(\frac{\pi}{n}\right)$-isosceles, $n > 4$ billiard trajectories are analogues over larger alphabets of the combinatorics for $\left(\frac{\pi}{4}\right)$-isosceles case. For $n = 2k \geq 4$ the coding alphabet on $\mathrm{P}^{\odot}_{2n}$ is $\mathscr{A}^{\odot}_{2n} = \{\beta_0, \beta_1, ..., \beta_{n-1}, \rho^{\pm}\}$. When n is odd, the edge that codes for passage of Σ_0 trajectories under the puncture is actually a reflection of the left leg of the base triangle, so is more appropriately labeled λ^-. For simplicity we will call the parallel reflected triangle legs that encode position with respect to the puncture $\rho^{\pm}$ in both cases. The alphabet $\mathscr{A}^{\odot}_{2n}$ is a disjoint union of $\mathscr{B}_{2n} = \{\beta_0, \beta_1, ..., \beta_n\}$ and $\overline{\mathscr{B}} = \{\rho^-, \rho^+\}$. The symmetries of $\mathrm{P}^{\odot}_{2n}$ allow us to restrict consideration to the angular sector $\Sigma^{2n}_0 = [0, \frac{\pi}{2n}]$. For each $\mathrm{P}^{\odot}_{2n}$ the one-step transition diagram $\mathfrak{D}^{2n}_j$ for $\Sigma^{2n}_j = [\frac{j\pi}{2n}, \frac{(j+1)\pi}{2n}]$, $j = 0, 1, ..., 4n-1$ is obtained from $\mathfrak{D}^{2n}_0$ (Figure 5.2) by a composition $\boldsymbol{\pi}_j = \pi^{\odot}_j \circ \pi_j$ of two permutations: the permutation π_j of vertex labels $\{\beta_0, ..., \beta_{n-1}\}$ corresponding to the isometry sending Σ^{2n}_j to Σ^{2n}_0, and the permutation $\pi^{\odot}_j$ of the set of length $n+2$ words in $\{\emptyset, \rho^-, \rho^+\}$ that, as an ordered $(n+2)$-tuple, label directed edges of diagrams

$\mathfrak{D}_i$,$i = 0, 1, ..., 4n - 1$ (see paragraph following Definition 4.1.0.1 of Section 4.1 and Remark **??** for details in the octagon case).

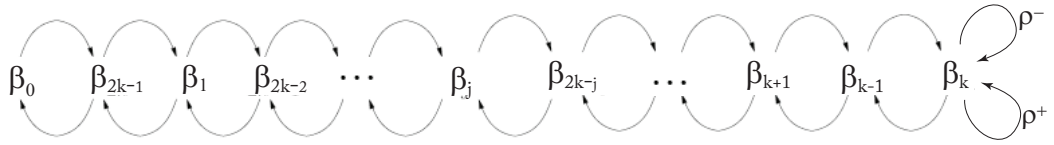

Figure 5.2: The one-step $\Sigma_0 = [0, \frac{\pi}{2n}]$ transition diagram $\mathfrak{D}_0^{2n}$ for $n = 2k \geq 4$. For $n = 2k + 1 \geq 5$, the ρ^- is replaced by a λ^- indicating a reflected copy of the left leg of the base triangle.

In Chapter 4, at each stage of the discussion, we take explicit account of the combinatorial asymmetry between sectors Σ_j and Σ_{j+2n}. Here we will simply make the following observations and proceed with a focus on Σ_j, $j = 0, 1, ..., 2n - 1$.

1. The permutation π_{j+2n} is equal to π_j for $j = 0, 1, ..., 2n - 1$.

2. The permutation $\pi^{\odot}_{j+2n}$ is equal to $(\rho^- \rho^+) \circ \pi^{\odot}_j$ for $j = 0, 1, ..., 2n - 1$

3. The composition $\boldsymbol{\pi}_{j+2n}$ is equal to $(\rho^- \rho^+) \circ \boldsymbol{\pi}_j$, $j = 0, 1, ..., 2n - 1$

4. A word w in $\mathscr{A}^{\odot}_{2n}$ is the cutting sequence of a sector Σ^{2n}_{j+2n} trajectory on $\mathrm{P}^{\odot}_{2n}$ if and only if $(\rho^- \rho^+) \cdot$ w is the cutting sequence of a sector Σ^{2n}_j trajectory, $j = 0, 1, ..., 2n - 1$

A word w $\in \left(\mathscr{A}^{\odot}_{2n}\right)^{\mathbb{Z}}$ is *weakly admissible* if it is realizable in $\mathfrak{D}^{2n}_i$ for some

$i \in \{0, 1, ..., 4n-1\}$. In this case $\mathtt{n}(\mathtt{w}) = \boldsymbol{\pi}_i \cdot \mathtt{w}$ is realizable in $\mathfrak{D}_0^{2n}$ and is called the *normalization* of w. If w is admissible and its normalization is realizable in the augmented almost-dual sector Σ_0^{2n} transition diagram $\mathfrak{D}_{2n}^*$ (Figure 5.3) in which vertices are labeled by boundary segments of the horizontal and angle-$\left(\frac{\pi}{2n}\right)$ cylinders in the augmented $2n$-gon $\widetilde{\mathrm{P}}_{2n}^{\odot}$ (see Figure 4.2 from Chapter 4 for the octagon case)

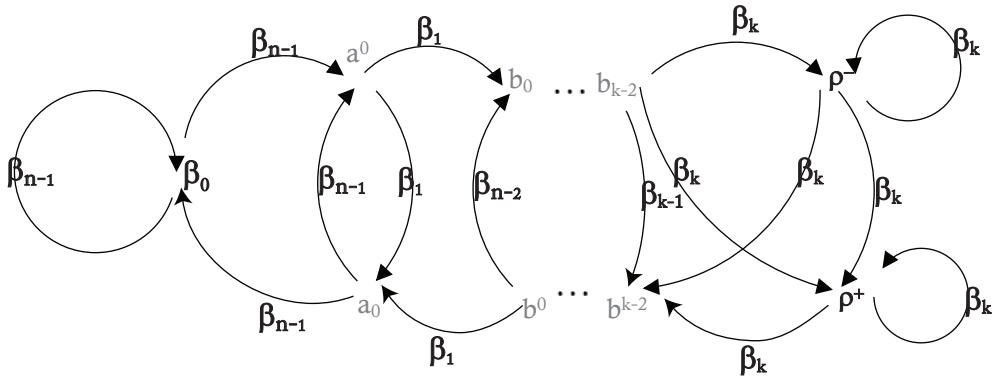

Figure 5.3: The 'almost dual' $\Sigma_0 = [0, \frac{\pi}{2n}]$ transition diagram $\mathfrak{D}_{2n}^*$ for $n = 2k \geq 4$. See Figure 4.19 (top) for the octagon case and Section 4.4 for detail on these transition diagrams for the octagon. For $n = 2k+1 \geq 5$, the ρ^- is replaced by a λ^- indicating a reflected copy of the left leg of the base triangle.

The correspondence between cutting sequences of linear trajectories on $\mathrm{P}_{2n}^{\odot}$ and hitting sequences of billiard trajectories on $\left(\frac{\pi}{n}\right)$-isosceles triangles is obtained exactly in the manner detailed for the $\left(\frac{\pi}{4}\right)$-isosceles triangle in Section 4.2.

For all $n \in \{4, 5, ...\}$, the orientation-reversing affine automorphism

$$\Psi_{2n} = \mathrm{h}_{2n}^{-1} \circ \kappa_{2n}^{-1} \circ r_v \circ \kappa_{2n} \circ \mathrm{h}_{2n}$$

has derivative $\mathrm{H}_{2n}^{-} = \mathrm{h}_{2n}^{-1} \circ r_v \circ \mathrm{h}_{2n}$ which is conjugate to orientation-reversing isometry r_v of $\mathrm{P}_{2n}^{\odot}$. Geometric derivation of Σ_0^{2n} trajectories in $\mathrm{P}_{2n}^{\odot}$ is accomplished by application of Ψ_{2n} (Figures 5.4 and 5.5). The almost-dual transition diagram $\mathfrak{D}_{2n}^{*'}$ (Figure 5.6) captures the two-step transitions possible for Σ_0^{2n} trajectories following renormalization.

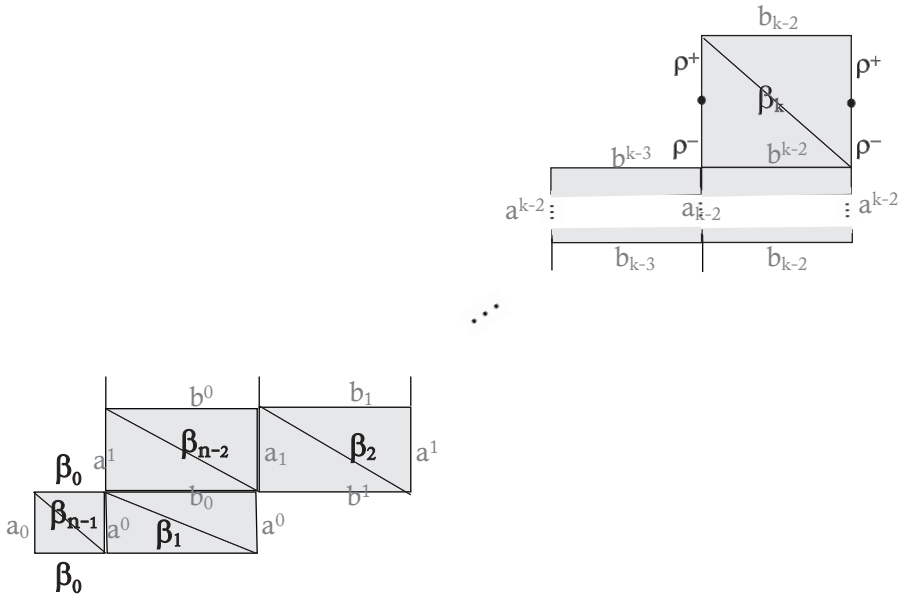

Figure 5.4: The L-shaped table $\mathcal{L}_{2n}^{\odot}$ obtained by applying the cut-and-paste map κ_{2n} to $\mathrm{h}_{2n} \cdot \mathrm{P}_{2n}^{\odot}$ for $n = 2k \geq 4$. (See Figure 4.10 for an analogous cut-and-paste map applied in the octagon case.) For $n = 2k+1 \geq 5$, the ρ^{-} is replaced by a λ^{-} indicating a reflected copy of the left leg of the base triangle.

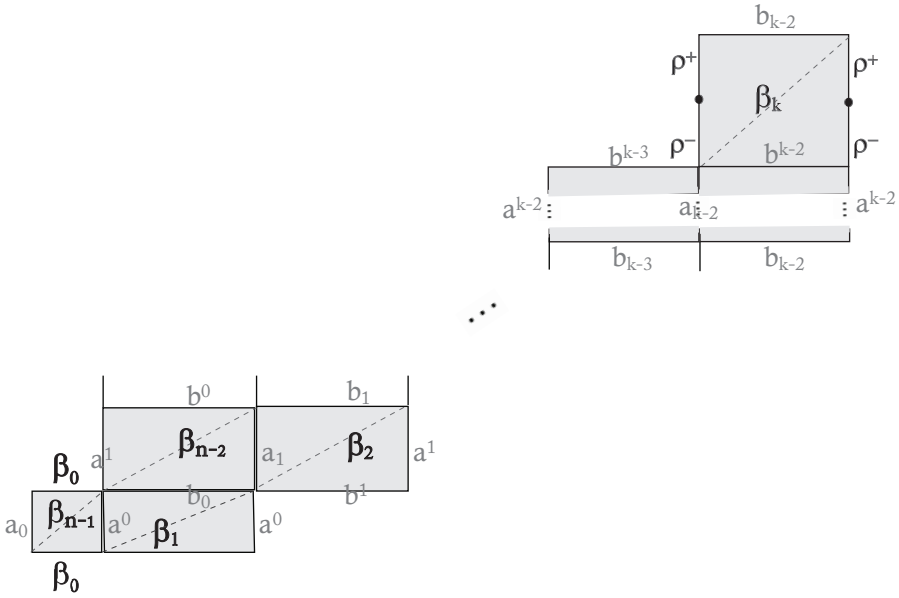

Figure 5.5: The reflected L-shaped table $\mathcal{L}_{2n}^{\odot\prime}$ obtained by reflecting each rectangle of $\mathcal{L}_{2n}^{\odot}$ about its central vertical axis, for $n = 2k \geq 4$. (See Figure 4.17 for octagon case.) For $n = 2k+1 \geq 5$ odd, the ρ^- is replaced by a λ^- indicating a reflected copy of the left leg of the base triangle.

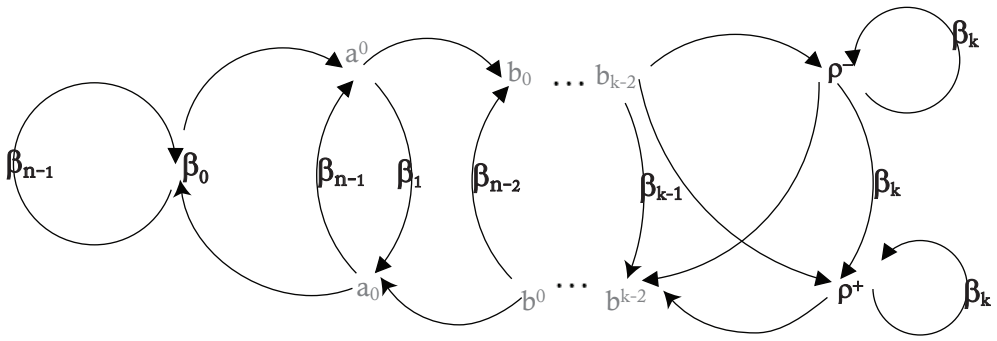

Figure 5.6: The post-renormalization 'almost dual' $\Sigma_0 = [0, \frac{\pi}{2n}]$ transition diagram $\mathfrak{D}_{2n}^{*\prime}$ for $n = 2k$. See Figure 4.19 (bottom) for the octagon case, and Section 4.4 for detail on these transition diagrams for the octagon. For $n = 2k+1 \geq 5$ the ρ^- is replaced by a λ^- indicating a reflected copy of the left leg of the base triangle.

The normalization $\mathtt{n}(\mathtt{w})$ of any admissible word $\mathtt{w} \in \left(\mathscr{A}_{2n}^{\odot}\right)^{\mathbb{Z}}$ is realizable by a path $\mathtt{p}$ through $\mathfrak{D}_{2n}^{*}$. The word $\mathtt{w}'$ obtained by tracing $\mathtt{p}$ through $\mathfrak{D}_{2n}^{*\prime}$ is

the *derivative* of w. The effect of derivation on $\mathtt{n}(\mathrm{w})$ is to retain every $\rho^{\pm}$ in and the sandwiched letters in $\mathtt{n}(\mathrm{w})\Big|_{\mathscr{B}}$. Proofs of the statements below exactly follow proofs of the analogous statements for centrally punctured octagon presented in Chapter 4.

Proposition 5.0.1.10. *For any $n \in \{4, 5, ...\}$, cutting sequences of linear trajectories on $\mathrm{P}^{\odot}_{2n}$ are weakly admissible, thus normalizable.*

Proposition 5.0.1.11. *For any $n \in \{4, 5, ...\}$, cutting sequences of linear trajectories on $\mathrm{P}^{\odot}_{2n}$ are admissible.*

Proposition 5.0.1.12. *For any $n \in \{4, 5, ...\}$, cutting sequences of linear trajectories on $\mathrm{P}^{\odot}_{2n}$ are deriveable, and the derived sequence is also the cutting sequence of a linear tajectory on $\mathrm{P}^{\odot}_{2n}$.*

Corollary 5.0.1.13. *For any $n \in \{4, 5, ...\}$, cutting sequences of linear trajectories on $\mathrm{P}^{\odot}_{2n}$ are infinitely deriveable.*

Although all cutting sequences of linear trajectories on $\mathrm{P}^{\odot}_{2n}$ are infinitely deriveable, not every infinitely deriveable sequence in $\mathscr{A}^{\odot}_{2n}$ is the cutting sequence of a linear trajectory. This is for the reasons discussed in connection with the centrally punctured octagon in Section 4.5. In continuing analogy with the octagon case, there is a set of *coherence conditions* on the restrictions $\mathtt{n}(\mathrm{w})\Big|_{\mathscr{B}}$ to $\mathscr{B}_{2n}$ of normalized sequences in $\mathscr{A}^{\odot}_{2n}$. Coherence conditions apply only the restrictions $\mathtt{n}(\mathrm{w})\Big|_{\mathscr{B}}$ to $\mathscr{B}_{2n}$ of normalied words in $\mathscr{A}^{\odot}_{2n}$, which is to say these conditions

ignore the puncture in $\mathrm{P}_{2n}^{\odot}$. For this reason all definitions and all results on the role of coherence in characterizing cutting sequences on non-punctured regular $2n$-gons in [76] carries over to the centrally punctured case without alteration. Corollary 5.0.1.13 combined with Theorem 6.3.2 from [76] yield a characterization of linear trajectory cutting sequences on $\mathrm{P}_{2n}^{\odot}$. The correspondence between cutting sequences on $\mathrm{P}_{2n}^{\odot}$ and hitting sequences on the $\left(\frac{\pi}{n}\right)$-isosceles triangle make this characterization of $\left(\frac{\pi}{n}\right)$-isosceles hitting sequences as well.

Theorem 5.0.1.14. *The closure of the set of cutting sequences on* $\mathrm{P}_{2n}^{\odot}$ *coincides with the set of infinitely coherent words in* $\mathscr{A}_{2n}^{\odot}$

CHAPTER 6

CONCLUSION AND FUTURE DIRECTIONS

We have completely characterized billiard trajectory hitting sequences in $\left(\frac{\pi}{n}\right)$-isosceles triangles for $n \geq 2$. These triangles constitute a significant subclass of triangles known to have the Veech property:

1. The acute $\left(\frac{\pi}{n}\right)$-isosceles triangles $n \geq 2$ [85].

2. The acute right triangles with interior angles $(\frac{\pi}{n}, \frac{(n-2)\pi}{2n}, \frac{\pi}{2})$ $n \geq 4$ [85].

3. The obtuse $\left(\frac{(n-2)\pi}{n}\right)$-isosceles triangles $n \geq 5$ [85].

4. The obtuse triangles with interior angles $(\frac{\pi}{n}, \frac{\pi}{2n}, \frac{2n-3}{2n})$ $n \geq 4$ [90].

5. The acute triangles with interior angles $(\frac{\pi}{4}, \frac{\pi}{3}, \frac{5\pi}{12})$ [85], $(\frac{\pi}{5}, \frac{\pi}{3}, \frac{7\pi}{12})$ [89] and $(\frac{2\pi}{9}, \frac{\pi}{3}, \frac{4\pi}{9})$ [47], and the obtuse triangle with interior angles $(\frac{\pi}{12}, \frac{\pi}{3}, \frac{7\pi}{12})$ [33].

Our techniques exploit the fact that the $\left(\frac{\pi}{n}\right)$-isosceles triangle are not just Veech triangles, but also *strongly Veech* in the sense of Definition 2.2.0.1.

For the $\left(\frac{\pi}{2}\right)$,$\left(\frac{\pi}{3}\right)$ and $\left(\frac{\pi}{4}\right)$-isosceles triangles we have detailed a renormalization scheme that operates on hitting sequences coded in the natural three-letter triangle alphabet. Combined with appropriate "coherence conditions" which

can be translated directly from the coherence conditions that apply in the regular $2n$-gon, this gives a different characterization of billiard trajectory hitting sequences these triangles.

Moving forward, there are several directions that seem worth pursuing. The most immediate follow-up to the work presented here would be a characterization of billiard trajectory hitting sequence on the right triangles that tile regular $2n$-gons. These triangles are also strongly Veech, and it is therefore not unreasonable to expect that some extension of methods employed in this thesis would suffice to characterize billiard trajectory hitting sequences $\left(\frac{\pi}{2n}, \frac{(2n-2)\pi}{4n}, \frac{\pi}{2}\right)$ right triangles as well.

The next step would be to apply the general philosophy of renormalization here to other strongly Veech triangles from the list above. The Veech groups of the translation surfaces induced by these triangles always contain parabolic shears that shorten angular sectors of the directional flow. These triangles will not have the symmetries that apply in triangles that tile regular $2n$-gons. However, there is reason to believe that a tractable combinatorial renormalization procedure adapted to specific angular sectors of the directional suface flow can be developed from a finite collection of parabolic elements of the Veech group. Finally, there are the $\left(\frac{2\pi}{n}\right)$-isosceles triangles that tile double centrally-punctured regular n-gons for $n \geq 5$ odd. These triangles are not Veech [52] but they tile Veech polygons (the unpunctured double regular $2k+1$-gons) in which the symbolic dynamics are already understood [19].

Combinatorial renormalization of billiard trajectories on the double regular $(2k+1)$-gon is the same as that on the regular $2k$-gon [19]. In the case of the $\left(\frac{\pi}{n}\right)$-

isosceles $n = 2k$ triangle, a combinatorial derivation rule comes from tracking the combinatorial consequences in $\mathrm{P}^{\odot}_{2k}$ of the same geometric renormalization strategy applied to the regular $2k$-gon. The situation in the double centrally-punctured $(2k+1)$-gon $\mathrm{P}^{\odot}_{2k+1}$ is fundamentally different. The renormalizing shear $\mathrm{H}^{+} = \begin{pmatrix} 1 & 2\cot\frac{\pi}{2k+1} \\ 0 & 1 \end{pmatrix}$ is the derivative of an affine automorphism of P_{2k+1} but *not* of $\mathrm{P}^{\odot}_{2k+1}$ (Figure 6.2). In fact, the $\left(\frac{2\pi}{n}\right)$-isosceles $n = 2k+1$ triangle surface $\mathrm{S}^{\odot}_{2k+1}$ is not a lattice surface and its Veech group need not contain any parabolic elements.

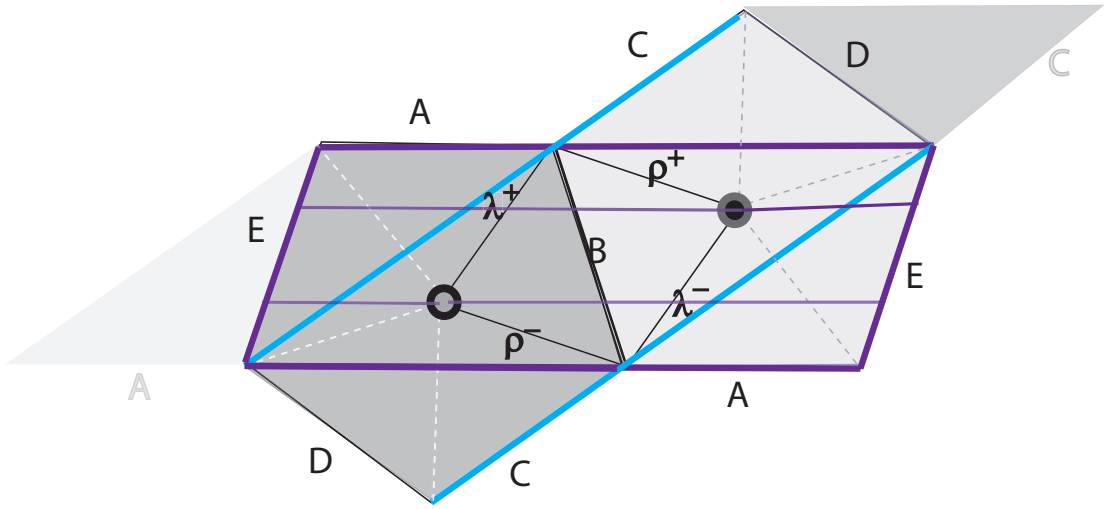

Figure 6.1: The centrally-punctured isosceles-tiled double regular pentagon with transverse cylinder decompositions in horizontal and angle-$\left(\frac{\pi}{5}\right)$ directions. The middle horizontal cylinders have rationally *in*commensurable inverse moduli. The ratio of the moduli of these two cylinders is in fact $\frac{1}{10}\sqrt{70+30\sqrt{5}}-1$. This means there cannot be an affine automorphism of the surface that is simultaneously an integer number of Dehn twists in each of the middle two horizontal cylinders and thus that H^{+} cannot be the derivative of such an automorphism.

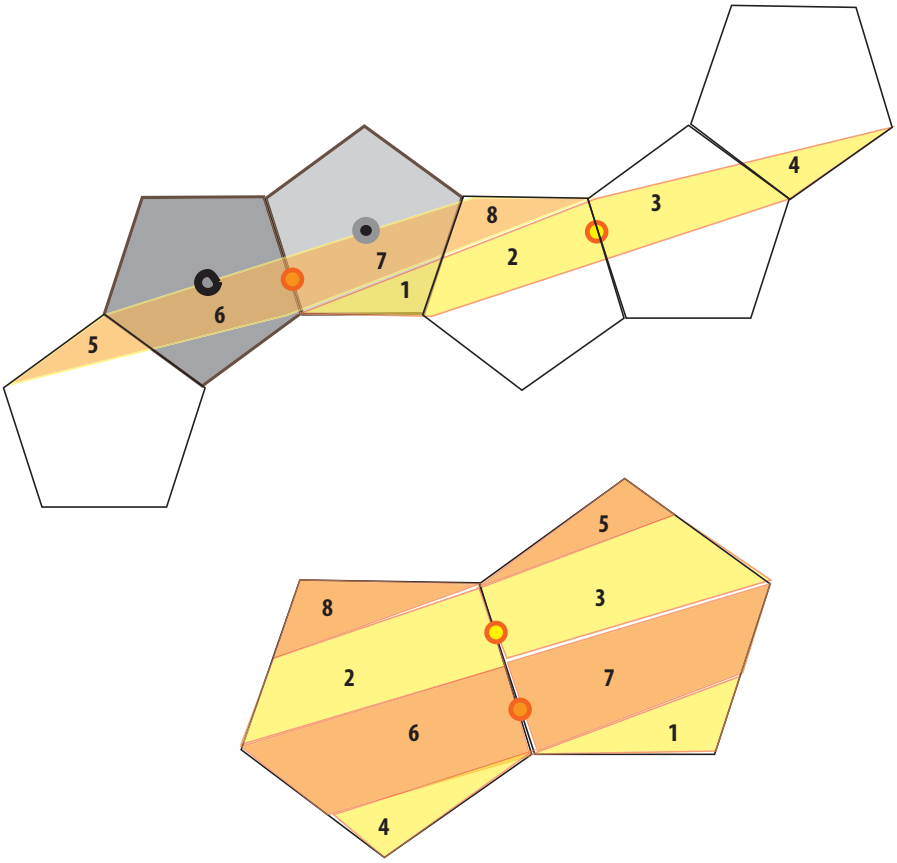

Figure 6.2: Although H^+ is not the derivative of an affine automorphism of the double centrally-punctured regular pentagon, it is in the Veech group of the non-punctured double regular pentagon surface. This is illustrated in the top subfigure. The grayscale centerpoints map to the orange/yellow points in the shears. In the bottom subfigure we see that postcomposing the indicated cut-and-paste map with H^+ is an automorphism of the double regular pentagon surface that does not map central punctures back to central punctures. It is not, therefore, an automorphism of the double centrally-punctured regular pentagon surface.

The methods of this thesis do not apply to the $\left(\frac{2\pi}{5}\right)$-isosceles triangle or to the double centrally-punctured pentagon. As an isosceles triangle that unfolds into a larger Veech polygon, the double-regular pentagon, with known symbolic dynamics [19], the $\left(\frac{2\pi}{5}\right)$-isosceles triangle is a compelling setting in which to start developing methods for characterizing billiard trajectory hitting sequences in non-Veech polygons.

Appendices

APPENDIX A

RENORMALIZATION SCHEMES ADAPTED FOR THREE LABELED TRIANGLE SIDES

A.1 Isosceles triangles that tile the plane

In the body of this thesis we have provide complete characterizations of $\left(\frac{\pi}{n}\right)$-isosceles triangle billiard trajectory hitting sequences for all $n \geq 2$. These characterizations have been achieved indirectly, by identifying the set of $\left(\frac{\pi}{n}\right)$-isosceles hitting sequences with the set of cutting sequences on a centrally-punctured regular $2n$-gon. It would be satisfying however to achieve a characterization based on conditions that apply directly to sequences in coded in the "intrinsic" three-letter alphabet $\{\beta, \lambda, \rho\}$ consisting of the labeled sides of the individual triangle in which the billiard trajectory is defined.

A.1.1 Characterization of hitting sequences for $\left(\frac{\pi}{2}\right)$-isosceles triangle hitting sequences

Reviewing Section 3.2 with an eye to the renormalizing the hitting sequences of $\left(\frac{\pi}{2}\right)$-isosceles billiard trajectories that are encoded in the "natural" three letter alphabet of labeled triangle sides, we note that the derivation process with respect to $\mathscr{B} \cup \overline{\mathscr{B}} \equiv \{A, B\} \cup \{R^{\pm}, L^{\pm}\}$ is actually performed on the two sub-alphabets $\mathscr{B}$ and $\overline{\mathscr{B}}$ independently: for Σ_0 trajectories, B's sandwiched between two A's or between two other B's in $\mathrm{w}\Big|_{\mathscr{B}}$ are retained, and $R^{\pm}$'s sandwiched

between two $L^{\pm}$'s or $R^{\pm}$'s in $\mathrm{w}\big|_{\overline{\mathscr{B}}}$ are retained, then reorganized according to the *3 letter subword swap* operation from Section 3.2. So in this case, a centrally punctured $2n$-gon point of view suffices to solve the coding problem for three labeled triangle sides. Working in the square unfolding of the $\left(\frac{\pi}{2}\right)$-triangle with edges simply labelled by $\mathscr{B} \cup \overline{\mathscr{B}} \equiv \{\beta\} \cup \{\lambda, \rho\}$ according to the side of the horizontally-positioned base triangle they unfolded from (Figure A.1), $\mathfrak{D}_0$ captures possible one-step transitions for a trajectory leaving the horizontal base at angle $\theta \in \bigcup_{j=0}^{4} \Sigma_{2j}$ and the "almost-dual" diagram $\mathfrak{D}_0^*$ (Figure A.3) shows gives two-step transitions. Transition diagrams for trajectories in angular sectors $\bigcup_{j=0}^{3} \Sigma_{2j+1}$ are obtained from $\mathfrak{D}_0$ and $\mathfrak{D}_0^*$ by applying the permutation $\pi_1 = (\lambda\, \rho)$ to edge and vertex labels.

Recall that cutting sequences on $\mathbb{T}_{\square}$ are almost constant (Definition 3.1.0.1). Furthermore, recall that a β-free subword is a subword with no β's and which is maximal in the sense that it cannot be expanded in either direction while retaining this property.

Definition A.1.1.1 (Almost constant sequences in $\{\beta, \lambda, \rho\}$)**.** *A word* $\mathrm{w} \in \{\beta, \lambda, \rho\}^{\mathbb{Z}}$ *is* almost constant *if there exists* $n \in \mathbb{N}$ *such that between any two* β*-free subwords of length one, there are either* n *or* $n+1$ β*-free subwords of length two.*

Note that if $[A\, B\, A]$ is a subword of the restricted cutting sequence $\mathrm{w}\big|_{\mathscr{B}}$ of some $\tau \in \mathcal{T}_0$ from Section 3.2, then the cutting sequence of τ coded in the 3-letter triangle alphabet $\{\beta, \lambda, \rho\}$ contains the subword $[\beta\, \rho\, \beta\, \rho\, \beta]$. Similarly, if $[A\, B\, B\, B\, A]$ is a subword of the restricted cutting sequence $\mathrm{w}\big|_{\mathscr{B}}$ of $\tau \in \mathcal{T}_0$, then

the same trajectory coded in $\{\beta, \lambda, \rho\}$ contains the subword $[\beta\rho\beta\lambda\rho\beta\rho\lambda\beta\rho\beta]$.

Following terminology introduced in Section 3.2 we say that the sequence $w \in \{\beta, \lambda, \rho\}^{\mathbb{Z}}$ is weakly admissible if w is almost constant and w or $\pi_1(w)$ can be realized in $\mathfrak{D}_0$. When w is weakly admissible, whichever of w or $\pi_1(w)$ is realizable in $\mathfrak{D}_0$ is referred to as the normalization, $n(w)$ of w. A weakly admissible word w whose normalization can be realized in $\mathfrak{D}_0^*$ is admissible.

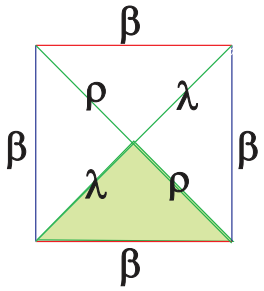

(a) Centrally Punctured Square from $\left(\frac{\pi}{2}\right)$-Isosceles Triangle

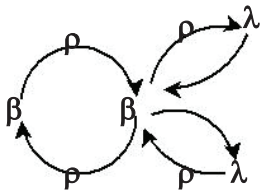

(b) One-Step Transition Diagram $\mathfrak{D}_0$ for $0 \leq \theta \leq \frac{\pi}{4}$

Figure A.1

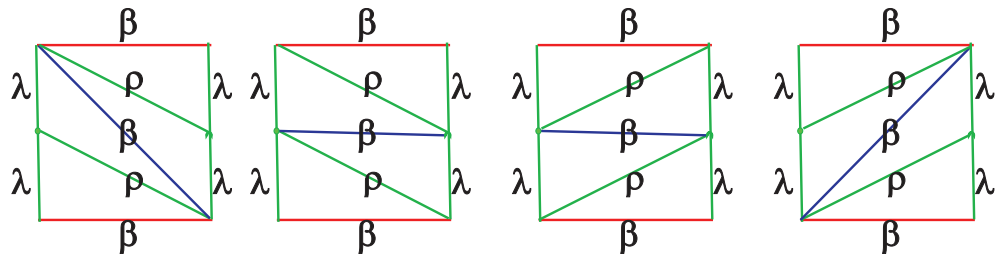

(a) Stage 0. Cut and paste along diagonal, then shear back to square shape.

(b) Stage 1. Flip main diagonal.

(c) Stage 2. Reflect about central vertical axis.

(d) Stage 3. Flip main diagonal again.

Figure A.2

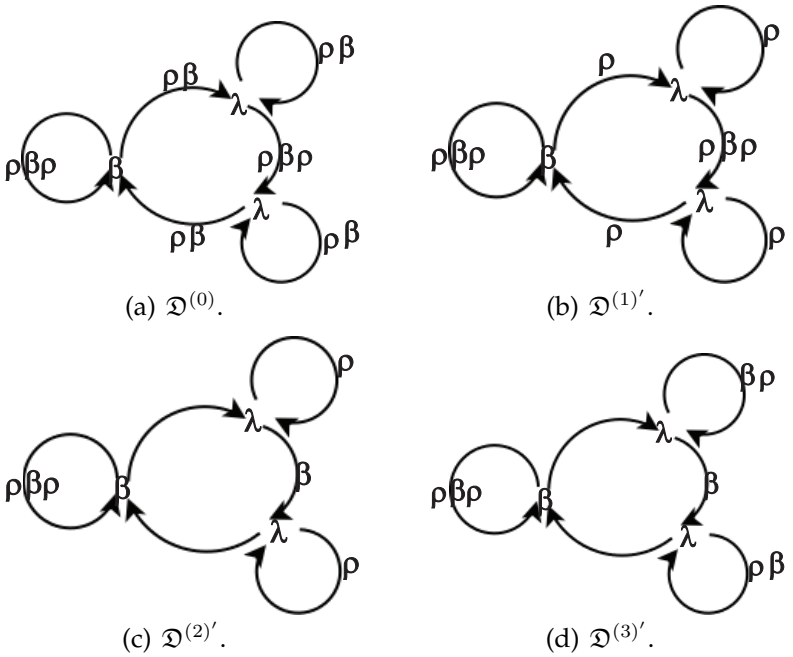

Figure A.3: Possible transitions of renormalized Σ_0 trajectories, in "almost dual" form: horizontal and vertical edges of Figure A.2 (a) are vertices, remaining edge(s) in Figure A.2 (a) label directed graph edges.

Let w be a word in $\{\beta, \lambda, \rho\}^{\mathbb{Z}}$ and $\mathrm{w}\big|_{\mathscr{B}}$, $\mathrm{w}\big|_{\overline{\mathscr{B}}}$ the restrictions of w to $\mathscr{B} = \{\beta\}$ and $\overline{\mathscr{B}} = \{\lambda, \rho\}$ respectively. The geometric renormalization (Figure A.2) is the shear-cut-paste-reflect operation from Section A.2 whose combinatorial effect (Figure A.3) on $\mathrm{n}(\mathrm{w}) \in \{\beta, \lambda, \rho\}^{\mathbb{Z}}$ is:

1. Drop every β in $\mathrm{n}(\mathrm{w})$ that is not sandwiched between two subwords from $\overline{\mathscr{B}}$ of the same length, either exactly length 1 or exactly length 2.

2. Drop every ρ that is not sandwiched between two λ's or two ρ's in $\mathrm{n}(\mathrm{w})\big|_{\overline{\mathscr{B}}}$.

3. (*3-letter subword swap*) Replace every occurance of $[\lambda\,\rho\,\beta]$ with $[\lambda\,\beta\,\rho]$, and every occurance of $[\beta\,\rho\,\lambda]$ with $[\rho\,\beta\,\lambda]$.

Example A.1.1.1. *Suppose*

$$\mathrm{w} = ...\beta\,\rho\,\beta\,\lambda\,\rho\,\beta\,\lambda\,\rho\,\beta\,\lambda\,\rho\,\beta\,\rho\,\lambda\,\beta\,\rho\,\lambda\,\beta\,\rho\,\lambda\,\beta\,\rho\,\beta...$$

encodes part of a billiard trajectory $\tau \in \mathcal{T}_0$ in the $\left(\frac{\pi}{2}\right)$-isosceles triangle. Since w *is admissible,* $\mathrm{n}(\mathrm{w})$ *can be realized in $\mathfrak{D}_0^*$. By Proposition 3.2.0.1,* $\mathrm{n}(\mathrm{w})$ *can also be realized by a path* p *in $\mathfrak{D}^{(0)}$. The effect of tracking* p *through transition diagrams $\mathfrak{D}^{(0)}$, $\mathfrak{D}^{(1)'}$, $\mathfrak{D}^{(2)'}$ and $\mathfrak{D}^{(3)'}$ from Figure A.3 successively are shown in Table A.1. The word* w′ *in the bottom row of Table A.1, obained by tracing* p *through $\mathfrak{D}^{(3)'}$, is the derived sequence of* w*. The word* w′ *is the cutting sequence of the trajectory $\tau^{(3)}$ that results from applying the affine automorphism illustrated in Figure* **??** *(a) through (d) to the isosceles-tiled square.*

Start	β	ρ	$\boldsymbol{\beta}$	λ		ρ	$\boldsymbol{\beta}$	λ		ρ	$\boldsymbol{\beta}$	λ	ρ	$\underline{\boldsymbol{\beta}}$	ρ	λ	$\boldsymbol{\beta}$	ρ		λ	$\boldsymbol{\beta}$	ρ		λ	$\boldsymbol{\beta}$	ρ	β
Step 1	β	ρ		λ		ρ		λ		ρ		λ	ρ	$\overline{\boldsymbol{\beta}}$	ρ	λ		ρ		λ		ρ		λ		ρ	β
Step 2	β			λ		ρ		λ		ρ		λ		$\overline{\boldsymbol{\beta}}$		λ		ρ		λ		ρ		λ			β
Final	β			λ	$\boldsymbol{\beta}$	ρ		λ	$\boldsymbol{\beta}$	ρ		λ		$\underline{\boldsymbol{\beta}}$		λ		ρ	$\boldsymbol{\beta}$	λ		ρ	$\boldsymbol{\beta}$	λ			β

Table A.1

Definition A.1.1.2. *The* derived sequence $\mathrm{w}' = \mathrm{D}(\mathrm{w})$ *of an admissible word* $\mathrm{w} \in \{\beta, \lambda, \rho\}^{\mathbb{Z}}$ *is obtained from* $\mathrm{n}(\mathrm{w})$ *by deleting the first and last β from each block of two or more consecutive β's in* $\mathrm{w}\big|_{\mathscr{B}}$ *and every ρ that is not sandwiched between two λ's or two ρ's in* $\mathrm{w}\big|_{\overline{\mathscr{B}}}$*, then performing the subword swap (point 3. above).*

Proposition A.1.1.1. *If* $\mathrm{w} \in \{\beta, \lambda, \rho\}^{\mathbb{Z}}$ *is the hitting sequence of a billiard trajectory in the $\left(\frac{\pi}{2}\right)$-isosceles triangle, then* $\mathrm{w}' = \mathrm{D}(\mathrm{w})$ *is as well.*

The proof of Proposition A.1.1.1 follows the same chain of reasoning as cases detailed in previous sections. This reasoning produces a geometric trajectory τ' such that $\mathrm{w}' = c(\tau)' = c(\tau')$, leading to the following corollary:

Corollary A.1.1.2. *The cutting sequence* $\mathrm{w} = c(\tau) \in \{\beta, \lambda, \rho\}^{\mathbb{Z}}$ *of any billiard trajectory* τ *on the* $\left(\frac{\pi}{2}\right)$*-isosceles triangle is infinitely deriveable.*

Theorem A.1.1.3. *The word* $\mathrm{w} \in \{\beta, \lambda, \rho\}^{\mathbb{Z}}$ *is in the closure of the set of billiard trajectory hitting sequences in the* $\left(\frac{\pi}{2}\right)$*-isosceles triangle if and only if it is infinitely deriveable.*

Proof of Theorem A.1.1.3. One direction follows from Corollary A.1.1.2. The other direction combines Corollary A.1.1.2, Proposition 2.3.1.1 and [71] (among others), but requires some additional steps. Following Series [71] and Smillie, Ulcigrai [76], we reason as follows:

Proposition A.1.1.4. *(Series) Every finite admissible word* $\mathrm{u} \in \{A, B\}$ *is realized by at least one line segment in* $\mathbb{R}^2$*.*

Proof of Proposition A.1.1.3. (following [71]) The proof follows from an elementary continued fraction argument based the first torus renormalization procedure detailed in Section 2.3.1. See [71] for details.

□

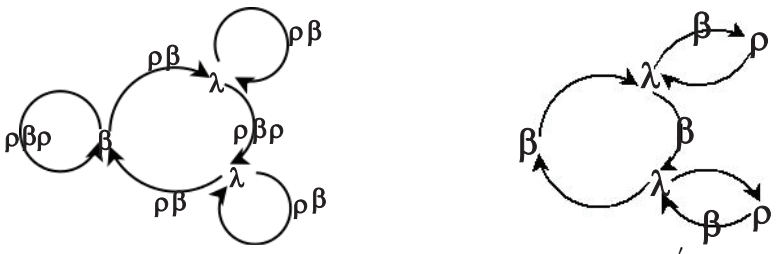

(a) $\mathfrak{D}^*$ (b) $\mathfrak{D}^{*'}$

Figure A.4: Possible transitions of Σ_0 (Left) and Σ_3 (Right) trajectories, in "almost dual" form: horizontal and interior triangle edges are vertices, remaining exterior polygon edge(s) label directed graph edges

Let $\mathrm{v} \in \{\beta, \lambda, \rho\}^m$ $m \geq 5$ be a finite admissible word realizable in $\mathfrak{D}^{*'}$. Words of this length can be realized by a unique path in only one of $\mathfrak{D}^*$ or $\mathfrak{D}^{*'}$ (Figure A.4). Let $\mathrm{p}(\mathrm{v})$ be the path in $\mathfrak{D}^{*'}$ realizing v. Tracing $\mathrm{p}(\mathrm{v})$ through any of the almost-dual diagrams $\mathfrak{D}_i$, $i = \{2, 3, 6, 7\}$ gives a word $\mathrm{w} \in \{A, B, L^{\pm}, R^{\pm}\}^m$ whose restriction to $\{A, B\}$ encodes a collection $\Lambda(\mathrm{w})$ of line segments in $\mathbb{R}^2$ with angles $\Omega(\mathrm{w}) \subset \pm[\frac{\pi}{4}, \frac{3\pi}{4}]$. By a classical continued fraction argument and, for example, Series [71], we know that as $m \to \infty$, $|\Omega| \to 0$. The important point is that $\Lambda(\mathrm{v}) = \Lambda(\mathrm{w})$ and $\Omega(\mathrm{v}) = \Omega(\mathrm{w})$, ensuring that v codes at least one linear segment $\overline{\tau}(\mathrm{v}) \in \mathbb{R}^2$. The geometric process of derivation on finite line segments in $\mathbb{R}^2$ (ie., finite billiard trajectory segments on $\mathrm{T}_{\frac{\pi}{2}}$) is an affine automorphism, thus invertible. The inverse operation and its combinatorial counterpart will be referred to as *generation*. From Figure A.5 we construct the generation diagram $\mathcal{G}^{*'}$ (Figure A.6) that interpolates between letters of v the labels of edges crossed by a Σ_0-trajectory segment $\overline{\tau}_{(1)}$ with combinatorial derivative v. The generation operator $\mathfrak{g}$ replaces v with an *interpolated* word $\mathrm{v}_{(1)} = \mathfrak{g}(\mathrm{v}) \in \Sigma'$ obtained by tracing $\mathrm{p}(\mathrm{v})$ through $\mathcal{G}^{*'}$ and sending the result back to Σ' via the permutation $\pi' = (\lambda\ \rho)$.

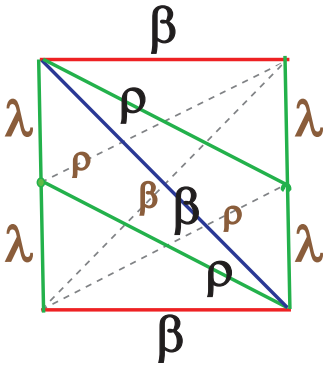

Figure A.5: Final renormalization (stage 3) in bold primary colors, large edge labels; initial renormalization (stage 0) dashed lines, brown edge labels.

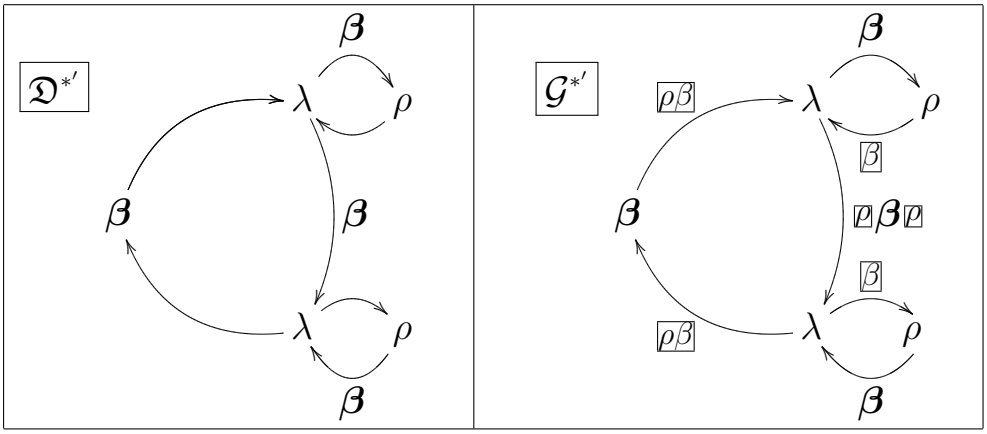

Figure A.6: (Left) $\Sigma' = [\frac{3\pi}{4}, \pi]$ Nearly-Dual Transition Diagram; (Right) The $(\frac{\pi}{2})$-Isosceles Generation Diagram, interpolated letters framed.

Example A.1.1.2. *Suppose*

$$\mathrm{v} = ...\beta\,\lambda\,\beta\,\rho\,\lambda\,\beta\,\rho\,\lambda\,\beta\,\lambda\,\rho\,\beta\,\lambda\,\rho\,\beta\,\lambda\,\beta...$$

is the renormalization of the word

$$\mathrm{w} = ...\beta\,\rho\,\beta\,\lambda\,\rho\,\beta\,\lambda\,\rho\,\beta\,\lambda\,\rho\,\beta\,\rho\,\lambda\,\beta\,\rho\,\lambda\,\beta\,\rho\,\lambda\,\beta\,\rho\,\beta...$$

from Example A.1.1.1. Tracing $\mathrm{p}(\mathrm{v})$ *through* $\mathcal{G}^{*'}$ *returns the original word,* $\mathrm{w} = \pi'(\mathfrak{g}(\mathrm{v}))$.

v	β			λ	$\boldsymbol{\beta}$	ρ		λ	$\boldsymbol{\beta}$	ρ		λ		$\underline{\boldsymbol{\beta}}$		λ		ρ	$\boldsymbol{\beta}$	λ		ρ	$\boldsymbol{\beta}$	λ			β
$\pi'(\mathfrak{g}(\mathrm{v}))$	β	ρ	$\boldsymbol{\beta}$	λ		ρ	$\boldsymbol{\beta}$	λ		ρ	$\boldsymbol{\beta}$	λ	ρ	$\underline{\boldsymbol{\beta}}$	ρ	λ	$\boldsymbol{\beta}$	ρ		λ	$\boldsymbol{\beta}$	ρ		λ	$\boldsymbol{\beta}$	ρ	β

Table A.2

Proposition A.1.1.5. *For finite* Σ'*-admissible* $\mathrm{v} \in \{\beta, \lambda, \rho\}^m$ $m \geq 5$*, the interpolated word* $\mathrm{v}_{(1)} = \mathfrak{g}(\mathrm{v})$ *has at most* $3m$ *letters (see Table A.6) and is realized by a linear segment* $\overline{\tau}_{(1)} \in \Lambda(\mathrm{v}_{(1)})$*, generated by inverse geometric derivation from a segment* $\overline{\tau}$ *coded by* v.

Proof of Propositon A.1.1.5. This follows from the invertibility of geometric derivation and inspection of Figures A.5 and A.6.

□

Corollary A.1.1.6. *For any* $m \geq 5, k \in \mathbb{N}$*, and* Σ'*-admissible* $\mathrm{v} \in \{\beta, \lambda, \rho\}^m$ *satisfying the* $n, n+1$ *property, there exists a linear segment* $\overline{\tau}_{(k)}$ *in* $\mathbb{R}^2$ *realizing the* k^{th} *generated interpolate* $\mathrm{v}_{(k)} = \mathfrak{g}^k(\mathrm{v})$ *of* v.

Proposition A.1.1.7. *If* u*,* $|u| \geq 2$ *is the longest common subword of two bi-infinite* Σ'*-admissible words* v *and* v'*, then* $|\mathfrak{g}(\mathrm{u})| > |\mathrm{u}|$ *where* $|^*|$ *denotes wordlength and the*

inequality is strict.

Proof. Generation clearly cannot strictly decrease the length of any Σ'-adimissible word. Further, the proof of Proposition A.1.1.7 is immediate from Figure A.6 when $|\mathrm{u}| \geq 4$. Suppose u, $2 \leq |\mathrm{u}| \leq 3$ with $|\mathfrak{g}(\mathrm{u})| = |\mathrm{u}|$ is common to Σ'-admissible v and v'. In this case u is realized along one of the loops on the top or bottom right corners of $\mathfrak{D}'^{*}$ (Figure A.4). However, any two such subwords by necessity have a common subword of length at least 4. Thus, if u satisfied the supposition, it would not be the longest subword common to v and v'.

□

As a subshift of finite type, the set of Σ'-admissible words is closed. Thus, Proposition A.1.1.7 together with Corollary A.1.1.6 imply that $\mathfrak{v} = \lim_{k\to\infty} \mathfrak{g}^k(\mathrm{v})$ is a limit of cutting sequences, proving theorem A.1.1.3.

□

A.1.2 The $\left(\frac{\pi}{3}\right)$-isosceles triangle

The transparent connection between combinatorial $\left(\frac{\pi}{n}\right)$-isosceles renormalization in the three letter triangle alphabet and the larger $2n$-gon alphabet breaks down for $n \geq 3$. Determining the specific sequence λ's and ρ's between two retained β's requires inputting subwords of length that grows quadratically in n. First observe from Figures A.7, A.8 and A.9 that the renormalization scheme for linear trajectories on the centrally-punctured square torus applies to the

centrally-punctured hexagonal torus as well.

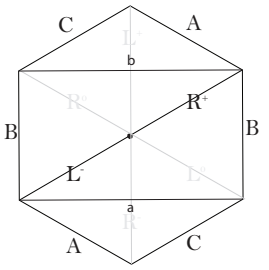

(a) Centrally Punctured Hexagon from $\left(\frac{\pi}{3}\right)$-Isosceles Triangle, with Auxilliary Interior Horizontals

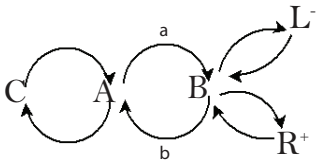

(b) Augemented One-Step Transition Diagram $\widetilde{\mathfrak{D}}_0$ for $0 \leq \theta \leq \frac{\pi}{6}$

Figure A.7

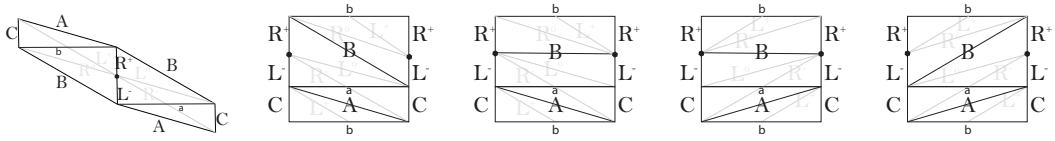

(a) Shear

(b) Cut-Paste into Rectangles

(c) Delaunay Flip

(d) Reflect about central vertical axis

(e) Flip Central Horizontal

Figure A.8: Geometric renormalization of cutting sequences in the centrally punctured hexagon, $0 \leq \theta \leq \frac{\pi}{6}$.

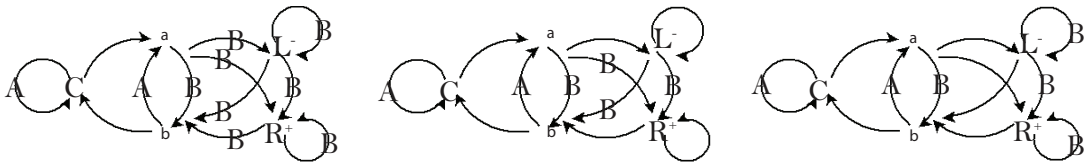

(a) Original transitions, preserved by shear-cut-paste

(b) Transitions following initial Delaunay flip and reflection

(c) Transitions following second flip of horizontal

Figure A.9: Possible transitions of renormalized Σ_0 trajectories, in 'almost dual' form: horizontal and auxiliary edge are vertices, remaining exterior polygon edge(s) label directed graph edges.

Pulling the faded $L^{\pm}$'s and $R^{\pm}$'s from Figure back into the analysis we might hope, based on recent experience with the square torus, for a nearly direct trans-

lation from renormalization of cutting sequences in $\mathscr{A}^{\odot}$ to renormalization of hitting sequences given in the triangle alphabet $\mathscr{A}^{\triangle}$. The differences in the hexagon case are immediately apparent. Auxiliary horizontals (Figure A.10) that bound punctured hexagon cylinders do not respect triangle edges, so a trajectory segment in $\Sigma_0 = [0, \frac{\pi}{6}]$ that intersects edges coded in $\{a, b, C, R^+, L^-\}$ only at its endpoints need not have a unique combinatorial path. For example (Figure A.10, (far left)), even before any geometric transformations are applied, a trajectory segment joining edge a to edge L^- can cross either L^0 and B, or R^- followed by L^0 and B (figure A.10).

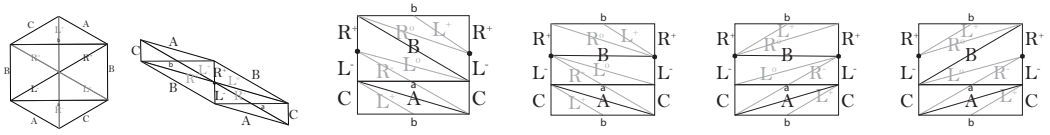

(a) 0. Isosceles Tiled Hexagon with Auxilliary Horizontals

(b) 1. Shear

(c) 2. Cut-Paste into Rectangles

(d) 3. Edge Flip (Delaunay in Shear

(e) 4. Reflect about central vertical axis

(f) 5. Second Edge Flip (Delaunay in Hexagon)

Figure A.10: Geometric renormalization of the centrally punctured hexagon with auxilliary horizontals, tiled by equilateral triangles.

The solution to this problem exploits the fact that cylinders of the sheared puctured hexagon are bounded by exterior edge β_2 and Delaunay flips of triangle legs $\lambda^{\pm}$, $\rho^{\pm}$ in the sheared hexagon (see Figure A.11). Geometric renormalization is really happening in the shear and the reflected shear, so we start there, working backwards and forwards from the shear to renormalize combinatorially.

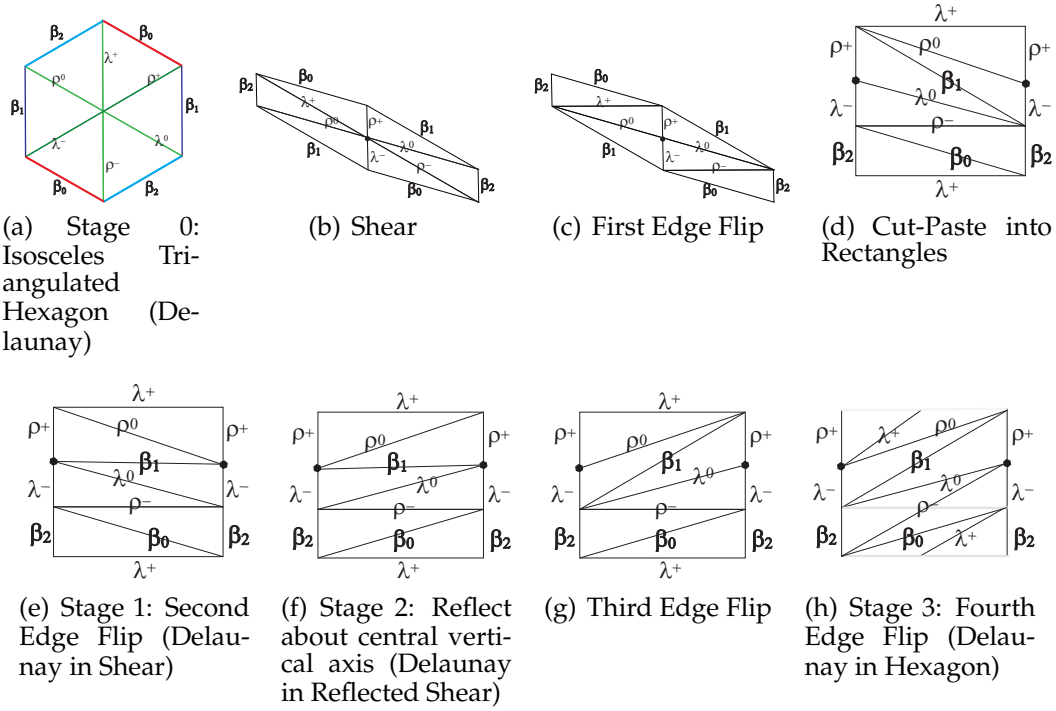

(a) Stage 0: Isosceles Triangulated Hexagon (Delaunay)

(b) Shear

(c) First Edge Flip

(d) Cut-Paste into Rectangles

(e) Stage 1: Second Edge Flip (Delaunay in Shear)

(f) Stage 2: Reflect about central vertical axis (Delaunay in Reflected Shear)

(g) Third Edge Flip

(h) Stage 3: Fourth Edge Flip (Delaunay in Hexagon)

Figure A.11: Geometric renormalization of the centrally punctured hexagon, tiled by equilateral triangles.

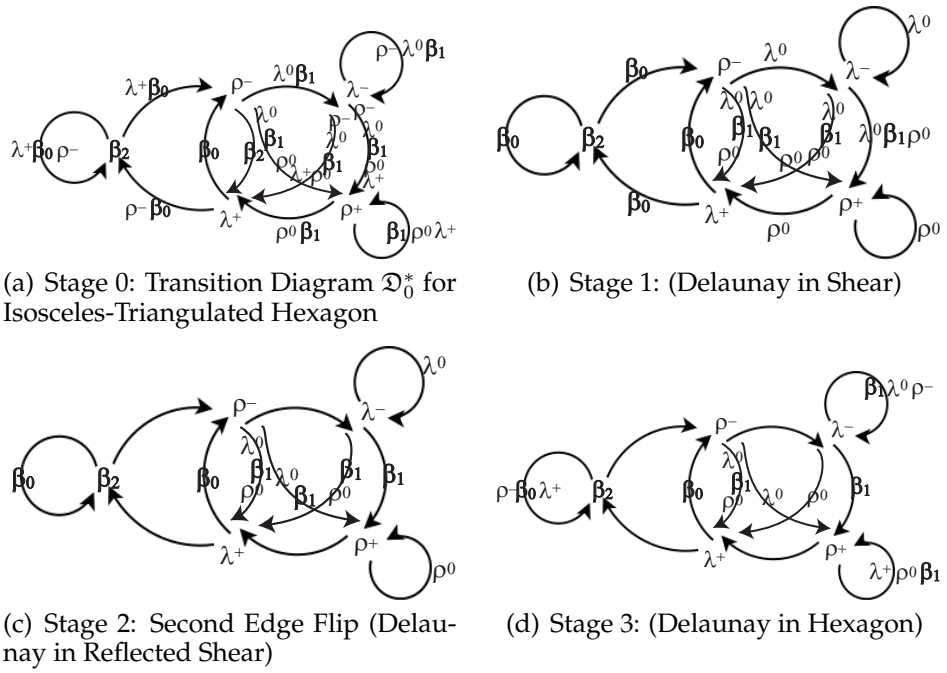

(a) Stage 0: Transition Diagram $\mathfrak{D}_0^*$ for Isosceles-Triangulated Hexagon

(b) Stage 1: (Delaunay in Shear)

(c) Stage 2: Second Edge Flip (Delaunay in Reflected Shear)

(d) Stage 3: (Delaunay in Hexagon)

Figure A.12: Combinatorial transitions in successive transformations of the isosceles-triangulated hexagon.

Let $\tau \in \mathcal{T}_0 = \{\tau^\theta : \theta \in [0, \frac{\pi}{6}]\}$ be a linear trajectory on the triangulated hexagonal torus $\mathbb{T}_{\text{hex}}$ (Figure A.11) and $\widetilde{\tau} = \begin{pmatrix} 1 & -\cot\frac{\pi}{6} \\ 0 & 1 \end{pmatrix} \cdot \tau$. The edges of $\mathfrak{D}_0^*$ are labeled in the usual way: by the isosceles-triangulated hexagon edges $\tau \in \mathcal{T}_0$ crosses in moving between edges represented by the diagram vertex labels.

Let Ψ denote the composition of transformations shown in Figure A.11.

Definition A.1.2.1. *The image τ' in $\Psi(\mathbb{T}_{\text{hex}})$ of $\tau \in \mathcal{T}_0$ is called the geometric derivative or renormalization of τ.*

Proposition A.1.2.1. *The geometric derivative of a trajectory $\tau \in \mathcal{T}_0$ is also a linear trajectory in $\mathbb{T}_{\text{hex}}$.*

Proof. It suffices to oberve that Ψ is an affine automorphism of the centrally-punctured hexagon.

□

Definition A.1.2.2. *A word* w *in $\{\beta_0, \beta_1, \beta_2\}$ will be be called* almost constant *if there exists $k \in \{0, 1, 2\}$ and $n \in \mathbb{N}$ such that every occurance of β_j, $j \neq k$ is isolated, and every β_k-block in* w *has length n or $n + 1$.*

For each angular sector $\Sigma_k = [\frac{k\pi}{6}, \frac{(k+1)\pi}{6}]$, $k = 0, 1, 2, ..., 11$ there is a diagram $\mathfrak{D}_k$ with the same topology as $\mathfrak{D}_0$ that captures the possible one-step transitions

for trajectories in directions $\theta \in \Sigma_k$.

Definition A.1.2.3. *A word* $\mathrm{w} \in \mathscr{A}^{\odot} \equiv \{\beta_0, \beta, \beta_2, \lambda^{0,\pm}, \rho^{0,\pm}\}^{\mathbb{Z}}$ *is weakly admissible if* w *is almost constant and can be realized by a path* p *in* $\mathfrak{D}_i$, $i \in \{0, 1, 2, ..., 11\}$. *If* w *is realizable in* $\mathfrak{D}_i$ *then* $\mathrm{n}(\mathrm{w}) = \boldsymbol{\pi}_i(\mathrm{w})$ *is realizable in* $\mathfrak{D}_0$ *and is called the* normalization *of* w.

Definition A.1.2.4. *The weakly admissible word* w *is* admissible *if its augmented normalization* $\widetilde{\mathrm{n}(\mathrm{w})}$ *can be realized in the almost-dual* Σ_0 *transition diagram* $\mathfrak{D}_0^*$ *(Figure A.9,(a)).*

The symmetries of P_{2n} discussed in Chapters 4 and 5 apply to the centrally-punctued hexagon. Elements ν_k of the dihedral group D_6 send trajectories in directions $\theta \in (\frac{\pi}{6}, 2\pi)$ to Σ_0 trajectories. Transition diagrams for Sectors $1, 2, ..., 11$ are obtained by corresponding permutations $\boldsymbol{\pi}_k^{-1}$ on edge and vertex labels of $\mathfrak{D}_0$, where the notation $\boldsymbol{\pi}_k$ is used both for the permutation on diagram labels and the associated mapping on admissible words (see Remark 4).

Proposition A.1.2.2. *If* $\mathrm{w} = \boldsymbol{c}(\tau) \in \left(\mathscr{A}^{\odot}\right)^{\mathbb{Z}}$ *is the cutting sequence of a trajectory* $\tau \in \mathcal{T}_0$ *then* w *is admissible.*

Proof. If w is the cutting sequence of a linear trajectory on the hexagonal torus, then by construction of the one-step transition diagrams, w is realizable in $\mathfrak{D}_i$ for some $i \in \{0, 1, 2, ..., 11\}$. Basic geometry constrains cutting sequences to be

almost constant (see Figure 3.3), and symmetries of the hexagonal torus allow us to consider only Σ_0 trajectories: a fixed-slope line in direction $\theta \in \Sigma_0$ cannot intersect β_1 both n times and $n+2$ times. Furthermore, simple inspection of Figure A.7 indicates that normalized cutting sequences of linear trajectories cannot contain the forbidden subword $[R^+ L^- R^+]$. Therefore the augmented normalization $\widetilde{\mathrm{n}(\mathrm{w})}$ of w is realizable in $\mathfrak{D}_0^*$

□

Definition A.1.2.5. *If* w *is admissible, then the result* $\mathrm{w}' = \mathrm{D}(\mathrm{w})$ *of sending* $\mathrm{n}(\mathrm{w})$ *successively through Stage* 1*, Stage* 2 *and Stage* 3 *diagrams in Figure A.12 is called the derived or renormalized sequence* w′ *of* w*.*

Definition A.1.2.6. *The admissible word* $\mathrm{w} \in \left(\mathscr{A}^{\odot}\right)^{\mathbb{Z}}$ *is* deriveable *if the derivative* w′ *of* w *is also admissible.*

Proposition A.1.2.3. *If* $\mathrm{w} = c(\tau)$ *is the cutting sequence of a trajectory on the hexagonal torus, then* w *is deriveable and the derivative* w′ *of* w *is the cutting sequence of a linear trajectory.*

Corollary A.1.2.4. *If* $\mathrm{w} = c(\tau)$ *is the cutting sequence of a linear trajectory on the hexagonal torus, then* w *infinitely deriveable.*

The proofs of Proposition A.1.2.3 and Corollary A.1.2.4 follow the same steps as our proofs of Propositions 3.1.0.3 and 4.4.0.1. The important point is that all of this remains true when we drop superscripts and subscripts of edge and vertex labels. Defining realizability and derivation from exisiting figures and dia-

grams *without* subscripts and superscripts, this observation combined with the propositions above yields a necessary condition for hitting sequences of billiard trajectories in the equilateral triangle (Figure A.13):

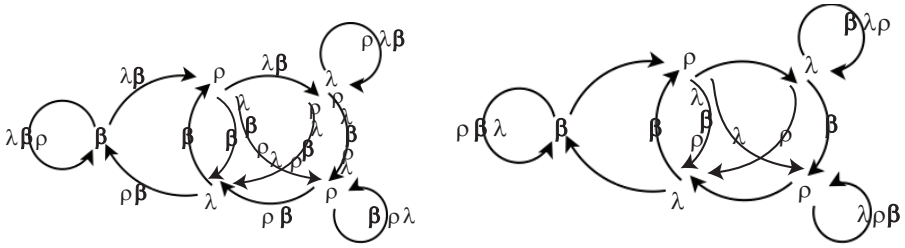

(a) Stage 0 Transition Diagram $\mathfrak{D}_0^*$ (b) Stage 3 Transition Diagram $\mathfrak{D}^{*'}$

Figure A.13: Combinatorial transitions in successive transformations of the unfolded equilateral triangle.

Theorem A.1.2.5. *If* $\mathrm{w} = c(\tau) \in \{\beta, \lambda, \rho\}^{\mathbb{Z}}$ *is the hitting sequence of a billiard trajectory in the equilateral triangle, then it is infinitely deriveable.*

Proof. Theorem A.1.2.5 follows from Corollary A.1.2.4 and by the construction of diagrams $\mathfrak{D}_0^*$ and $\mathfrak{D}^{*'}$ in Figure A.13.

□

A.2 The $\left(\frac{\pi}{4}\right)$-isosceles triangle

To suport our claim that the approach in Section A.1.2 scales with n, we sketch an extension of the method to a triangle that does not tile the plane: the $\left(\frac{\pi}{4}\right)$-isosceles triangle.

In Section 4 we described an orientation-reversing affine automorphism $\Psi = \mathrm{h}^{-1} \circ \kappa^{-1} \circ r_v \circ \kappa \circ \mathrm{h}$ of the centrally punctured octagon $\mathcal{O}^{\odot}$ that is conjugate to an isometry by the linear transformation $\mathrm{h} = \begin{pmatrix} -1 & \cot\frac{\pi}{4} \\ 0 & 1 \end{pmatrix}$. Following the procedure from Section A.1.2 we apply h to the isosceles-triangulated octagon (Figure A.14 (a)), flip edges until the resulting triangulation is Delaunay (Figure A.14 (b),(c)) in the sheared octagon. Cut and paste into the familiar L-shaped diagram $\mathcal{L}$ (Figure A.14 (d)). After reflecting rectangles of $\mathcal{L}$ about their central vertical axes, flip edges until the resulting triangulation is Delaunay in $\mathcal{O}^{\odot}$ (Figure A.14 (e), (f), (g)). Finally apply $\mathrm{h}^{-1} \circ \kappa^{-1}$ to go back to the isosceles-triangulated octagon.

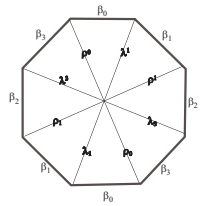

(a) Stage 0: Isosceles Triangulated Octagon (Delaunay)

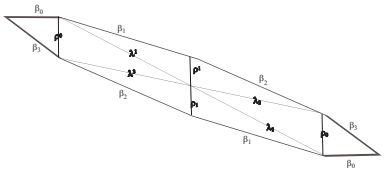

(b) Shear, first edge-flip

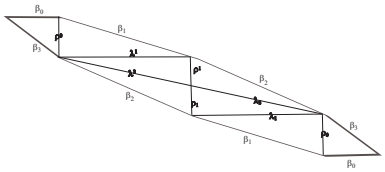

(c) Shear, second edge-flip (Delaunay in Shear

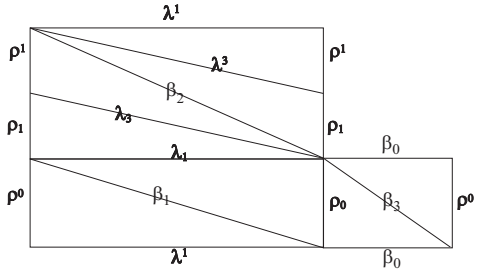

(d) Stage 1: Cut-Paste shear into rectangles (Delaunay in Shear)

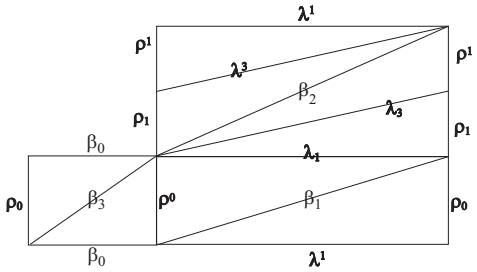

(e) Stage 2: Reflect about central vertical axis (Delaunay in Reflected Shear)

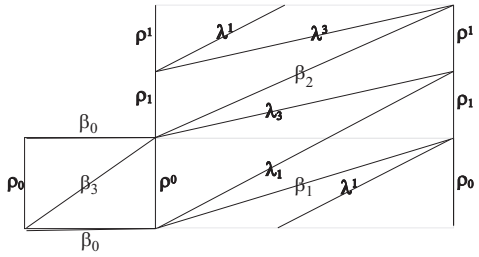

(f) Stage 2: Undo first Delaunay edge-flip

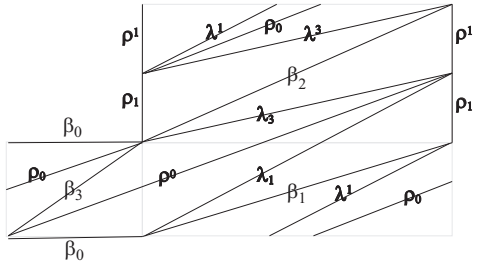

(g) Stage 3: Undo second Delaunay edg-flip (Delaunay in Octagon

Figure A.14: Geometric renormalization of the centrally punctured octagon, tiled by $\left(\frac{\pi}{4}\right)$-isosceles triangles.

Using the edges that bound rectangles in the Delaunay-triangulation of the sheared isosceles-triangulated octagon, create the 'almost-dual' Σ_0 transition diagram (Figure A.15, (a)). Arguments from Section 4 suggest that hitting sequences of Σ_i, $i \neq 0$ trajectories are realizable in $\mathfrak{D}_0^*$ after applying appropriate permutations to vertex and edge labels. Combinatorial derivation will involve

recoding sequences which can be realized by the path p in $\mathfrak{D}_0^*$ after appropriate permutations according to the labels picked up following the same path through $\mathfrak{D}^{*'}$ (Figure A.15, (b)).

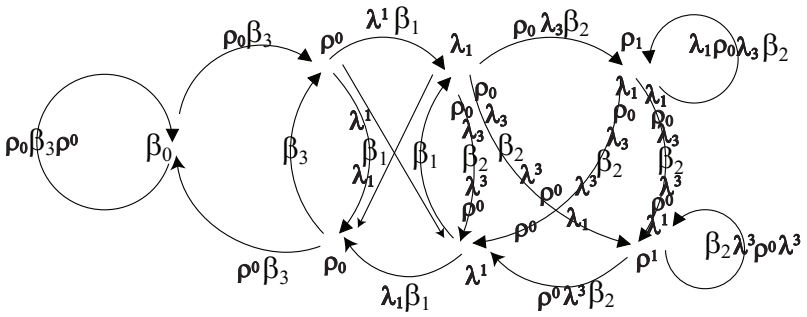

(a) Stage 0: Transition Diagram $\mathfrak{D}_0^*$ for $\left(\frac{\pi}{4}\right)$-isosceles trianglulated octagon (Triangulation Delaunay in Octagon)

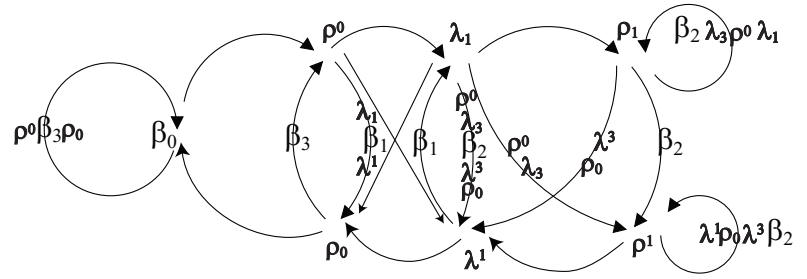

(b) Stage 3: Transition Diagram $\mathfrak{D}^{*'}$ for renormalized octagon (Triangulation Delaunay in Octagon)

Figure A.15: Combinatorial transitions in successive transformations of the $\left(\frac{\pi}{4}\right)$-isosceles triangulated octagon.

Removing subscripts and superscripts Figure A.16 yields a corresponding intrinsic combinatorial derivation on the $\left(\frac{\pi}{4}\right)$-isosceles triangle.

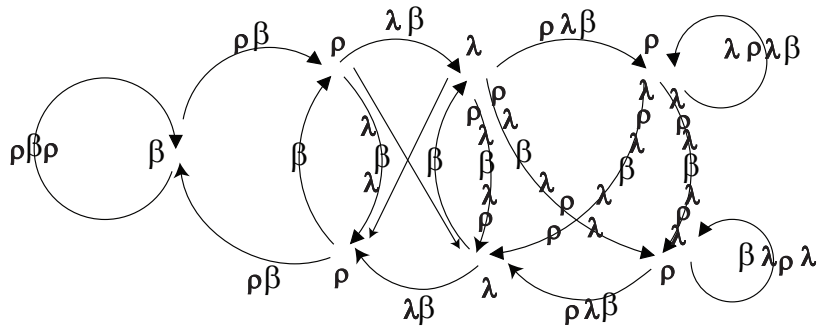

(a) Stage 0: Transition Diagram $\mathfrak{D}_0^*$ for unfolded $\left(\frac{\pi}{4}\right)$-isosceles triangle (Delaunay in Octagon)

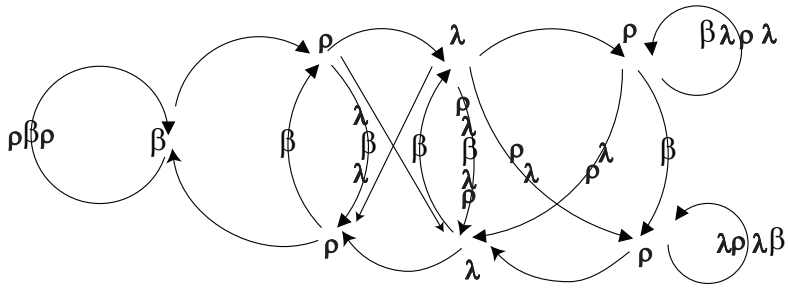

(b) Stage 3: Transition Diagram $\mathfrak{D}^{*'}$ for unfolded $\left(\frac{\pi}{4}\right)$-isosceles triangle after renormalization(Delaunay in Octagon)

Figure A.16: Combinatorial transitions in successive transformations of the unfolded $\left(\frac{\pi}{4}\right)$-isosceles triangle.

The coherence conditions from Section 4.5 and [76] can be translated, dictionary-style, into the intrinsic three-letter triangle alphabet.

Definition A.2.0.1. *The word in* $\{\beta, \lambda, \rho\}^{\mathbb{Z}}$ *obtained from*

$$\mathrm{w} \in \left(\{\beta_i\}_{i\in\{0,\ldots,3\}} \cup \{\rho_j.\rho^j, \lambda_k, \lambda^k\}_{j=0,1;k=1,3}\right)^{\mathbb{Z}}$$

by stripping off all subscripts and superscripts is the triangle projection *of* w.

Definition A.2.0.2. *A* β-free subword *of* $\mathrm{w} \in \{\beta, \lambda, \rho\}^{\mathbb{Z}}$ *is a subword consisting only of* λ*'s and* ρ*'s that is maximal, in that cannot be extended in either direction while retaining this property.*

Example A.2.0.1. *The successive* β*-free subwords of the finite word:*

$$\mathrm{w} = \beta\,\rho\,\beta\,\rho\,\lambda\,\beta\,\lambda\,\rho\,\lambda\,\rho\,\beta\,\lambda\;\rho\,\lambda\,\beta$$

are $[\rho]$*,* $[\rho\,\lambda]$*,* $[\lambda\,\rho\,\lambda]$*,* $[\lambda\,\rho\,\lambda\,\rho]$ *and* $[\lambda\,\rho\,\lambda]$*.*

Definition A.2.0.3. *The word* $\mathrm{w} \in \{\beta, \lambda, \rho\}^{\mathbb{Z}}$ *is* deriveable *if* w *or* $(\lambda\,\rho) \cdot \mathrm{w}$ *is realizable in* $\mathfrak{D}_0^*$*. In this case, whichever of* w *or* $\lambda\,\rho) \cdot \mathrm{w}$ *can be realized in* $\mathfrak{D}_0^*$ *called the* normalization $\mathrm{n}(\mathrm{w})$ *of* w*.*

Definition A.2.0.4. *The combinatorial* derivative *of a normalizable word* $\mathrm{w} \in \{\beta, \lambda, \rho\}^{\mathbb{Z}}$ *is the word* $\mathrm{D}(\mathrm{w}) \equiv \mathrm{w}'$ *obtained by tracing the path* p *realizing* $\mathrm{n}(\mathrm{w})$ *in* $\mathfrak{D}_0^*$ *through* $\mathfrak{D}^{*'}$*. A normalizable word is* deriveable *if its derivative is also normalizable.*

Coherence Conditions: A $T_4^{\triangle}$-deriveable word **w** is $T_4^{\triangle}$-***coherent*** if the pairs of adjacent same-length β-free subwords in the triangle-projection of its normalization **n(w)** fall only into the categories given for $\mathcal{G}_k$, k = 0,1,2,3 shown below.

for $\mathcal{G}_0$	[ρ] [ρ]	[λρλ] [λρλ]	[λρλ] [λρλ]	[ρ] [ρ]
for $\mathcal{G}_1$	[ρ] [ρ]	[λρλ] [λρλ]	[λρλ] [λρλ]	[λρ] [ρλ]
for $\mathcal{G}_2$	[ρ] [ρ]	[λρλ] [λρλ]	[ρλρλ] [ρλρλ] [ρλρλ][λρλρ] [λρλρ][λρλρ]	[λρ] [ρλ]
for $\mathcal{G}_3$	[ρ] [ρ]	[ρλ] [λρ]	[ρλρλ] [ρλρλ] [ρλρλ][λρλρ] [λρλρ][λρλρ]	[λρ] [ρλ]

Figure A.17: Coherence conditions from Section 4.5 and [76] translated into identical conditions on the three letter triangle alphabet $\{\beta, \lambda, \rho\}$ labeling sides of the $\left(\frac{\pi}{4}\right)$-isosceles triangle.

Definition A.2.0.5. *If pairs of successive same-length β-free subwords of the normalized derivative* $\mathrm{n}(\mathrm{w}')$ *of a deriveable word* $\mathrm{w} \in \{\beta, \lambda, \rho\}^{\mathbb{Z}}$ *fall exclusively into one of the categories from the table in Figure A.17 then* w *is* coherent.

Theorem A.2.0.1. *The closure of the set of hitting sequences on the $\left(\frac{\pi}{4}\right)$-isosceles triangle is exactly the set of infinitely coherent sequences in $\{\beta, \lambda, \rho\}^{\mathbb{Z}}$.*

Conjecture A.2.1. *The closure of the set of hitting sequences on the $\left(\frac{\pi}{4n}\right)$-isosceles triangle is exactly the set of infinitely coherent sequences in $\{\beta, \lambda, \rho\}^{\mathbb{Z}}$, where the properties of deriveability and coherence follow from appropriate, immediate analogues, of figures from Figure A.14, diagrams in Figure A.16 and the table in Figure A.17.*

APPENDIX B

PLANE GEOMETRY AND ISOSCELES TRIANGLE HITTING SEQUENCES

A simple necessary condition for general isosceles triangle hitting sequences can be obtained directly from plane geometry.

Theorem B.0.0.2. *Let $\alpha \leq \frac{\pi}{2}$ be the apex angle of an isosceles triangle T_α. For $\mathrm{w} \in \left(\mathscr{B} \cup \overline{\mathscr{B}}\right)^{\mathbb{Z}}$, $\mathscr{B} = \{\beta\}$, $\overline{\mathscr{B}} = \{\lambda, \rho\}$ to be the hitting sequence of a billiard trajectory on T_α, it must satisfy the following conditions:*

1. *No letter immediately succeeds itself in* w.

2. *There exists $n \geq 2$ such that every $\overline{\mathscr{B}}$-block separating successive β's in* w *has length at most n.*

3. *The $\overline{\mathscr{B}}$-blocks separating a given β in* w *from its predecessor and successor β's differ in length by at most* 1.

Proof. Condition (1) is self-evident and holds in any triangle whatsoever. For conditions (2) and (3), let $0 < \alpha \leq \frac{\pi}{2}$, and $n_\alpha = \lceil \frac{\pi}{\alpha} \rceil$ where $\lceil \cdot \rceil$ denotes 'smallest integer larger than.' Let T_α^0 be situated with its base $\boldsymbol{\beta}_0$ horizontal and apex lying above $\boldsymbol{\beta}_0$ (Figure B.1). Take $\overline{\tau}$ to be an arbitrary billiard trajectory segment in T_α^0 that departs $\boldsymbol{\beta}_0$ at $t = t_0$ and next intersects $\boldsymbol{\beta}_0$ at $t = t_1 > t_0$. Due to symmetry, the conditions of Theorem B.0.0.2 are invariant under reflection through the

horizontal and vertical axes, so without loss of generality, we may assume that $\overline{\tau}$ leaves $\boldsymbol{\beta}_0$ at angle $\theta \in [0, \frac{\pi}{2}]$ and makes its next subsequent edge-intersection with $\boldsymbol{\rho}_0$.

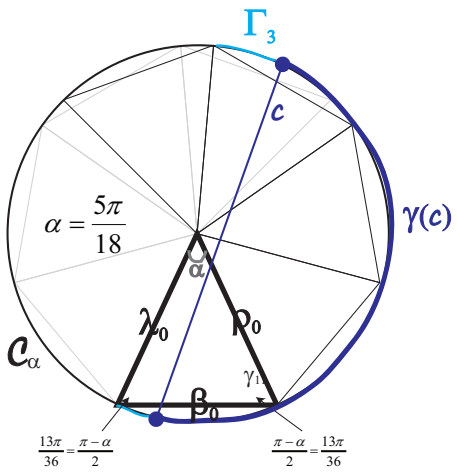

β ρ λ ρ β
(a)

Figure B.1

Setting up the figures (Figures B.1, B.2 and B.3) that will be used to prove (2) and (3): Let $\mathcal{C}_\alpha$ be the circumscribed circle about the polygonal unfolding of T^0_α $n_\alpha = \lceil \frac{\pi}{\alpha} \rceil$ times counterclockwise exclusively through ρ's and λ's. Oriented counterclockwise β_{n_α} will have nonpositive direction with respect to the horizontal.

Definition B.0.0.6. *A reflection of* T_α *through either* λ *or* ρ *is a* side-reflection, *while its reflection through* β *is a* base-reflection.

The piecewise linear ordered concatenation of β_i, $i = 0, 1, .., j$ will be $\mathcal{B}_j$; the

minor arc on $\mathcal{C}_\alpha$ subtended by β_i is γ_i and $\mathbf{\Gamma}_j$ is the ordered concatenation of γ_i, $i = 1, 2, .., j$. Finally, if c is an oriented chord or concatenated sequence of chords in $\mathcal{C}_\alpha$, $\gamma(c)$ is the counterclockwise arc bounded by its initial and terminal point; its arclength is $\ell(\gamma(c))$.

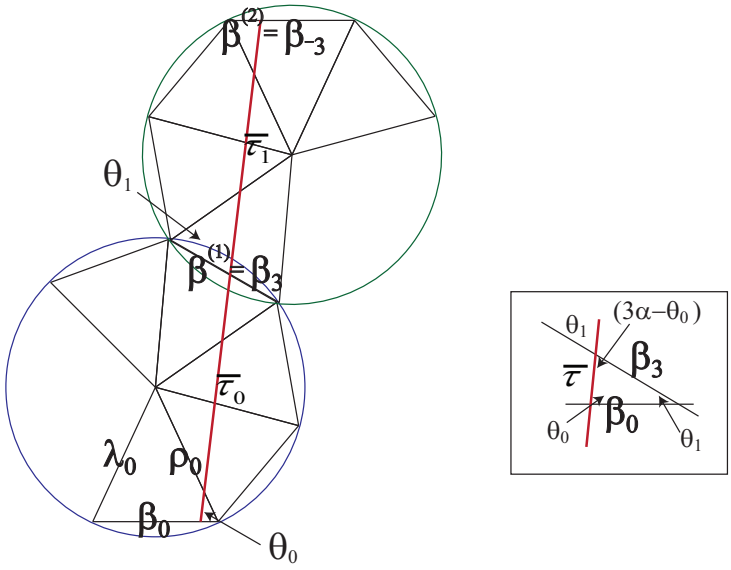

(a)

Figure B.2

Proof of Theorem B.0.0.2, Part (2): Any point on $\mathcal{C}_\alpha$ will be contained in an arc subtended by β_i, where $i \leq n_\alpha = \lceil \frac{\pi}{\alpha} \rceil$ is the i^{th} successive clockwise or i^{th} successive counterclockwise side-reflection of T^0_α. Suppose $\overline{\tau}$ is the unfolding of a billiard trajectory segment in T^0_α that starts at $\boldsymbol{\beta}_0$, next hits $\boldsymbol{\rho}_0$ and terminates upon its second intersection with $\boldsymbol{\beta}_0$. The line in $\mathbb{R}^2$ containing $\overline{\tau}$ also contains the chord $c(\overline{\tau})$ of $\mathcal{C}_\alpha$. The endpoints of $c(\overline{\tau})$ are necessarily both contained in Γ_{n_α}. So $\overline{\tau}$ intersects at most n_α successive counterclockwise side-reflections of T^0_α, which is to say it hits at most n_α ρ's and λ's between any two consecutive intersections with β.

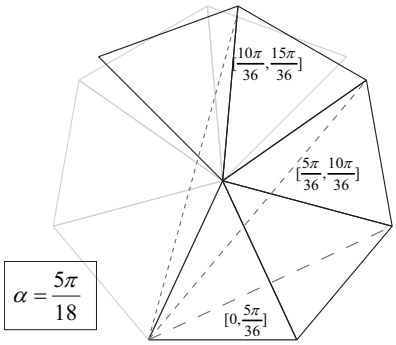

(a) Angular Sectors

$\alpha \le \frac{\pi}{2}$			
Angular Sector	# of Side-Crossings	# of Side-Crossings	Angular Sectors
$\Sigma_0 = [0, \frac{\alpha}{2}]$	1	1	$\Sigma_0 \cup \Sigma_1 = [0, \alpha]$
$\Sigma_1 = [\frac{\alpha}{2}, \alpha]$	1,2	2	$\Sigma_1 \cup \Sigma_2 = [\alpha, 2\alpha]$
$\Sigma_2 = [\alpha, \frac{3\alpha}{2}]$	2,3	3	$\Sigma_2 \cup \Sigma_3 = [2\alpha, 3\alpha]$
$\Sigma_{n_\alpha} = [\frac{(n_\alpha - 1)\alpha}{2}, \frac{n_\alpha \alpha}{2}]$	$n_\alpha - 1, n_\alpha$	n_α	$\Sigma_{n_\alpha - 1} \cup \Sigma_{n_\alpha} = [(n_\alpha - 1)\alpha, n_\alpha \alpha]$

(b) Angle Sector and # of Side-Crossings

Figure B.3

Proof of Theorem B.0.0.2, Part (3): Now let $\overline{\tau}$ be the concatenation of two parallel β-to-β trajectory segments $\overline{\tau}_0$ and $\overline{\tau}_1$ of the type described above (Figure B.3). Assume that $\overline{\tau}_0$ makes k_0 side-crossings between $\boldsymbol{\beta}_0$ and its next base-intersection, $\beta^{(1)} = \beta_{k_0}$. By Figure B.3 (Figure (left) and Table (right)), this implies that $\overline{\tau}_0$ has angle

$$\theta_0 \in \Sigma_{k_0-1} \cup \Sigma_{k_0} \equiv \left[\frac{(k_0-1)\alpha}{2}, \frac{k_0\alpha}{2}\right] \cup \left[\frac{k_0\alpha}{2}, \frac{(k_0+1)\alpha}{2}\right] = \left[\frac{(k_0-1)\alpha}{2}, \frac{(k_0+1)\alpha}{2}\right]$$

with respect to the horizontal edge $\boldsymbol{\beta}_0$. Setting θ_1 to be the angle that the extension $\overline{\tau}_1$ of $\overline{\tau}_0$ through $\beta^{(1)} = \beta_{k_0}$ makes with β_{k_0}, we get:

$$\begin{aligned}\theta_1 = \pi - \theta_0 - (\pi - (k_0 - 1)\alpha) &= k_0\alpha - \theta_0 \\ &\in \left[\frac{(k_0 - 1)\alpha}{2}, \frac{(k_0 + 1)\alpha}{2}\right] \\ &= \Sigma_{k_0 - 1} \cup \Sigma_{k_0}\end{aligned}$$

for $\theta_0 \in \left[\frac{(k_0-1)\alpha}{2}, \frac{(k_0+1)\alpha}{2}\right]$. Trajectories in Σ_{k_0-1} can make $(k_0 - 1)$ or k_0 side-crossings before their next base-intersection (Table in Figure B.3), while trajectories in Σ_{k_0} can make k_0 or $k_0 + 1$ such side-crossings (Table in Figure B.3). To summarize: the extension through $\beta^{(1)}$ of a trajectory segment $\overline{\tau}_0$ that made k_0 side-crossings getting from $\boldsymbol{\beta}_0$ to $\beta^{(1)}$ makes $k_1 \in \{k_0-1, k_0, k_0+1\}$ side-crossings before next intersecting β, proving that successive $\overline{\mathscr{B}}$-blocks in α-isosceles hitting sequences differ in length by at most 1.

□

BIBLIOGRAPHY

[1] Pierre Arnoux and Pascal Hubert. Fractions continues sur les surfaces de veech. *Journal dAnalyse Mathématique*, 81(1):35–64, 2000.

[2] Jayadev S Athreya. Quantitative recurrence and large deviations for teichmuller geodesic flow. *Geometriae Dedicata*, 119(1):121–140, 2006.

[3] Jayadev S Athreya, Alex Eskin, and Anton Zorich. Right-angled billiards and volumes of moduli spaces of quadratic differentials on cp. *arXiv preprint arXiv:1212.1660*, 2012.

[4] Jayadev S Athreya and Giovanni Forni. Deviation of ergodic averages for rational polygonal billiards. *Duke Mathematical Journal*, 144(2):285–319, 2008.

[5] A Avila and P Hubert. Recurrence for the wind-tree model. *preprint*.

[6] Artur Avila, Marcelo Viana, et al. Dynamics in the moduli space of abelian differentials. *Portugaliae Mathematica*, 62(4):531, 2005.

[7] Tim Bedford, Michael Keane, and Caroline Series. *Ergodic theory, symbolic dynamics, and hyperbolic spaces*. Oxford University Press Oxford, 1991.

[8] Jozef Bobok and Serge Troubetzkoy. Does a billiard orbit determine its (polygonal) table? *arXiv preprint arXiv:0811.1094*, 2008.

[9] Jozef Bobok and Serge Troubetzkoy. Code and order in polygonal billiards. *Topology and its Applications*, 159(1):236–247, 2012.

[10] Corentin Boissy and Erwan Lanneau. Dynamics and geometry of the rauzy-veech induction for quadratic differentials. *Ergodic Theory and Dynamical Systems*, 29(3):767, 2009.

[11] M Boshernitzan, G Galperin, T Krüger, and S Troubetzkoy. Periodic billiard orbits are dense in rational polygons. *Transactions of the American Mathematical Society*, 350(9):3523–3535, 1998.

[12] Michael D Boshernitzan. Billiards and rational periodic directions in polygons. *The American mathematical monthly*, 99(6):522–529, 1992.

[13] Irene I Bouw and Martin Möller. Teichmüller curves, triangle groups, and lyapunov exponents. *Annals of Mathematics*, 172:139–185, 2010.

[14] Joshua P Bowman. Teichmüller geodesics, delaunay triangulations, and veech groups. In *Proceedings of the International Workshop on Teichmüller theory and moduli problems*, 2008.

[15] Xavier Bressaud, Alexander I Bufetov, and Pascal Hubert. Deviation of ergodic averages for substitution dynamical systems with eigenvalues of modulus one. *arXiv preprint arXiv:1106.2666*, 2011.

[16] J Cassaigne, Pascal Hubert, Serge Troubetzkoy, et al. Complexity and growth for polygonal billiards. In *Annales de l'institut Fourier*, volume 52, pages 835–848. Chartres: L'Institut, 1950-, 2002.

[17] Yitwah Cheung and Alex Eskin. Slow divergence and unique ergodicity. *arXiv preprint arXiv:0711.0240*, 2007.

[18] Yitwah Cheung and Howard Masur. Minimal non-ergodic directions on genus-2 translation surfaces. *Ergodic Theory and Dynamical Systems*, 26(2):341, 2006.

[19] Diana Davis. Cutting sequences, regular polygons, and the veech group. *Geometriae Dedicata*, 162(1):231–261, 2013.

[20] Diana Davis, Dmitry Fuchs, and Serge Tabachnikov. Periodic trajectories in the regular pentagon. *Moscow Math. J*, 11:1–23, 2011.

[21] Laura DeMarco. The conformal geometry of billiards. *Bulletin of the American Mathematical Society*, 48(1):33–52, 2011.

[22] N Pytheas Fogg and Valérie Berthé. *Substitutions in dynamics, arithmetics and combinatorics*, volume 1794. Springer, 2002.

[23] Giovanni Forni and Carlos Matheus. Introduction to teichmuller theory and its applications to dynamics of interval exchange transformations, flows on surfaces and billiards. 2012.

[24] Ralph H Fox and Richard B Kershner. Concerning the transitive properties of geodesics on a rational polyhedron. *Duke Mathematical Journal*, 2(1):147–150, 1936.

[25] Dmitry Fuchs and Serge Tabachnikov. Periodic trajectories in the regular pentagon, ii. *arXiv preprint arXiv:1201.0026*, 2011.

[26] Eugene Gutkin. Billiard dynamics: An updated survey with the emphasis on open problems. *Chaos: An Interdisciplinary Journal of Nonlinear Science*, 22(2):026116–026116, 2012.

[27] Eugene Gutkin, Pascal Hubert, and Thomas A Schmidt. Affine diffeomorphisms of translation surfaces: periodic points, fuchsian groups, and arithmeticity. In *Annales Scientifiques de lÉcole Normale Supérieure*, volume 36, pages 847–866. Elsevier, 2003.

[28] Eugene Gutkin and Chris Judge. The geometry and arithmetic of translation surfaces with applications to polygonal billiards. *Mathematical Research Letters*, 3:391–404, 1996.

[29] Eugene Gutkin and Serge Troubetzkoy. Directional flows and strong recurrence for polygonal billiards. *Pitman Research Notes in Mathematics Series*, pages 21–45, 1996.

[30] Lorenz Halbeisen and Norbert Hungerbühler. On periodic billiard trajectories in obtuse triangles. *SIAM review*, 42(4):657–670, 2000.

[31] W Patrick Hooper. Periodic billiard paths in right triangles are unstable. *Geometriae Dedicata*, 125(1):39–46, 2007.

[32] W Patrick Hooper. An infinite surface with the lattice property i: Veech groups and coding geodesics. *arXiv preprint arXiv:1011.0700*, 2010.

[33] W Patrick Hooper. Another veech triangle. *arXiv preprint arXiv:1107.5054*, 2011.

[34] W Patrick Hooper, Pascal Hubert, and Barak Weiss. Dynamics on the infinite staircase. *Discret. Continuous Dyn. Syst. Ser. A (to appear)*, 2010.

[35] W Patrick Hooper and Richard Evan Schwartz. Billiards in nearly isosceles triangles. *arXiv preprint arXiv:0807.3498*, 2008.

[36] John Hubbard and Howard Masur. Quadratic differentials and foliations. *Acta Mathematica*, 142(1):221–274, 1979.

[37] John H Hubbard. *Teichmüller theory and applications to geometry, topology, and dynamics*, volume 1. Matrix Pr, 2006.

[38] John H Hubbard and Howard Masur. On the existence and uniqueness of strebel differentials. *Bulletin (New Series) of the American Mathematical Society*, 82(1):77–79, 1976.

[39] Pascal Hubert, Samuel Lelievre, and Serge Troubetzkoy. The ehrenfest wind-tree model: periodic directions, recurrence, diffusion. *Journal für die reine und angewandte Mathematik (Crelles Journal)*, 2011(656):223–244, 2011.

[40] Pascal Hubert and Thomas A Schmidt. Veech groups and polygonal coverings. *Journal of Geometry and Physics*, 35(1):75–91, 2000.

[41] Pascal Hubert and Thomas A Schmidt. An introduction to veech surfaces. *Handbook of dynamical systems*, 1:501–526, 2006.

[42] Pascal Hubert and Barak Weiss. Ergodicity for infinite periodic translation surfaces.

[43] A Katok. Billiard table as a mathematicians playground. In *Student colloquium lecture series*, volume 2, pages 8–36. Citeseer, 2002.

[44] Svetlana Katok. *Fuchsian groups*. University of Chicago press, 1992.

[45] Svetlana Katok. Coding of closed geodesics after gauss and morse. *Geometriae Dedicata*, 63(2):123–145, 1996.

[46] Svetlana Katok and Ilie Ugarcovici. Symbolic dynamics for the modular surface and beyond. *Bulletin of the American Mathematical Society*, 44(1):87–132, 2007.

[47] Richard Kenyon and John Smillie. Billiards on rational-angled triangles. *Commentarii Mathematici Helvetici*, 75(1):65–108, 2000.

[48] Steven Kerckhoff, Howard Masur, and John Smillie. A rational billiard flow is uniquely ergodic in almost every direction. *Bulletin of the American Mathematical Society*, 13(2):141–142, 1985.

[49] Steven Kerckhoff, Howard Masur, and John Smillie. Ergodicity of billiard flows and quadratic differentials. *The Annals of Mathematics*, 124(2):293–311, 1986.

[50] Michel L Lapidus and Robert G Niemeyer. The current state of fractal billiards. *arXiv preprint arXiv:1210.0282*, 2012.

[51] Michel L Lapidus and Robert G Niemeyer. Sequences of compatible periodic hybrid orbits of prefractal koch snowflake billiards. *arXiv preprint arXiv:1204.3133*, 2012.

[52] Samuel Lelièvre. Veech surfaces associated with rational billiards. *arXiv preprint math/0205249*, 2002.

[53] Richard L Liboff. Classical irreversibility and mapping of the isosceles triangle billiard. *International Journal of Theoretical Physics*, 35(1):189–198, 1996.

[54] Douglas Alan Lind. *An introduction to symbolic dynamics and coding*. Cambridge University Press, 1995.

[55] Howard Masur. The growth rate of trajectories of a quadratic differential. *Ergodic Theory Dynam. Systems*, 10(1):151–176, 1990.

[56] Howard Masur. Ergodic theory of translation surfaces. *Handbook of dynamical systems*, 1:527–547, 2006.

[57] Howard Masur and Serge Tabachnikov. Rational billiards and flat structures. *Handbook of dynamical systems*, 1:1015–1089, 2002.

[58] Curtis McMullen. Billiards and teichmüller curves on hilbert modular surfaces. *Journal of the American Mathematical Society*, 16(4):857–885, 2003.

[59] Curtis T McMullen. Dynamics of over moduli space in genus two. *Annals of mathematics*, pages 397–456, 2007.

[60] Marston Morse and Gustav A Hedlund. Symbolic dynamics. *American Journal of Mathematics*, 60(4):815–866, 1938.

[61] Marston Morse and Gustav A Hedlund. Symbolic dynamics ii. sturmian trajectories. *American Journal of Mathematics*, 62(1):1–42, 1940.

[62] Gérard Rauzy. Échanges d'intervalles et transformations induites. *Acta Arithmetica*, 34(4):315–328, 1979.

[63] Dmitri Scheglov. Growth of periodic orbits and generalized diagonals for typical triangular billiards. 2012.

[64] Jean-Christophe Schlage-Puchta. On triangular billiards. *Commentarii Mathematici Helvetici*, 76(3):501–505, 2001.

[65] Jason Schmurr. Translation covers of triangular billiards surfaces. *arXiv preprint arXiv:0810.3353*, 2008.

[66] R Schwartz. Billiards obtuse and irrational. *Preprint*, 2005.

[67] Richard Evan Schwartz. Obtuse triangular billiards i: near the (2, 3, 6) triangle. *Experimental Mathematics*, 15(2):161–182, 2006.

[68] Richard Evan Schwartz. Obtuse triangular billiards ii: One hundred degrees worth of periodic trajectories. *Experimental Mathematics*, 18(2):137–171, 2009.

[69] Richard Evan Schwartz. *Mostly surfaces*, volume 60. AMS Bookstore, 2011.

[70] Caroline Series. Non-euclidean geometry, continued fractions, and ergodic theory. *The Mathematical Intelligencer*, 4(1):24–31, 1982.

[71] Caroline Series. The geometry of markoff numbers. *The mathematical intelligencer*, 7(3):20–29, 1985.

[72] Caroline Series. The modular surface and continued fractions. *Journal of the London Mathematical Society*, 2(1):69–80, 1985.

[73] J Smillie. The dynamics of billiard flows in rational polygons of dynamical systems. *Dynamical systems, ergodic theory and applications*, 1:360, 2000.

[74] John Smillie and Corinna Ulcigrai. Symbolic coding for linear trajectories in the regular octagon. *arXiv preprint arXiv:0905.0871*, 2009.

[75] John Smillie and Corinna Ulcigrai. Geodesic flow on the teichmuller disk of the regular octagon, cutting sequences and octagon continued fractions maps. In *Dynamical Numbers: Interplay Between Dynamical Systems and Number Theory: a Special Program, May 1-July 31, 2009: International Conference, July 20-24, 2009, Max Planck Institute for Mathematics, Bonn, Germany*, volume 532, page 29. AMS Bookstore, 2010.

[76] John Smillie and Corinna Ulcigrai. Beyond sturmian sequences: coding linear trajectories in the regular octagon. *Proceedings of the London Mathematical Society*, 102(2):291–340, 2011.

[77] John Smillie and Barak Weiss. Veechs dichotomy and the lattice property. *Ergodic Theory Dynam. Systems*, 28(6):1959–1972, 2008.

[78] John Smillie and Barak Weiss. Characterizations of lattice surfaces. *Inventiones mathematicae*, 180(3):535–557, 2010.

[79] John Stillwell. Classical topology and combinatorial group theory. *Graduate Texts in Mathematics*, 72, 1980.

[80] Serge Tabachnikov. *Billiards*. Société mathématique de France Paris, 1995.

[81] Sergej L'vovivc Tabavcnikov. *Geometry and billiards*, volume 30. AMS Bookstore, 2005.

[82] Rodrigo Treviño. On the ergodicity of flat surfaces of finite area. *arXiv preprint arXiv:1211.1313*, 2012.

[83] Serge Troubetzkoy. Recurrence and periodic billiard orbits in polygons. *Regular and Chaotic Dynamics*, 9(1):1–12, 2004.

[84] Serge Troubetzkoy. Periodic billiard orbits in right triangles. In *Annales de l'institut Fourier*, volume 55, pages 29–46. Chartres: L'Institut, 1950-, 2005.

[85] William A Veech. Teichmüller curves in moduli space, eisenstein series and an application to triangular billiards. *Inventiones mathematicae*, 97(3):553–583, 1989.

[86] William A Veech. The billiard in a regular polygon. *Geometric and Functional Analysis*, 2(3):341–379, 1992.

[87] Marcelo Viana. Ergodic theory of interval exchange maps. *Revista Matemática Complutense*, 19(1):7–100, 2006.

[88] Marcelo Viana. Dynamics of interval exchange transformations and teichmüller flows. *Lecture Notes. http://w3. impa. br/˜ viana/out/ietf. pdf*, 2008.

[89] Ya B Vorobets. Planar structures and billiards in rational polygons: the veech alternative. *Russian Mathematical Surveys*, 51(5):779–817, 1996.

[90] Clayton C Ward. Calculation of fuchsian groups associated to billiards in a rational triangle. *Ergodic Theory and Dynamical Systems*, 18(4):1019–1042, 1998.

[91] Alex Wright. Schwarz triangle mappings and teichmüller curves: the veech–ward–bouw–möller curves. *Geometric and Functional Analysis*, pages 1–34, 2013.

[92] Jean-Christophe Yoccoz. Continued fraction algorithms for interval exchange maps: an introduction. *Frontiers in number theory, physics, and geometry I*, pages 403–437, 2006.

[93] Jean-Christophe Yoccoz. Interval exchange maps and translation surfaces. *Lecture Notes: Pisa Lectures*, 2007.

[94] AN Zemlyakov and Anatolii Borisovich Katok. Topological transitivity of billiards in polygons. *Mathematical Notes of the Academy of Sciences of the USSR*, 18(2):760–764, 1975.

[95] Anton Zorich. Flat surfaces. *Frontiers in number theory, physics, and geometry I*, pages 439–585, 2006.